Planck and next generation CMB experiments

Francesco Piacentini

University of Roma "La Sapienza"
Planck HFI Collaboration

December 18, 2013

Outline

planck

- The Planck 2013 results (highlights)
- Planck and gravitational lensing
- Planck and dark matter annihilation
- Cosmic Microwave Background polarization
- Next generation CMB missions

Planck (Max)

- In order to explain the blackbody measured radiation, Max Planck found an *empirical equation*, working very well

$$E=\frac{C\lambda^{-5}}{e^{c/\lambda T}-1},$$

which, as far as I can see at the moment, fits the observational data, published up to now, as satisfactorily as the best equations put forward for the spectrum, namely those of Thiesen,*[17] Lummer–Jahnke,† and Lummer–Pringsheim.‡ (This was demonstrated by some numerical examples.[18]) I should therefore be permitted to draw your attention to this new formula which I consider to be the simplest possible, apart from Wien's expression, from the point of view of the electromagnetic theory of radiation.

- Then, he wanted a physical explanation
  - He HAD to introduce the quantization of electromagnetic energy $E=h\nu$
  - That was *"an act of desperation"*

    ...as you can see from his evolution

Planck (Max)

before

Planck (Max)

before

1901

Planck (Max)

before

1901

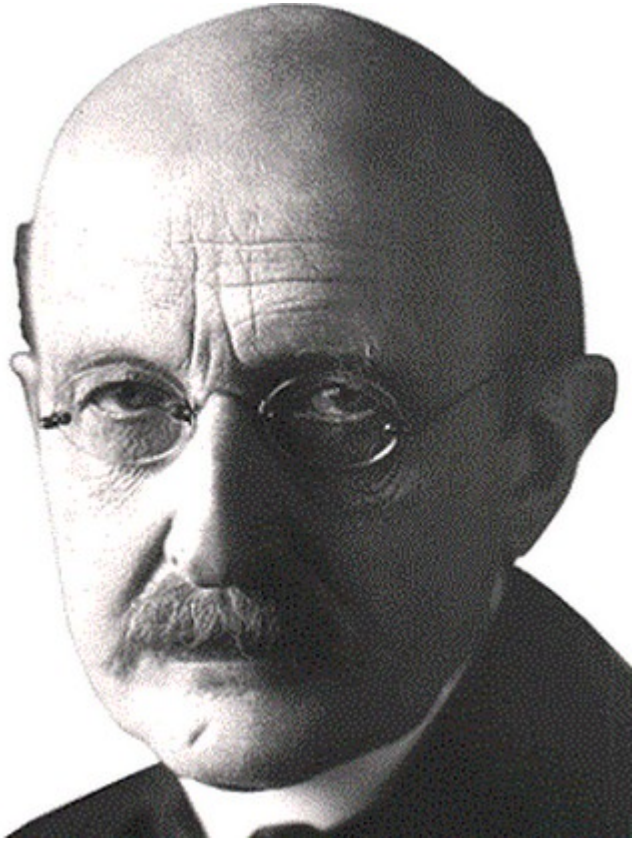

after

Kragh, Helge. "Max Planck: The Reluctant Revolutionary," Physics World, December 2000.

Dark matter

- In a similar fashion, Dark Matter HAD to be introduced, in order to explain several astrophysical phenomena
  - Speed of galaxies in galaxy clusters (F. Zwicky, 1933)
    - They are so fast that there must be a strong gravitational potential to keep them bound
  - Rotation of stars spiral galaxies (V. Rubin, 1970)
    - There must be an invisible halo of *matter*, in order to explain the rotation speed of stars around the galactic center
  - Faintness of Cosmic Microwave Background anisotropy (1990)
    - Is not possible to explain structures formation, unless a form of dark matter was collapsing before Early Universe plasma recombination, unaffected by radiation pressure
  - Details of the CMB anisotropy angular power spectrum (2000)

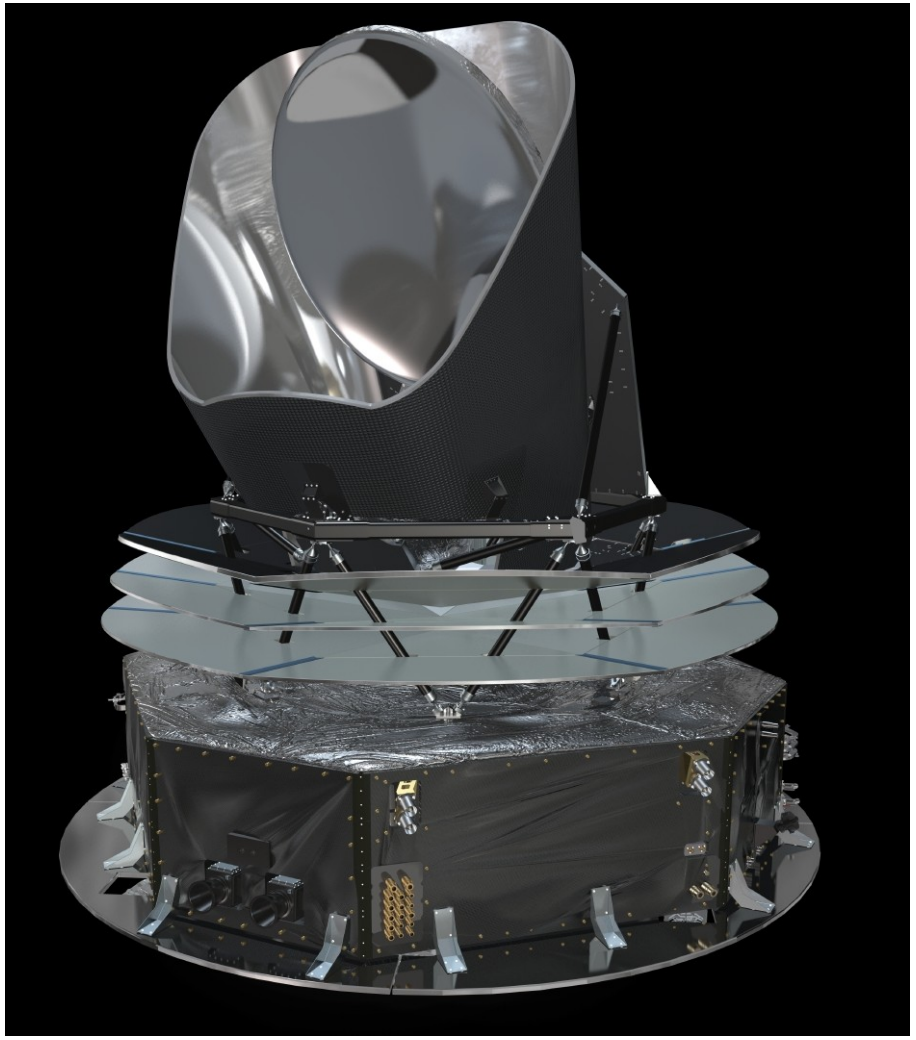

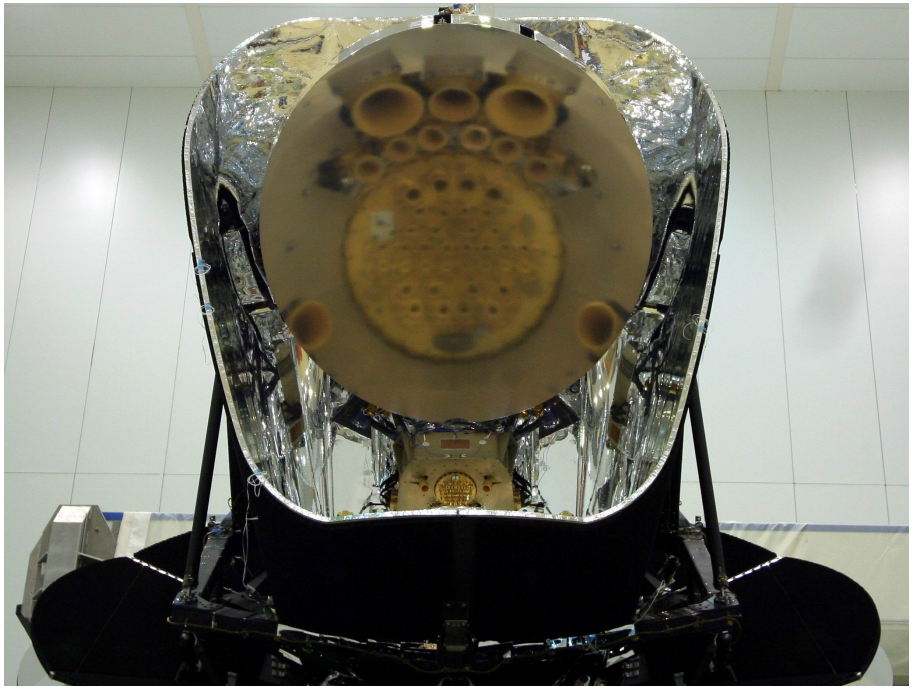

Planck – the spacecraft

- ESA Medium class mission,
  - selected in 1996,
    - launch 14-May-2009, in Kourou (with Herschel)
    - 29 months of operation at L2, 5 HFI sky surveys, +3 extra LFI surveys
- Planck is designed to extract
  - **all of the information in the CMB temperature anisotropies**.
  - measure the **polarization of CMB** anisotropies, which encodes not only a wealth of cosmological information but also provides a unique probe of the thermal history of the Universe
- It will survey the whole sky with **unprecedented combination of:**
  - 2 instruments, **74 detectors**
  - **frequency coverage,** 33, 44, 70 100, 143, 217, 353, 545, 857 GHz
  - **angular resolution**, 32, 27, 13, 10, 7, 5, 5, 5, 4 arcmin
  - **Sensitivity**, ~5 μK/beam, providing data valuable for a broad range of astrophysics
  - In orbit around Sun-Earth L2 point

Observation frequencies

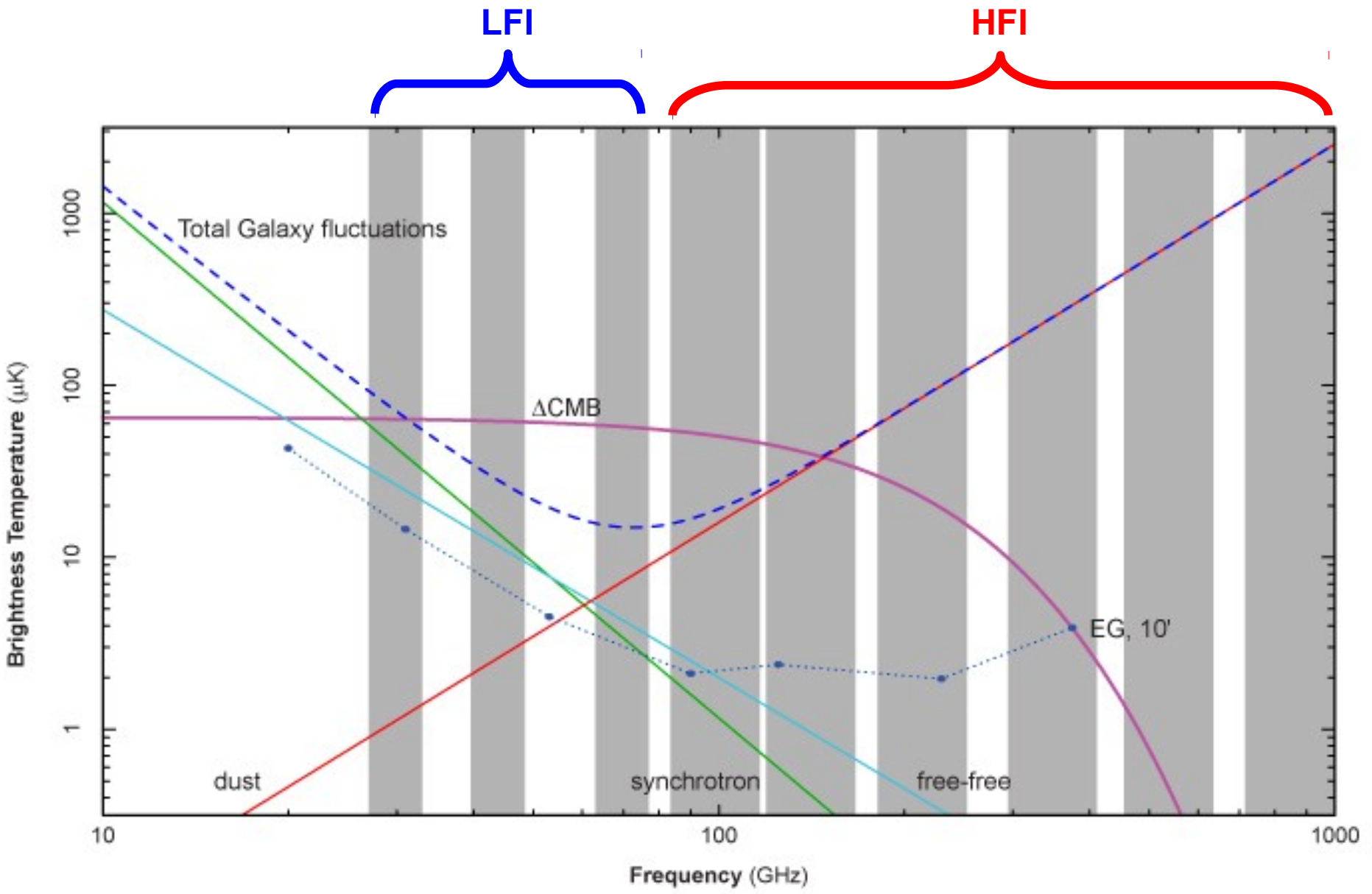

Mission timeline

- Launch 14 May 2009
- Start of operations 14 May 2009
- Cooldown/trip to L2 June 2009
- Calibration and performance verification Mid June – mid August 2009
- First light survey August 2009
- Survey 1 August 2009 – February 2010
- Survey 2 Feb 2010 – Aug 2010
- Survey 3 Aug 2010 – Feb 2011
- Survey 4 Feb 2011 – Aug 2011
- Survey 5 Aug 2011 – Dec 2011
- HFI End Of Life tests Dec 2011 – Aug 2013
- HFI End of Helium 13 January 2012
- Survey 6, 7, 8 (LFI only) Feb 2012 – Aug 2013
- Switch-off 23 October 2013

CMB observation

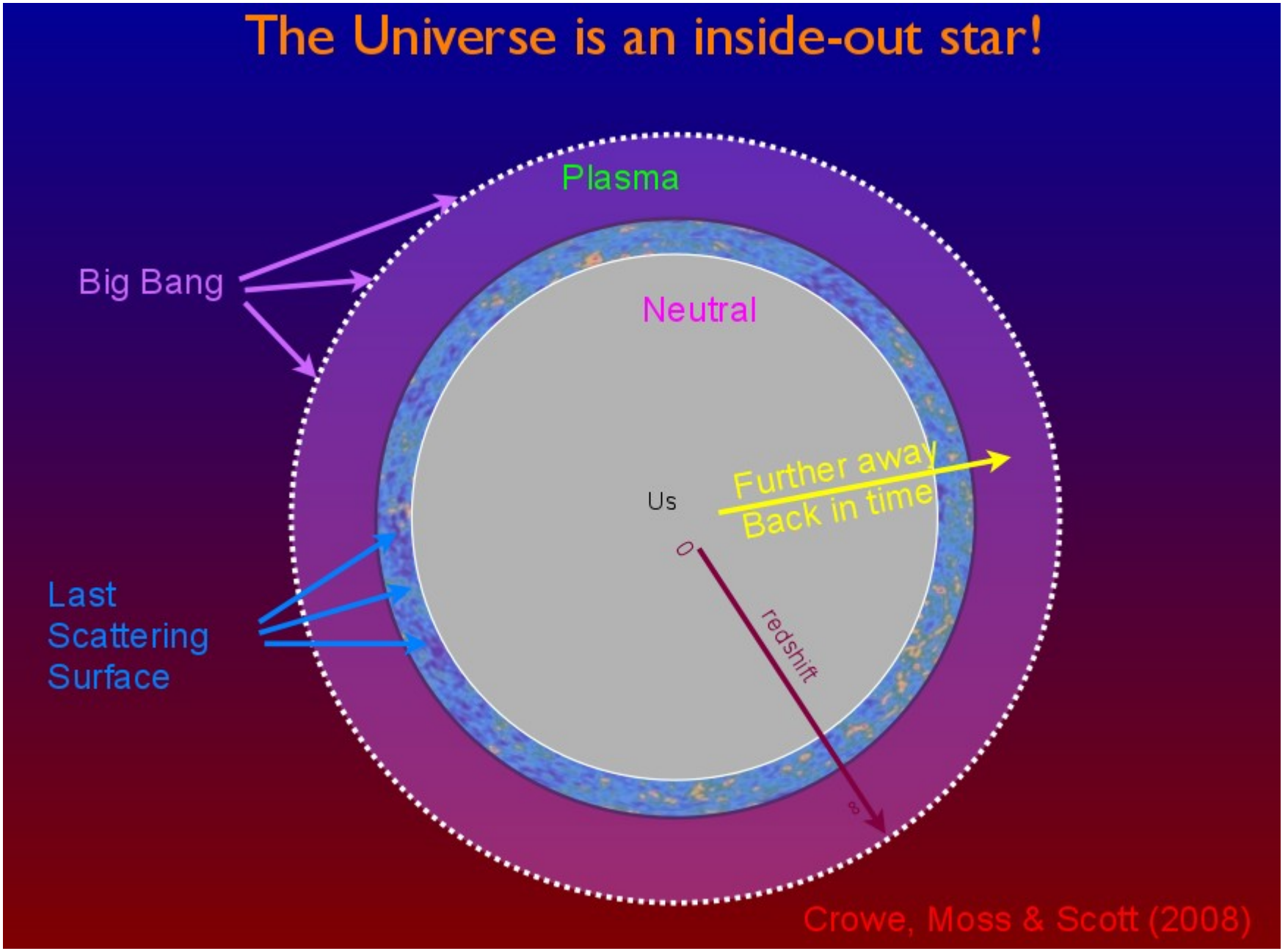

Sky maps

1 year of data, more than 2.5 are available

Maps properties (1 year)

Table 6. Properties of the *Planck* maps[a]

Property	Applies to	Frequency [GHz] 30	44	70	100	143	217	353	545	857
Effective frequency [GHz]	Mean	28.4	44.1	70.4	100	143	217	353	545	857
Noise rms per pixel [μK_{CMB}]	Median	9.2	12.5	23.2	11	6	12	43	...	...
[MJy sr^{-1}]	Median	...	...	...	...	...	...	...	0.0149	0.0155
Gain calibration uncertainty[b]	All sky	0.82 %	0.55 %	0.62 %	0.5 %	0.5 %	0.5 %	1.2 %	10 %	10 %
Zero level[c] [MJy sr^{-1}]	All sky	0	0	0	0.0047	0.0136	0.0384	0.0885	0.1065	0.1470
Zero level uncertainty [μK_{CMB}]	All sky	±2.23	±0.78	±0.64	...	...	...	...	...	...
[MJy sr^{-1}]	All sky	...	...	...	±0.0008	±0.001	±0.0024	±0.0067	±0.0165	±0.0147
Color correction unc.[d]	non-CMB emission	0.1β %	0.3β %	0.2β %	0.11$\Delta\alpha$ %	0.031$\Delta\alpha$ %	0.007$\Delta\alpha$ %	0.006$\Delta\alpha$ %	0.020$\Delta\alpha$ %	0.048$\Delta\alpha$ %
Beam Color correction unc.[e]	non-CMB emission	0.5 %	0.1 %	0.3 %	<0.3 %	<0.3 %	<0.3 %	<0.5 %	<2.0 %	<1.0 %

[a] The HFI default maps do not include removal of zodiacal emission.

[b] Includes the absolute uncertainty (0.24 %) of the calibration standard used, which is the CMB dipole estimated by WMAP7 (Hinshaw et al. 2009).

[c] A zero level has been removed from the LFI maps (−300.84, −22.83, and −28.09 μK_{CMB} at 30, 44, and 70 GHz), but not from the HFI maps. The value given in this table corresponds to an estimate zero level of Galactic emission (Planck Collaboration VIII 2013) in the maps which include zodiacal emission. For total emission studies, the level contributed by the Cosmic Infrared Background must be added (Planck Collaboration VIII 2013).

[d] β is the temperature spectral index of the source, see Planck Collaboration IV (2013). $\Delta\alpha$ is the difference in source spectral index from −1 (i.e., νI_ν = constant for $\alpha = -1$ following the IRAS convention), see Planck Collaboration IX (2013). No uncertainties are assumed on α and β.

[e] For the HFI channels, we show the upper limit in solid angle change due to color correction from a planet spectrum source (roughly ν^2) to *IRAS* convention (ν^{-1}).

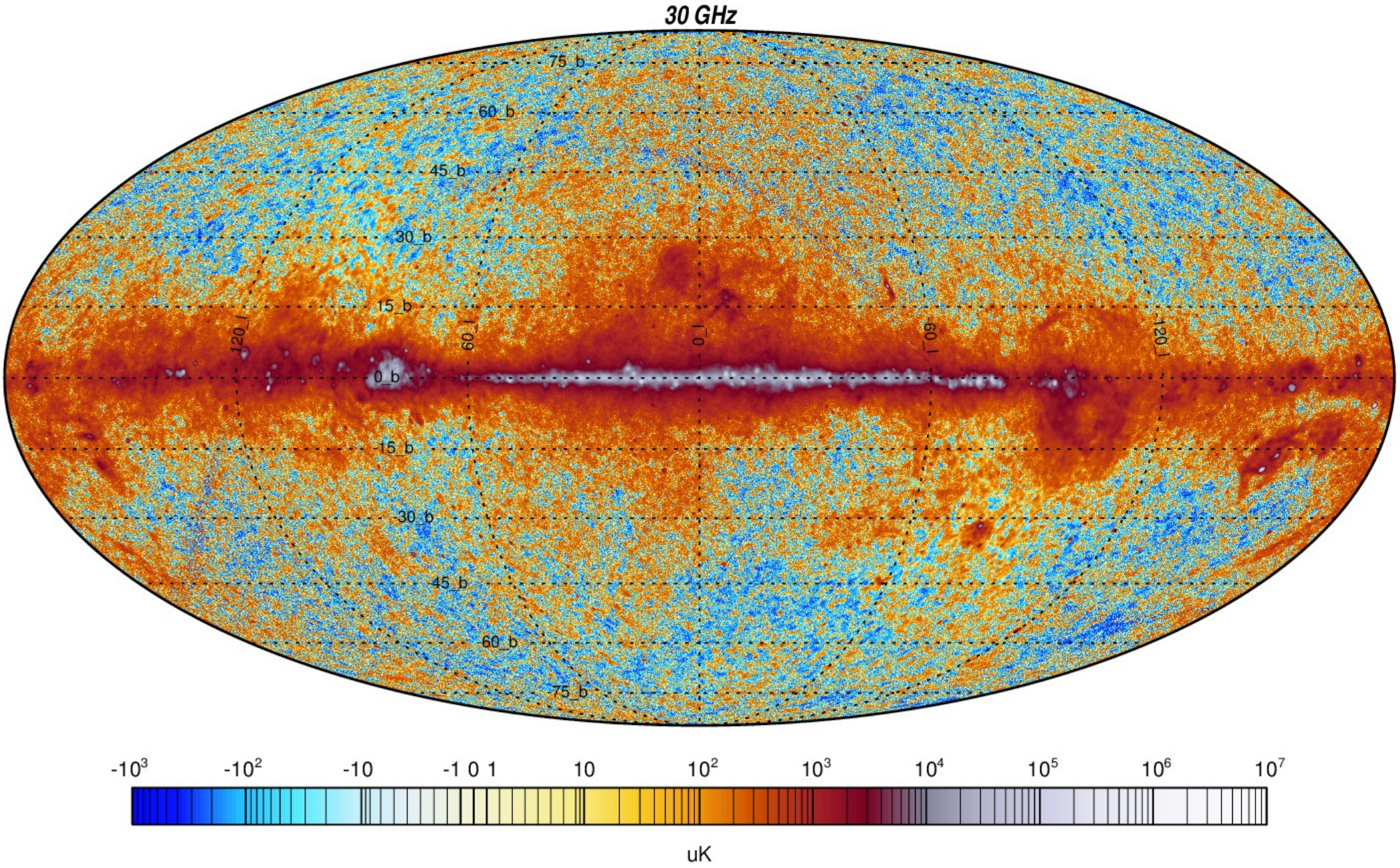
30 GHz
75_b
60_b
45_b
30_b
15_b
0_b
-15_b
-30_b
-45_b
-60_b
-75_b
120_l
60_l
0_l
-60_l
-120_l
-10^3
-10^2
-10
-1 0 1
10
10^2
10^3
10^4
10^5
10^6
10^7
uK

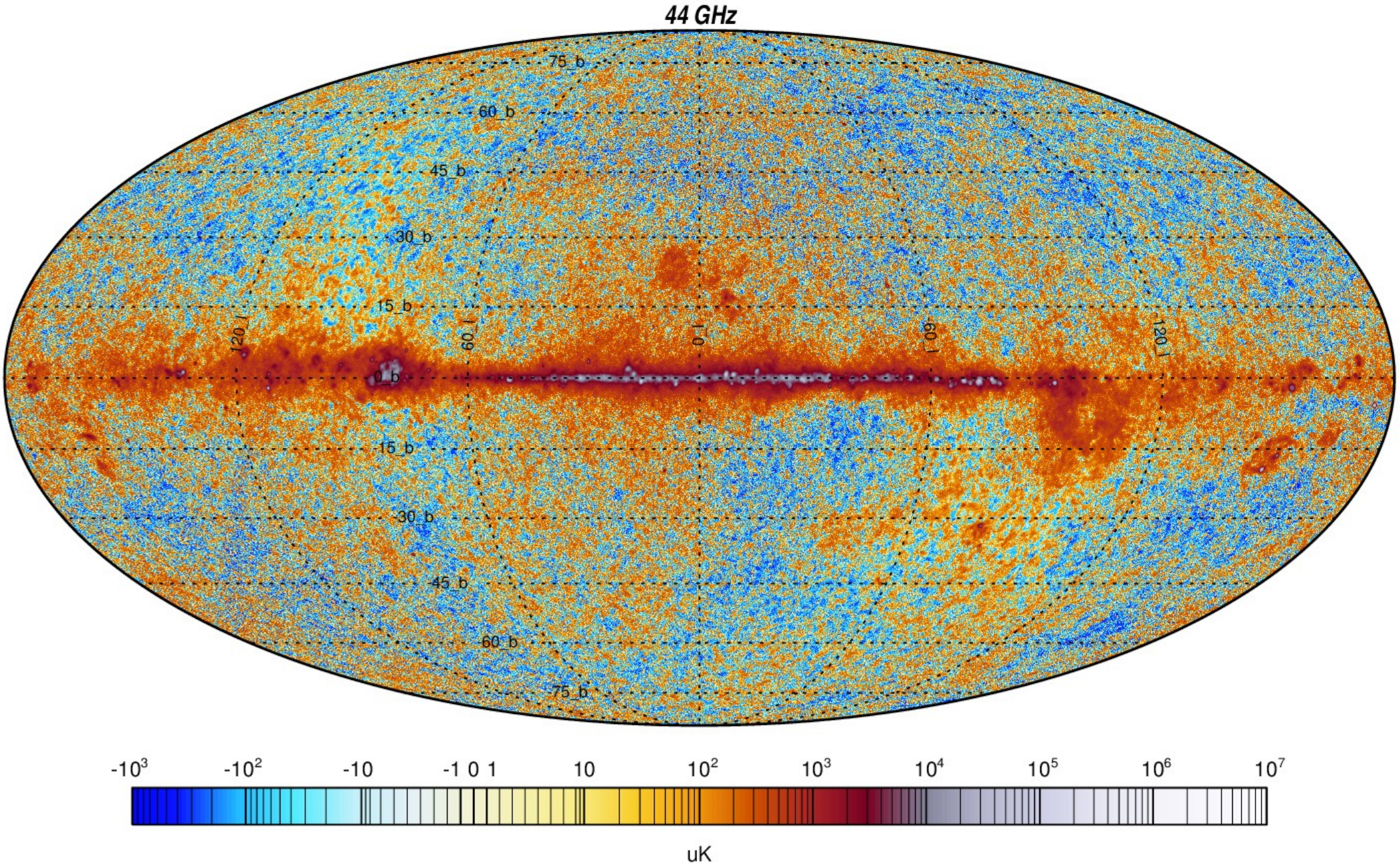
44 GHz
75_b
60_b
45_b
30_b
15_b
0_b
120_l
60_l
0_l
60_l
120_l
-10^3
-10^2
-10
-1 0 1
10
10^2
10^3
10^4
10^5
10^6
10^7
uK

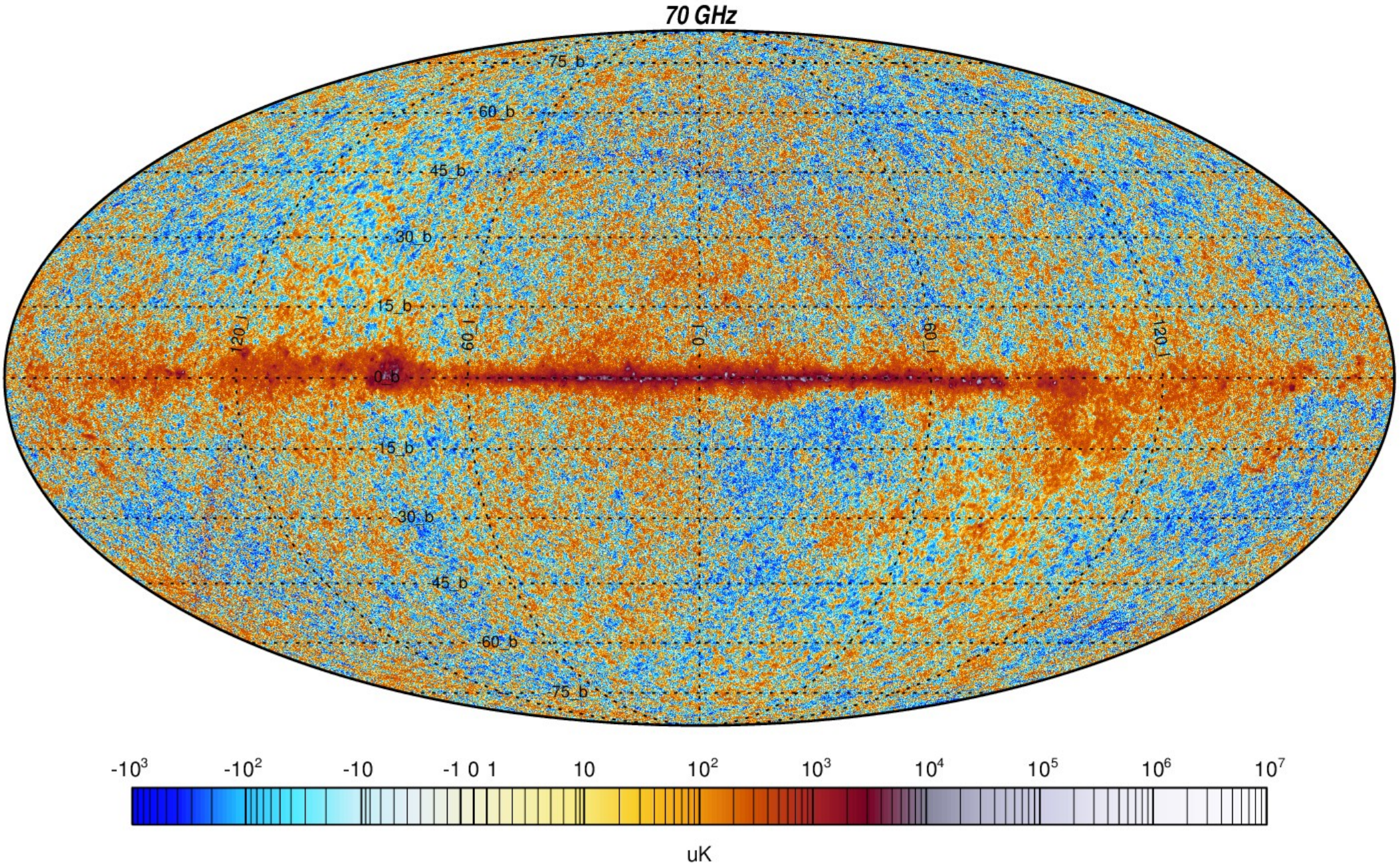
70 GHz
75_b
60_b
45_b
30_b
15_b
120_l
60_l
0_l
60_l
120_l
0_b
15_b
30_b
45_b
60_b
75_b
-10^3
-10^2
-10
-1 0 1
10
10^2
10^3
10^4
10^5
10^6
10^7
uK

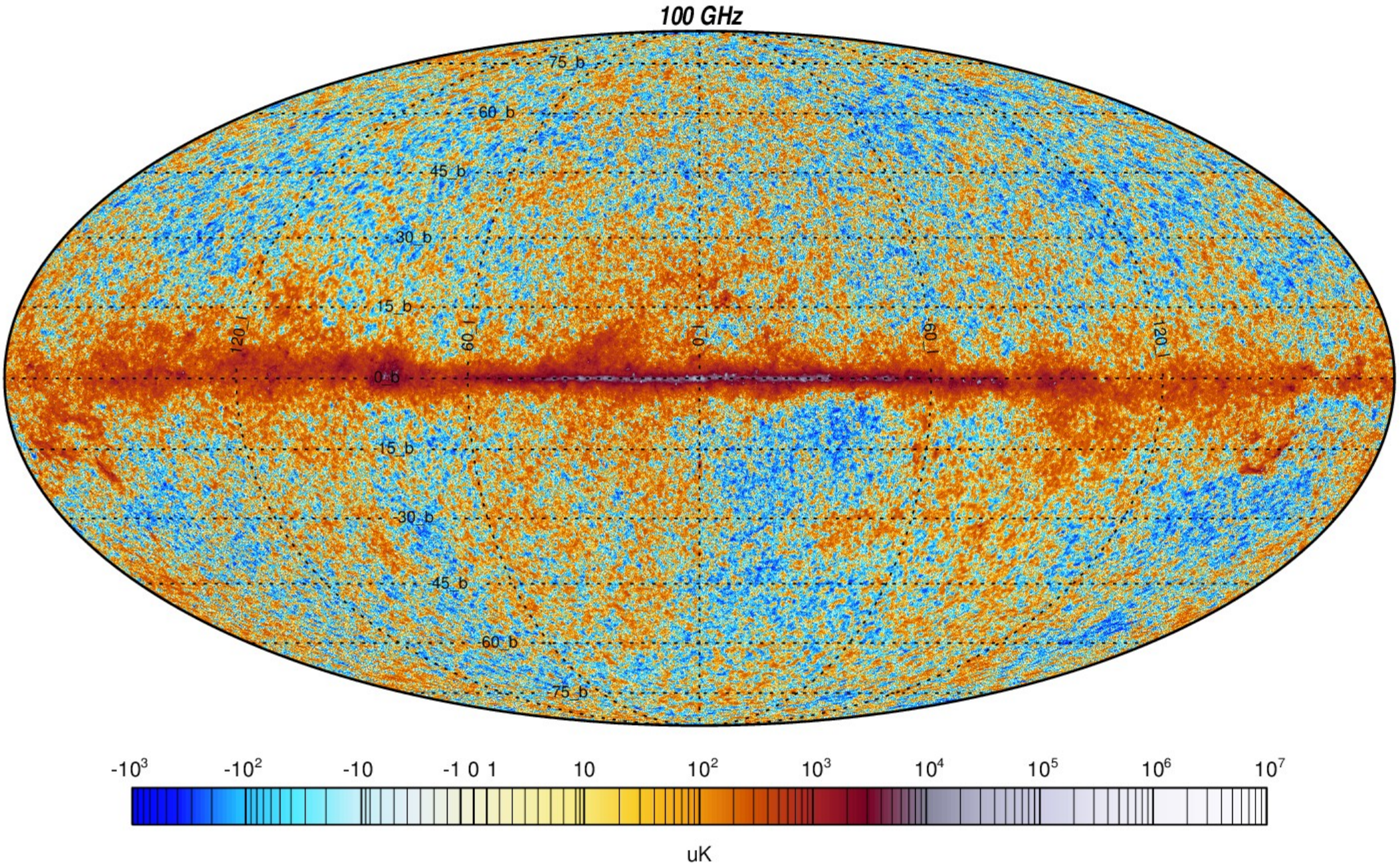
100 GHz
75_b
60_b
45_b
30_b
15_b
0_b
120_l
60_l
0_l
60_l
120_l
-10^3
-10^2
-10
-1 0 1
10
10^2
10^3
10^4
10^5
10^6
10^7
uK

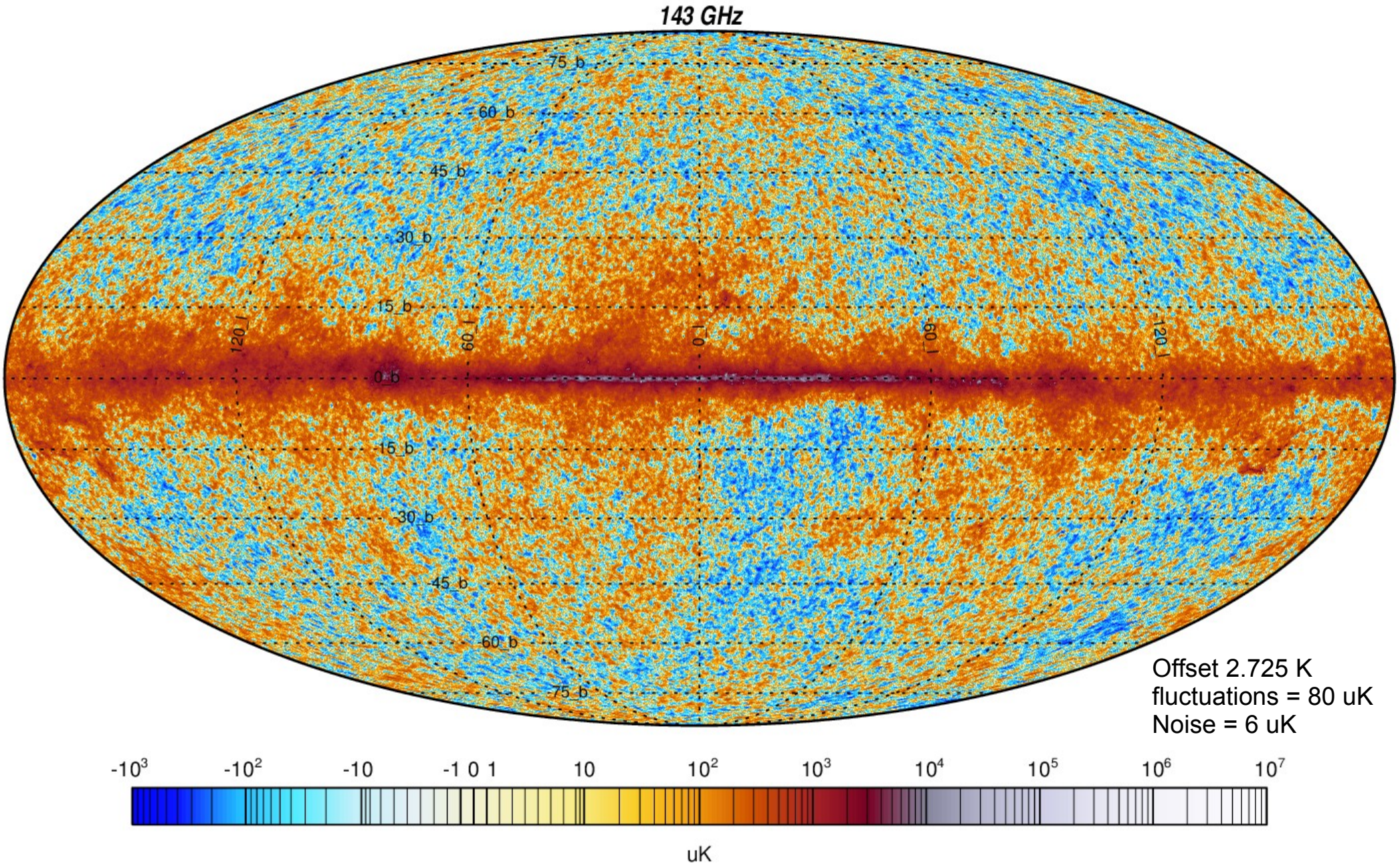

Offset 2.725 K
fluctuations = 80 uK
Noise = 6 uK

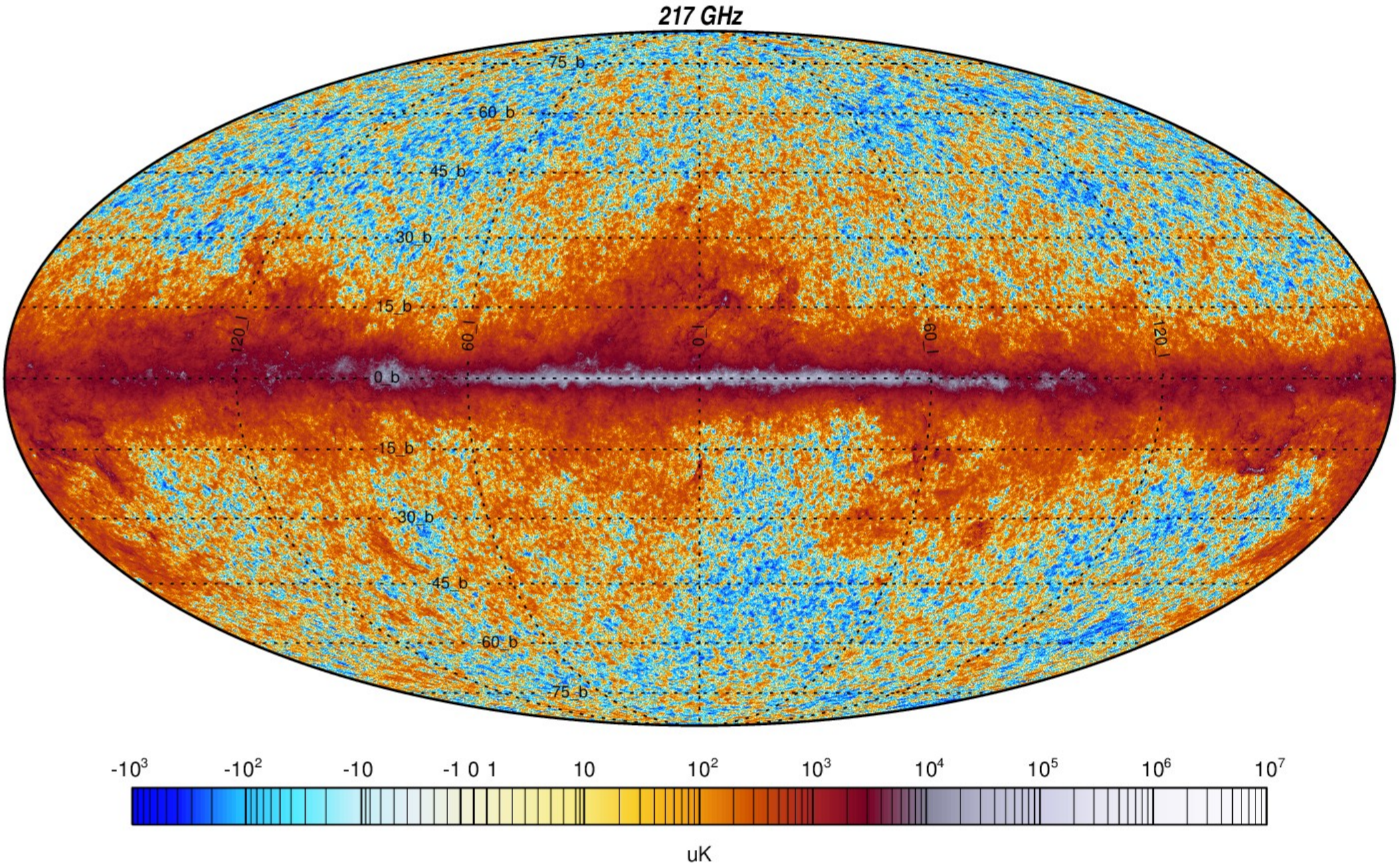
217 GHz
75_b
60_b
45_b
30_b
15_b
0_b
120_l
60_l
0_l
60_l
120_l
-10^3
-10^2
-10
-1 0 1
10
10^2
10^3
10^4
10^5
10^6
10^7
uK

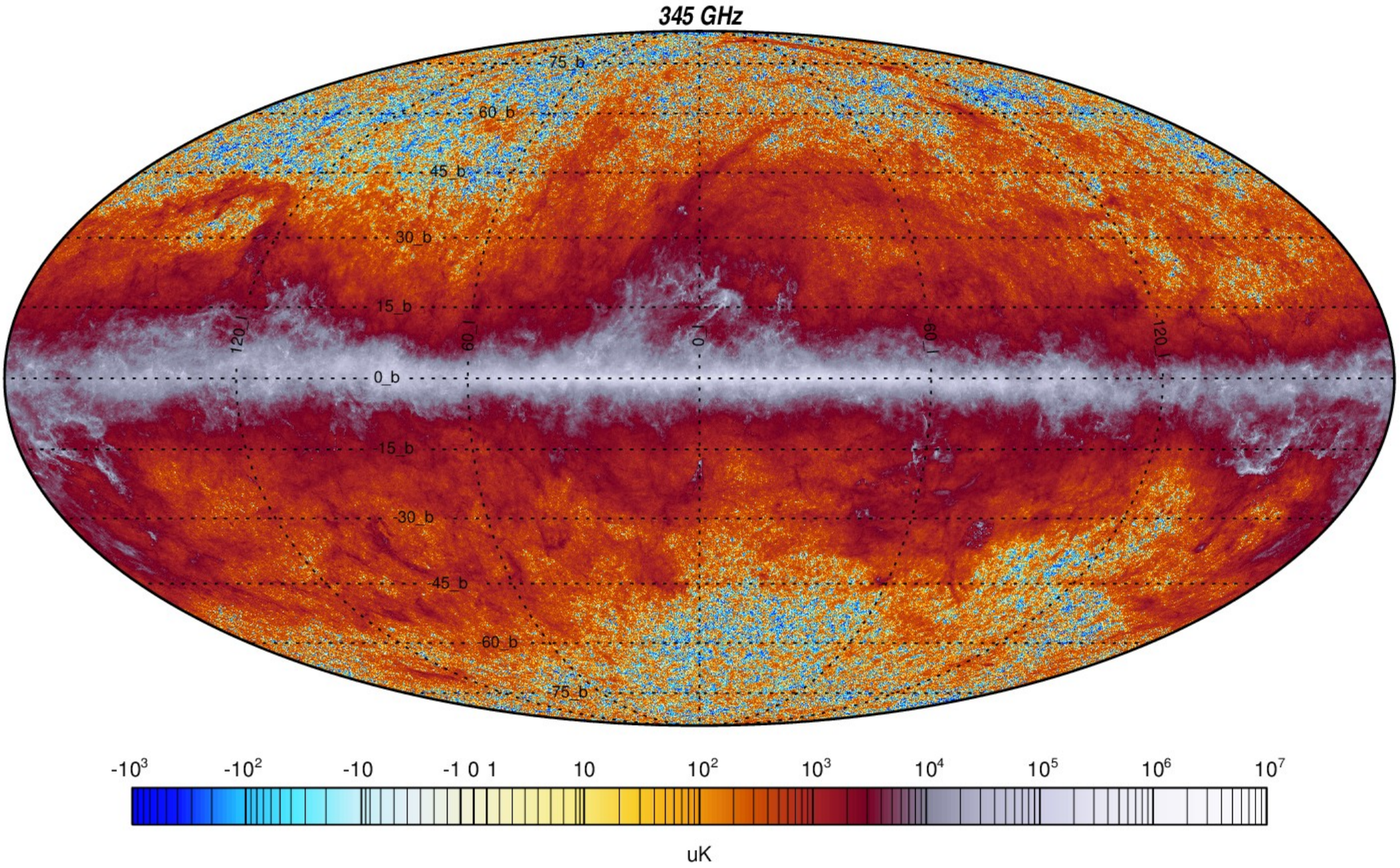
345 GHz
75_b
60_b
45_b
30_b
15_b
0_b
-15_b
-30_b
-45_b
-60_b
-75_b
120_l
60_l
0_l
-60_l
-120_l
-10^3
-10^2
-10
-1 0 1
10
10^2
10^3
10^4
10^5
10^6
10^7
uK

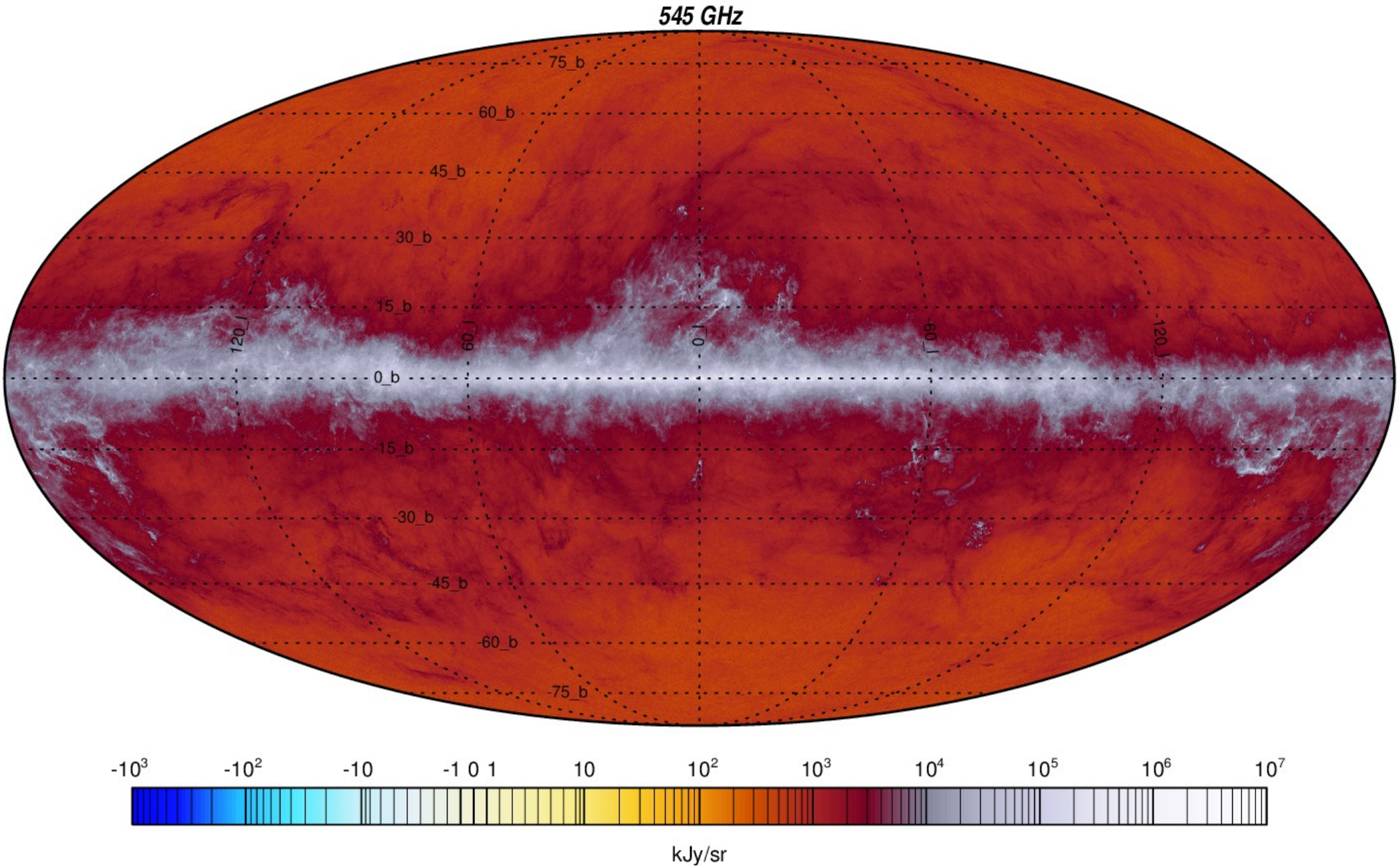
545 GHz
75_b
60_b
45_b
30_b
15_b
0_b
-15_b
-30_b
-45_b
-60_b
-75_b
120_l
60_l
0_l
-60_l
-120_l
-10^3
-10^2
-10
-1 0 1
10
10^2
10^3
10^4
10^5
10^6
10^7
kJy/sr

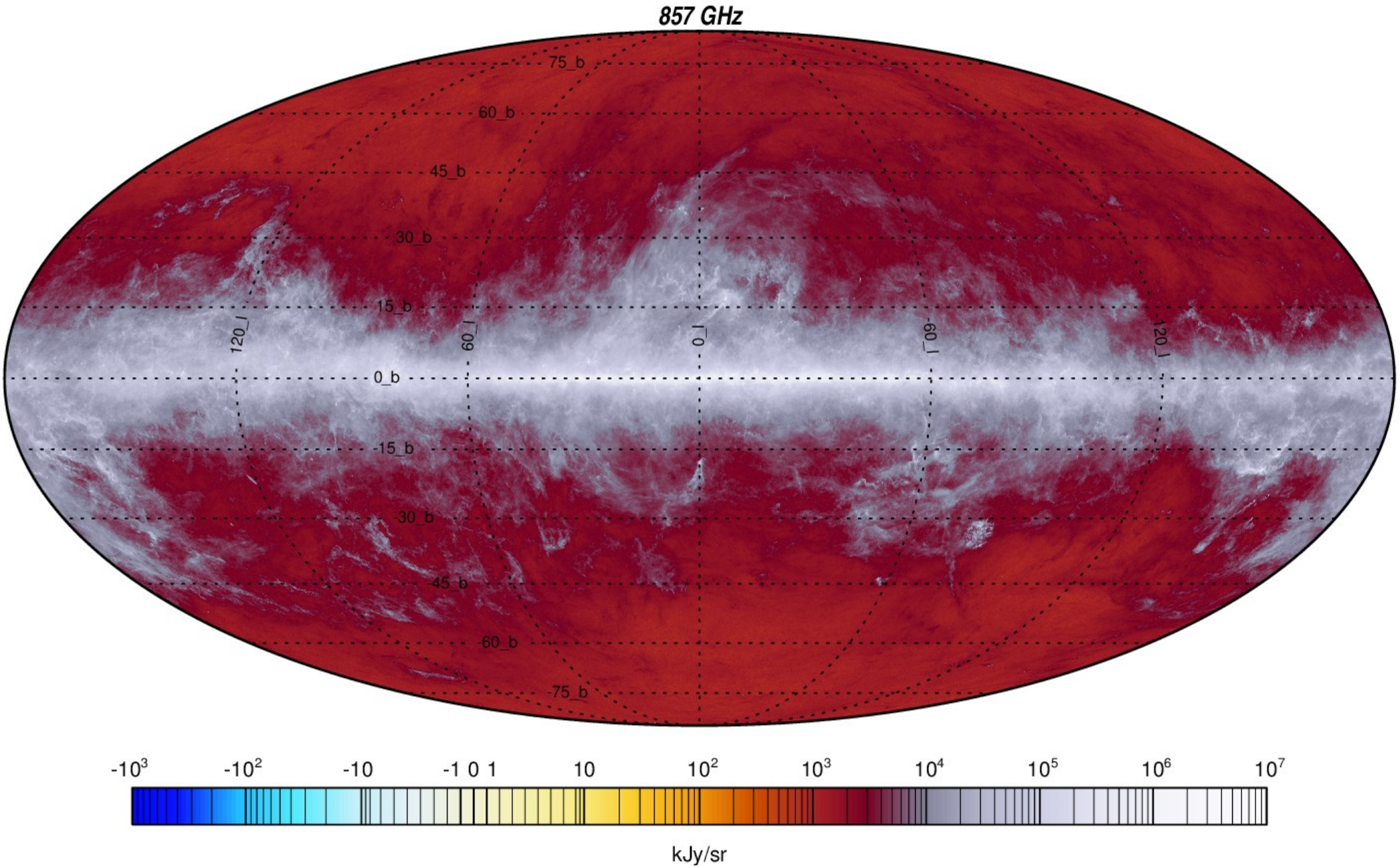
857 GHz
75_b
60_b
45_b
30_b
15_b
0_b
-15_b
-30_b
-45_b
-60_b
-75_b
120_l
60_l
0_l
-60_l
-120_l
-10^3
-10^2
-10
-1 0 1
10
10^2
10^3
10^4
10^5
10^6
10^7
kJy/sr

Extracted CMB

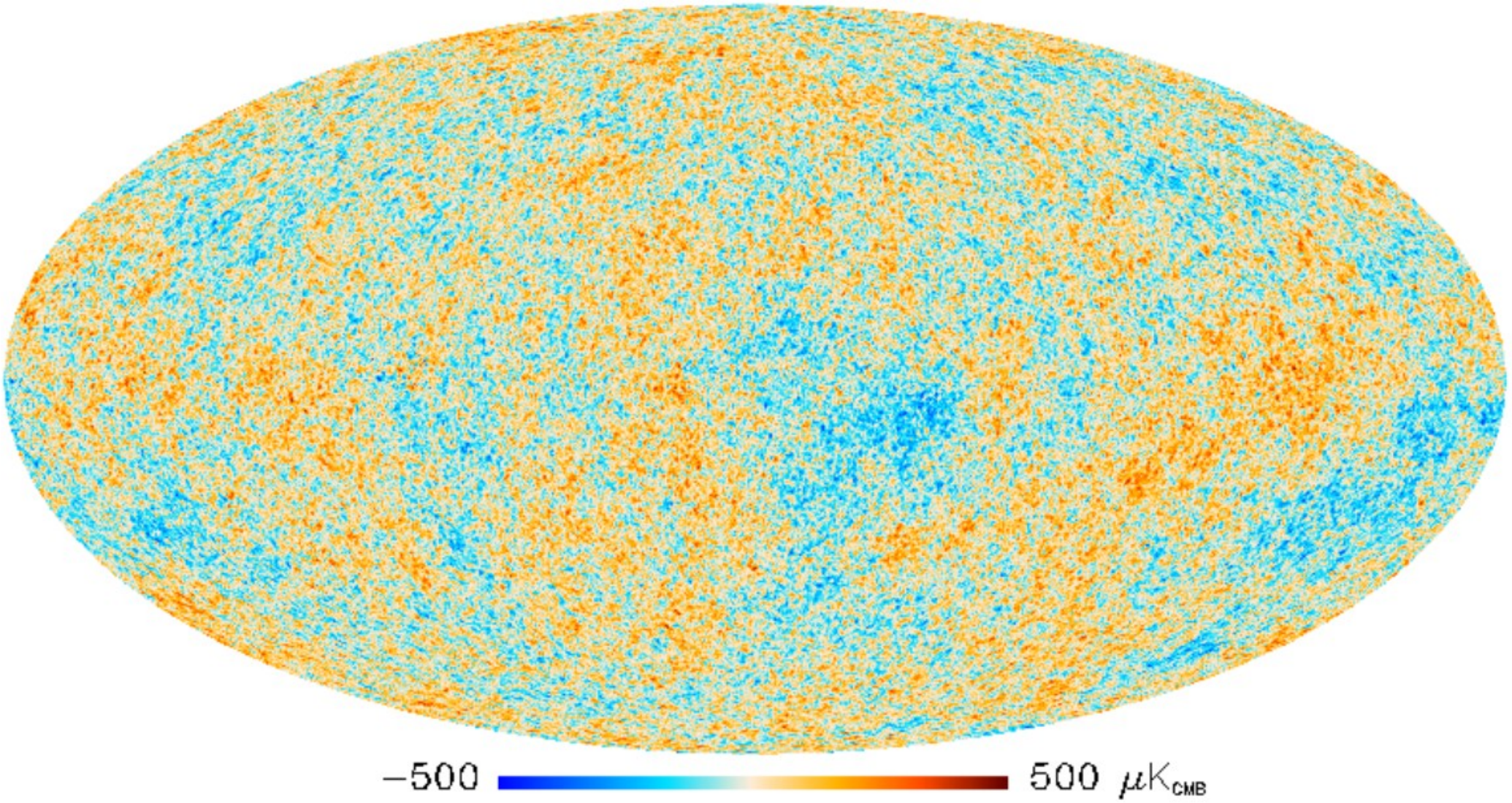

Combined frequencies map

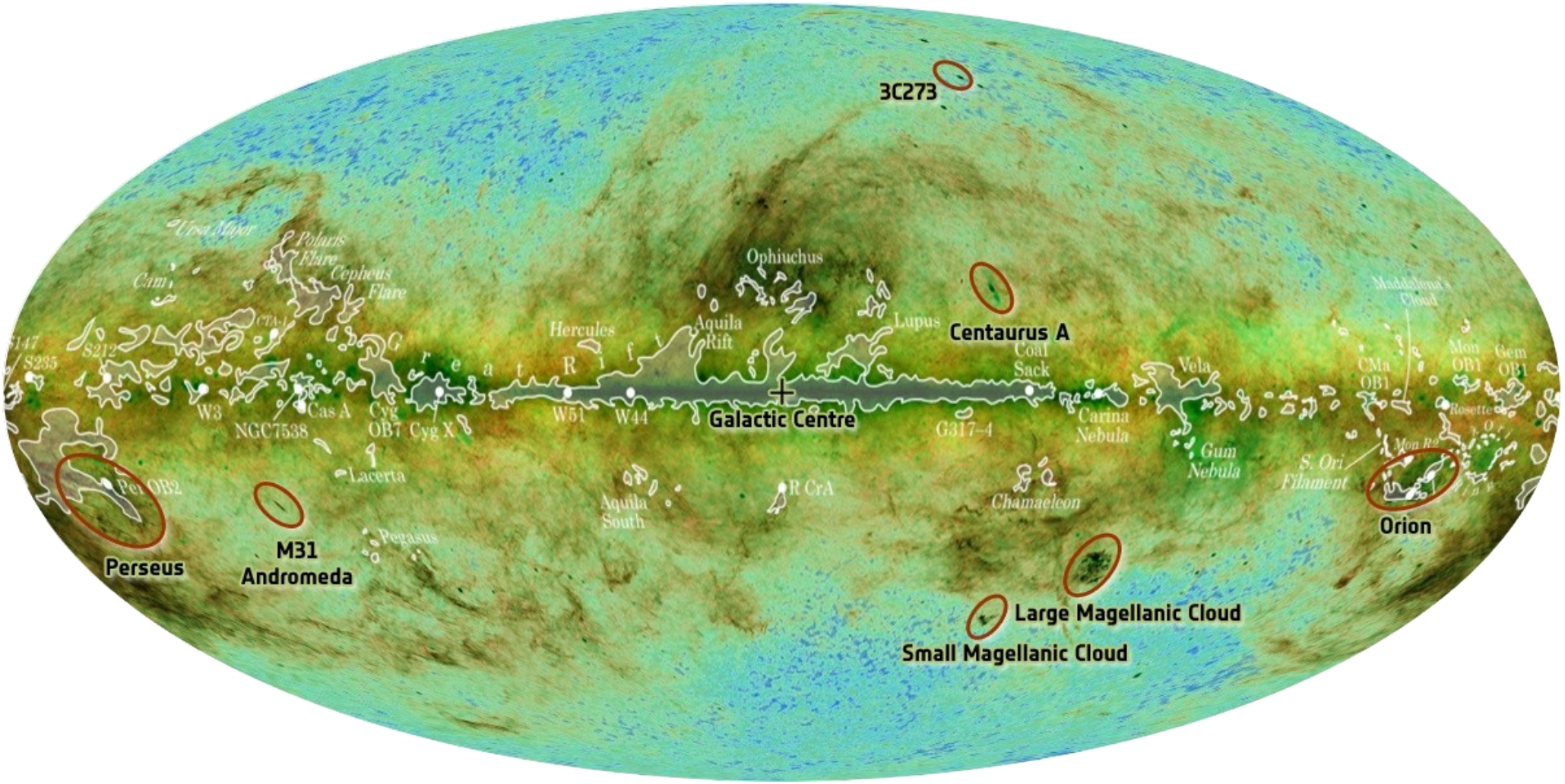

(c) HFI, LFI and ESA Consortia (2009)

Noise and Systematic effects

- Planck sensitivity is extremely high
  - Systematic effects dominate over noise
- NOISE
  - Null test on 30 minutes timescale with same scanning path
- Systematic effects
  - Null test on 6 months timescales with different scanning path

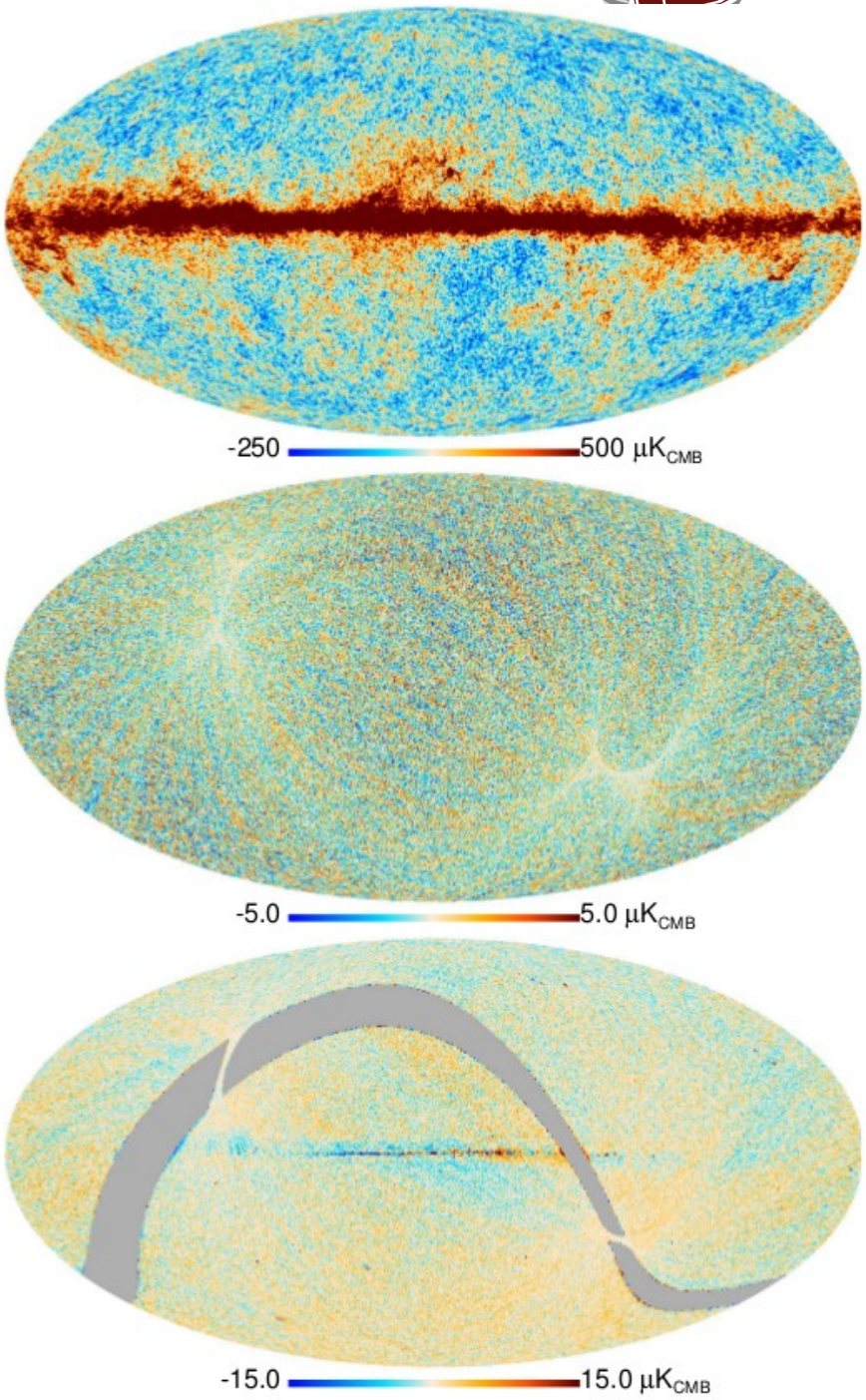

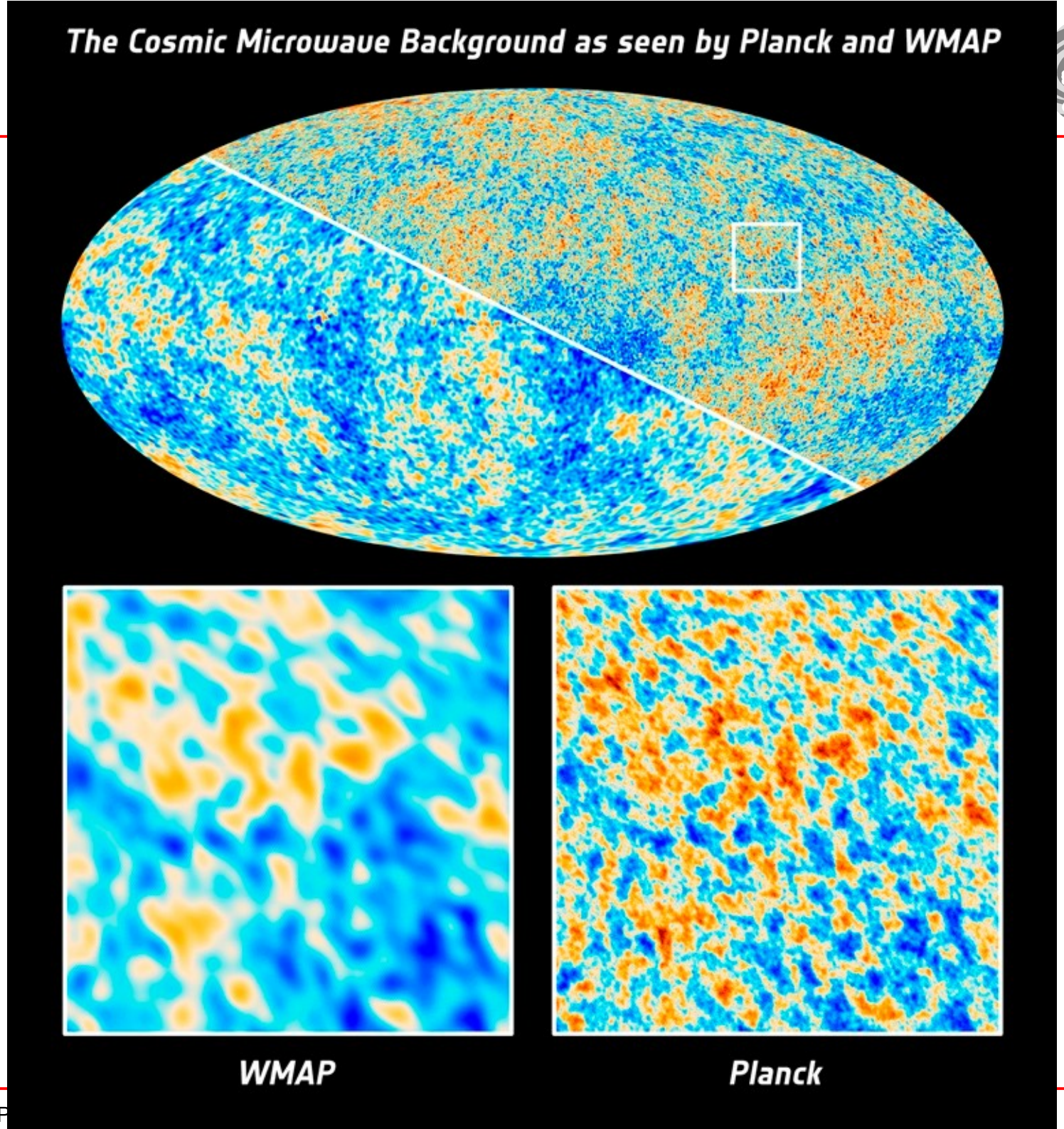
The Cosmic Microwave Background as seen by Planck and WMAP
WMAP
Planck

Planck results - highlights

Angular power spectrum

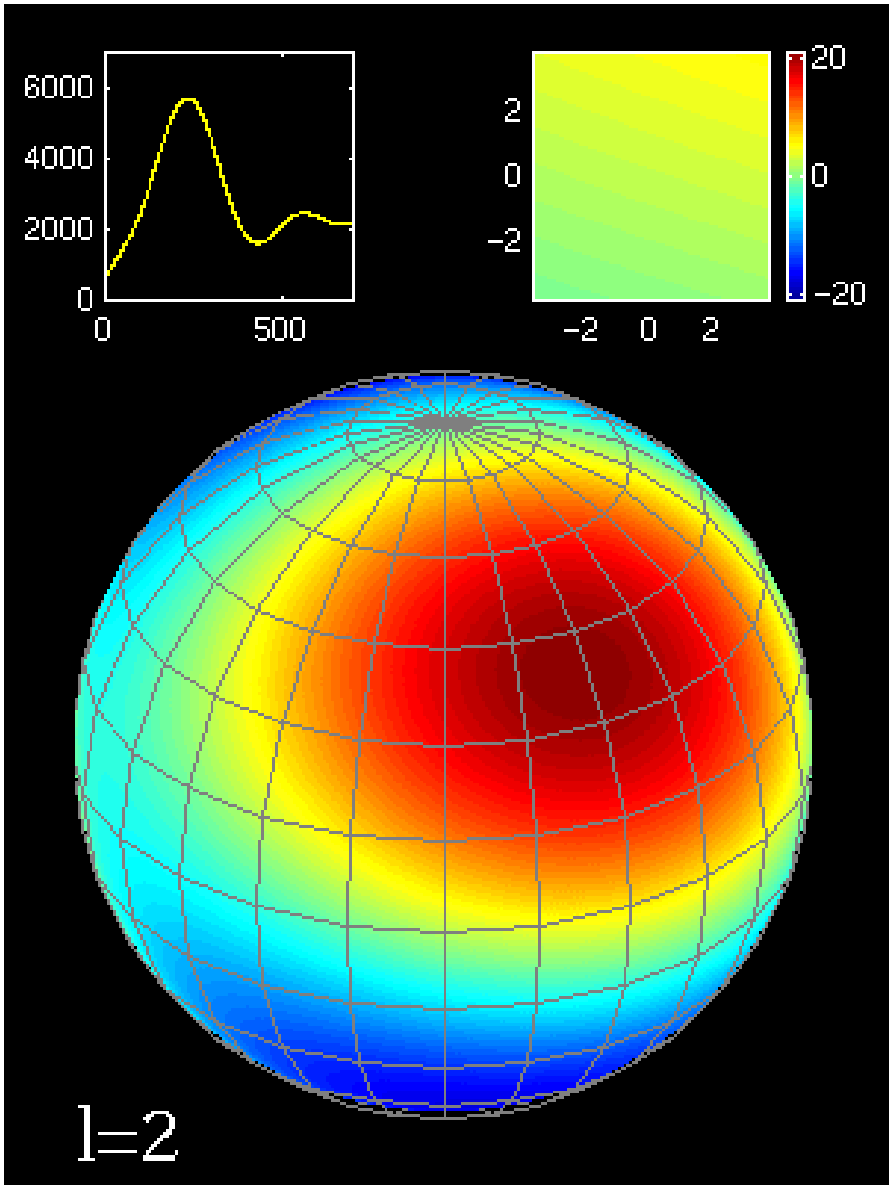

- rms of the signal as a function of the angular scale

Clem Pryke web page

Angular power spectrum

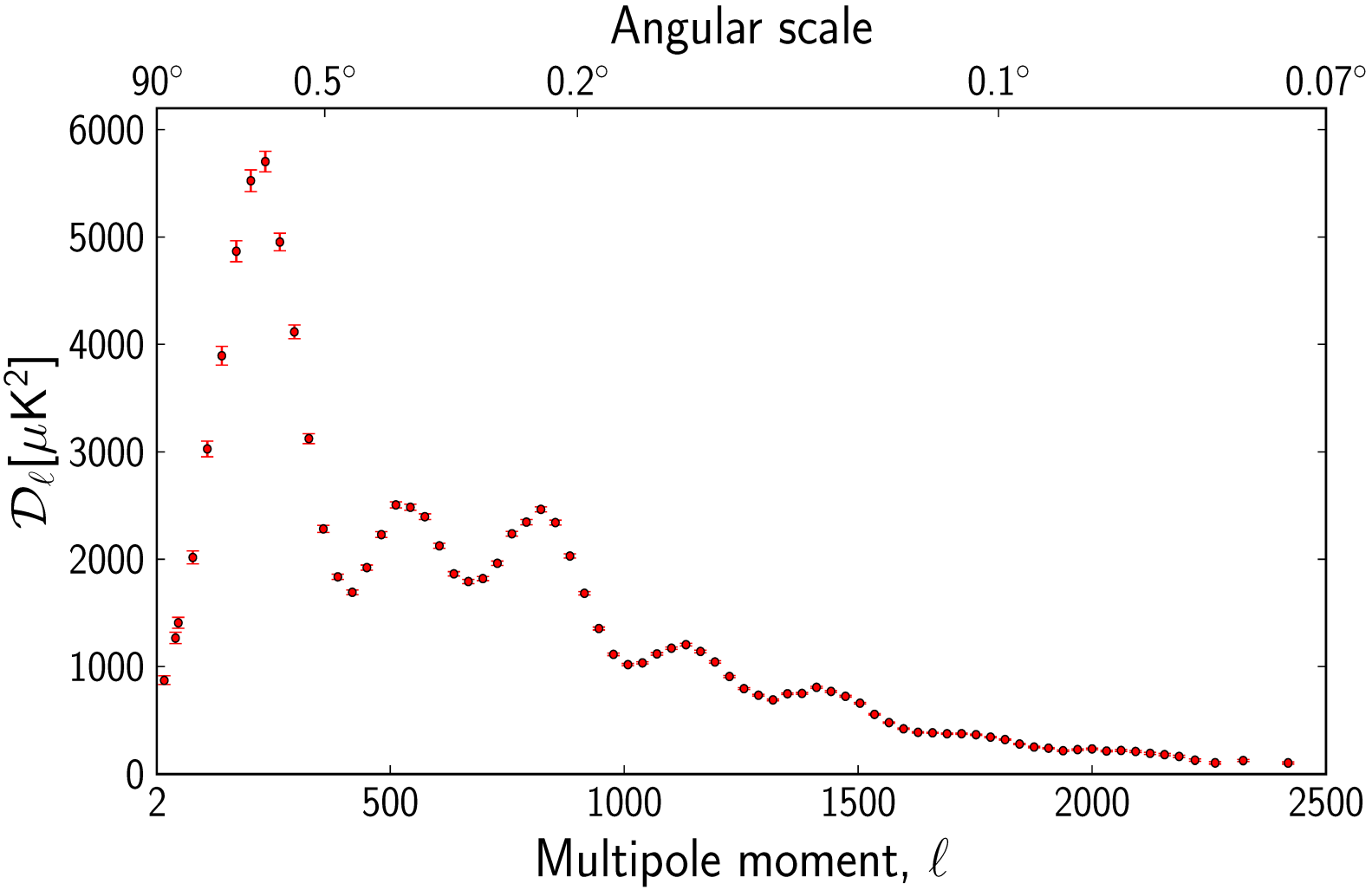

Angular power spectrum

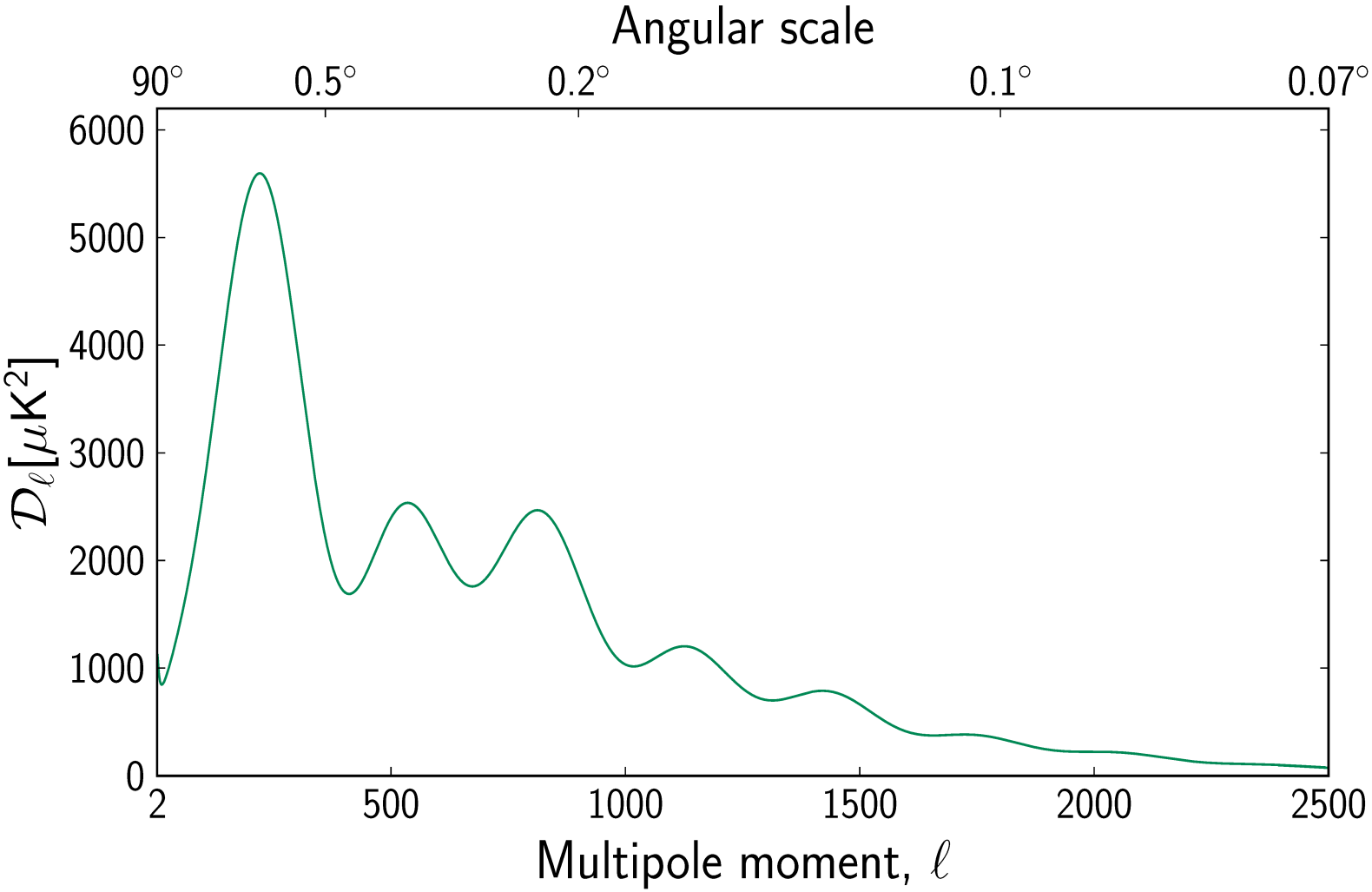

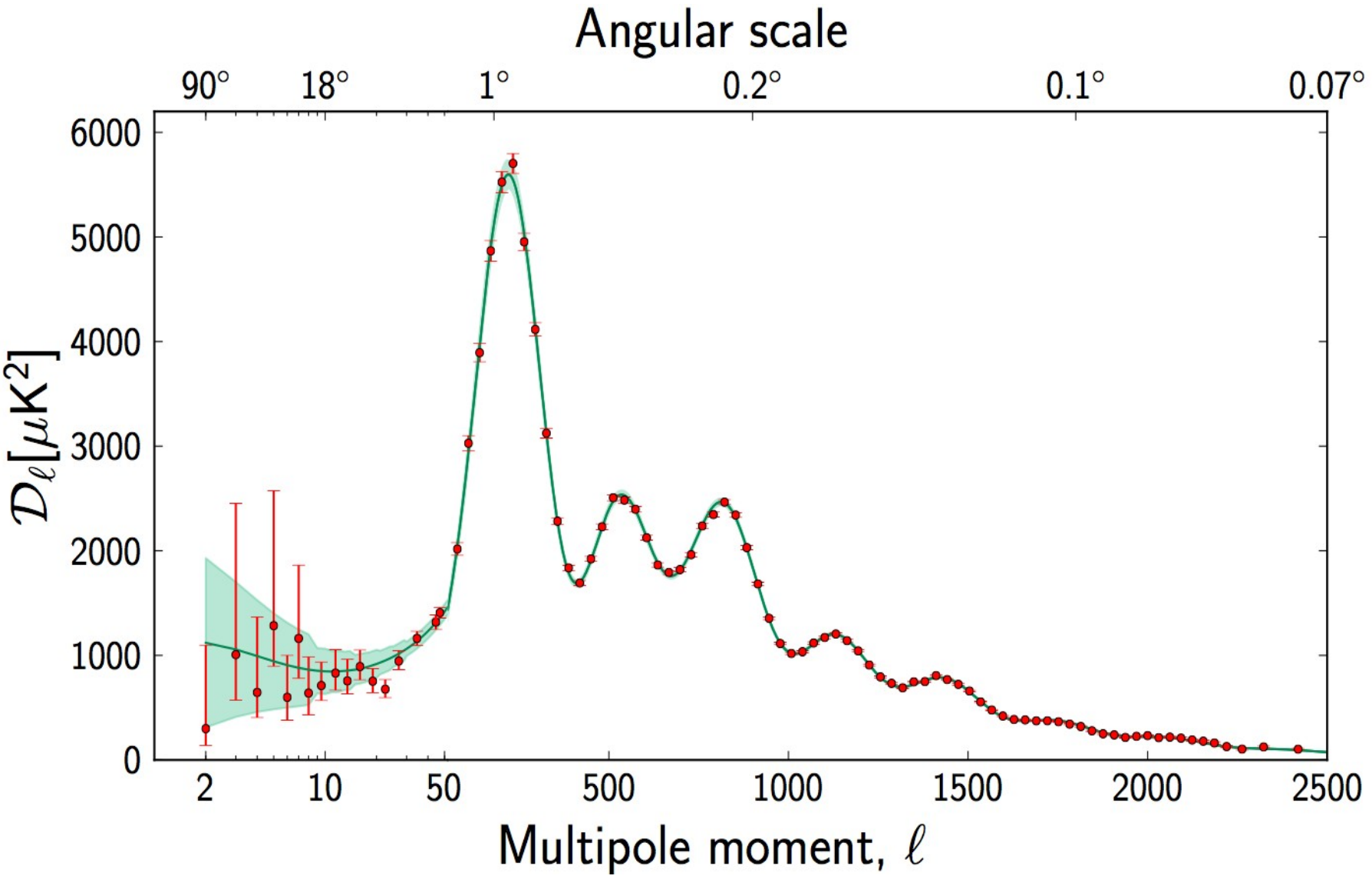
Angular scale
90°
18°
1°
0.2°
0.1°
0.07°
6000
5000
4000
3000
2000
1000
0
$\mathcal{D}_\ell [\mu K^2]$
2
10
50
500
1000
1500
2000
2500
Multipole moment, ℓ

Combined with other experiments

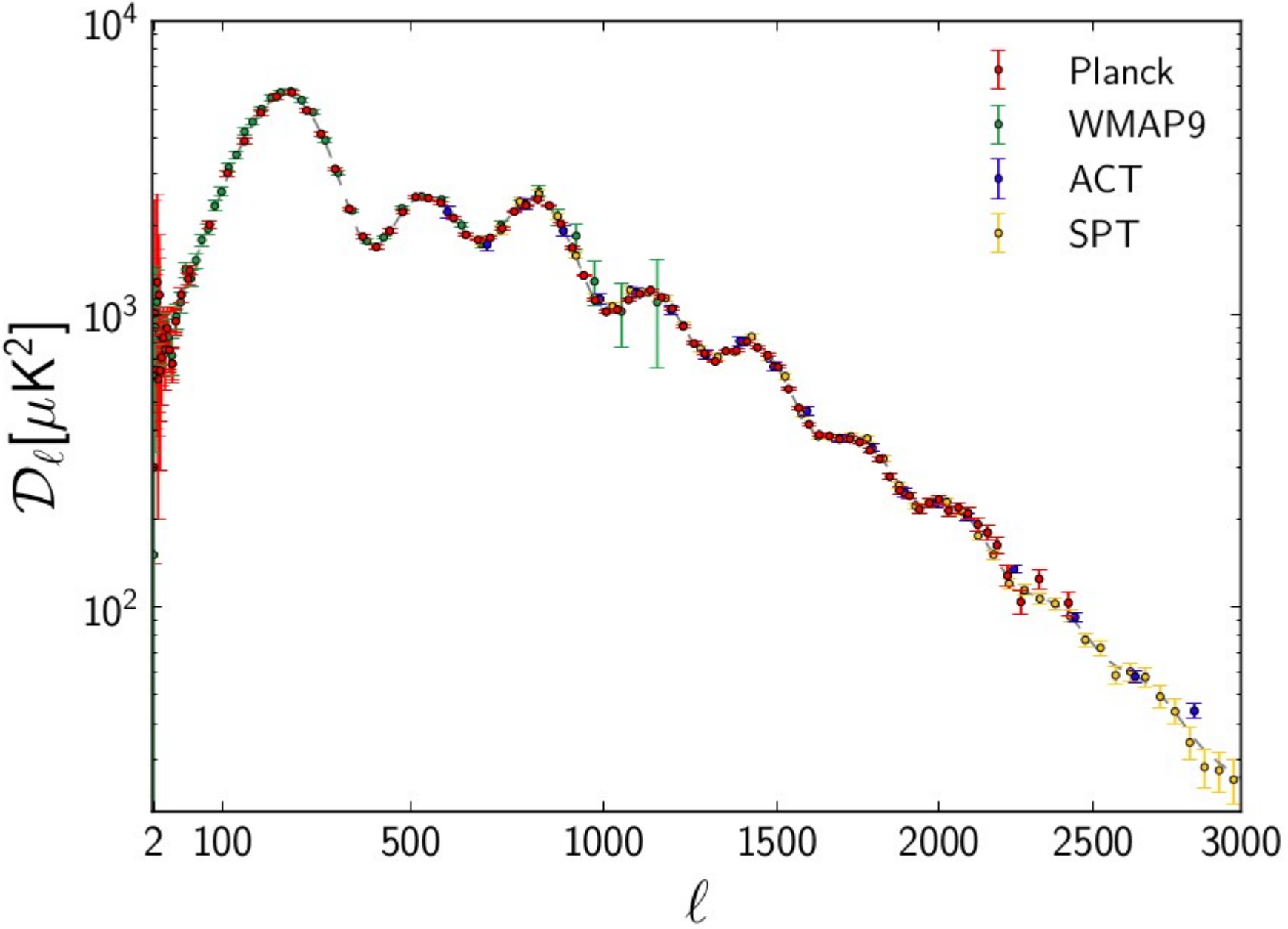

Fig. 25. Measured angular power spectra of *Planck*, WMAP9, ACT, and SPT. The model plotted is *Planck*'s best-fit model including *Planck* temperature, WMAP polarization, ACT, and SPT (the model is labelled [Planck+WP+HighL] in Planck Collaboration XVI (2013)). Error bars include cosmic variance. The horizontal axis is $\ell^{0.8}$.

ΛCDM – 6 parameters model

- Assumed Curvature: 0, flat universe
- **3** parameters to set the dynamic of the universe (based on GR)
  - $\Omega_b h^2$: Baryon density today
  - $\Omega_c h^2$: Cold dark matter density today
  - θ: angle of the sound horizon as seen in the CMB
- **1** parameter to capture the effect of re-ionization of the Universe
  - τ: optical depth = fraction of CMB photon re-scattered
- **2** parameter to describe the primordial fluctuations
  - A_s: amplitude
  - n_s: power law (n_s-1 measured departure from scale invariance)

- Derived parameters
  - Ω_Λ: "Dark Energy" density
  - H_0: Hubble constant = expansion rate today
  - t_0: age of the Universe

ΛCDM – 6 parameters model

Baryon density

CDM density

sound horizon (rad)

reionization opacity

Primordial spectrum

Assumed Curvature: 0
Goodness of fit:
2000 deg. of freedom
Chi2 of 1+-5E-2,
DeltaChi2<1.6 sigma

Parameter	*Planck* (CMB+lensing) Best fit	*Planck* (CMB+lensing) 68 % limits
$\Omega_b h^2$	0.022242	0.02217 ± 0.00033
$\Omega_c h^2$	0.11805	0.1186 ± 0.0031
$100\theta_{MC}$	1.04150	1.04141 ± 0.00067
τ	0.0949	0.089 ± 0.032
n_s	0.9675	0.9635 ± 0.0094
$\ln(10^{10} A_s)$	3.098	3.085 ± 0.057
Ω_Λ	0.6964	0.693 ± 0.019
σ_8	0.8285	0.823 ± 0.018
z_{re}	11.45	$10.8^{+3.1}_{-2.5}$
H_0	68.14	67.9 ± 1.5
Age/Gyr	13.784	13.796 ± 0.058
$100\theta_*$	1.04164	1.04156 ± 0.00066
r_{drag}	147.74	147.70 ± 0.63
$r_{drag}/D_V(0.57)$	0.07207	0.0719 ± 0.0011

Baryonic Acoustic Oscillations

- In early universe plasma Baryon perturbations propagate as sound waves
- After recombination the sound speed drops
- This leave imprinted in the structure distribution some level of correlation
- Observed in the galaxies surveys
- Proportional to baryon density

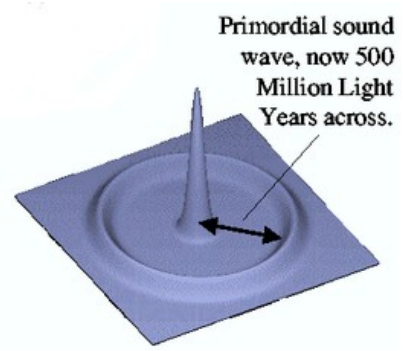

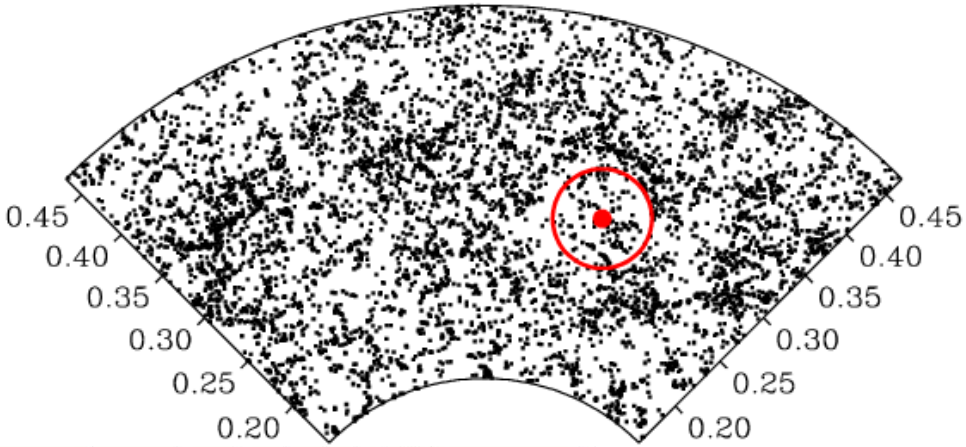

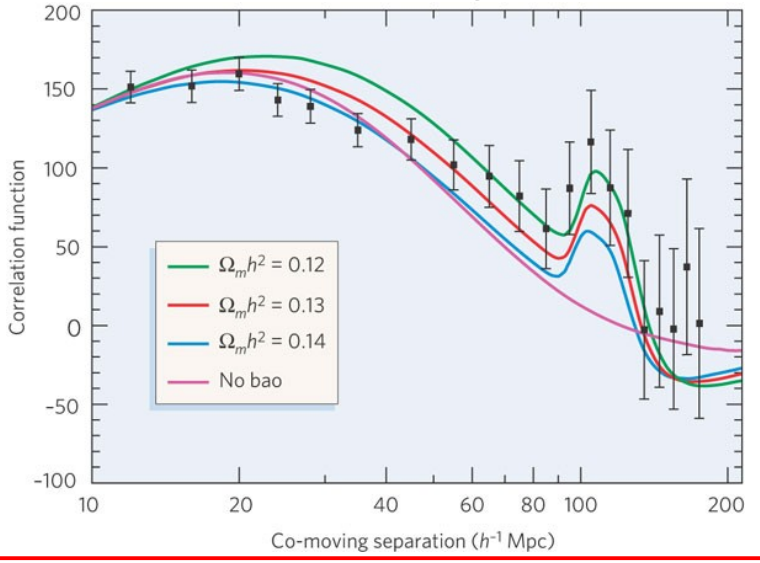

- CMB results and BAO are in agreement
- Data can be combined

ΛCDM – 6 parameters model

Baryon density

CDM density

sound horizon (rad)

reionization opacity

Primordial spectrum

Assumed Curvature: 0
Goodness of fit:
2000 deg. of freedom
Chi2 of 1+-5E-2,
DeltaChi2<1.6 sigma

	Planck (CMB+lensing)		*Planck*+WP+highL+BAO	
Parameter	Best fit	68 % limits	Best fit	68 % limits
$\Omega_b h^2$	0.022242	0.02217 ± 0.00033	0.022161	0.02214 ± 0.00024
$\Omega_c h^2$	0.11805	0.1186 ± 0.0031	0.11889	0.1187 ± 0.0017
$100\theta_{MC}$	1.04150	1.04141 ± 0.00067	1.04148	1.04147 ± 0.00056
τ	0.0949	0.089 ± 0.032	0.0952	0.092 ± 0.013
n_s	0.9675	0.9635 ± 0.0094	0.9611	0.9608 ± 0.0054
$\ln(10^{10} A_s)$	3.098	3.085 ± 0.057	3.0973	3.091 ± 0.025
Ω_Λ	0.6964	0.693 ± 0.019	0.6914	0.692 ± 0.010
σ_8	0.8285	0.823 ± 0.018	0.8288	0.826 ± 0.012
z_{re}	11.45	$10.8^{+3.1}_{-2.5}$	11.52	11.3 ± 1.1
H_0	68.14	67.9 ± 1.5	67.77	67.80 ± 0.77
Age/Gyr	13.784	13.796 ± 0.058	13.7965	13.798 ± 0.037
$100\theta_*$	1.04164	1.04156 ± 0.00066	1.04163	1.04162 ± 0.00056
r_{drag}	147.74	147.70 ± 0.63	147.611	147.68 ± 0.45
$r_{drag}/D_V(0.57)$	0.07207	0.0719 ± 0.0011		

Model extensions

- Curvature
- Neutrino mass
- Neutrino effective number
- Helium primordial abundance
- Slope variation of ns
- Tensor to scalar ratio
- Dark energy equation of state

Planck Collaboration: Cosmological parameters

	Planck+WP		*Planck*+WP+BAO		*Planck*+WP+highL		*Planck*+WP+highL+BAO	
Parameter	Best fit	95% limits	Best fit	95% limits	Best fit	95% limits	Best fit	95% limits
Ω_K	−0.0105	$-0.037^{+0.043}_{-0.049}$	0.0000	$0.0000^{+0.0066}_{-0.0067}$	−0.0111	$-0.042^{+0.043}_{-0.048}$	0.0009	$-0.0005^{+0.0065}_{-0.0066}$
Σm_ν [eV]	0.022	< 0.933	0.002	< 0.247	0.023	< 0.663	0.000	< 0.230
$N_{\rm eff}$	3.08	$3.51^{+0.80}_{-0.74}$	3.08	$3.40^{+0.59}_{-0.57}$	3.23	$3.36^{+0.68}_{-0.64}$	3.22	$3.30^{+0.54}_{-0.51}$
$Y_{\rm P}$	0.2583	$0.283^{+0.045}_{-0.048}$	0.2736	$0.283^{+0.043}_{-0.045}$	0.2612	$0.266^{+0.040}_{-0.042}$	0.2615	$0.267^{+0.038}_{-0.040}$
$dn_s/d\ln k$	−0.0090	$-0.013^{+0.018}_{-0.018}$	−0.0102	$-0.013^{+0.018}_{-0.018}$	−0.0106	$-0.015^{+0.017}_{-0.017}$	−0.0103	$-0.014^{+0.016}_{-0.017}$
$r_{0.002}$	0.000	< 0.120	0.000	< 0.122	0.000	< 0.108	0.000	< 0.111
w	−1.20	$-1.49^{+0.65}_{-0.57}$	−1.076	$-1.13^{+0.24}_{-0.25}$	−1.20	$-1.51^{+0.62}_{-0.53}$	−1.109	$-1.13^{+0.23}_{-0.25}$

Table 10. Constraints on one-parameter extensions to the base ΛCDM model. Data combinations all include *Planck* combined with *WMAP* polarization, and results are shown for combinations with high-ℓ CMB data and BAO. Note that we quote 95% limits here.

Cosmic recipe

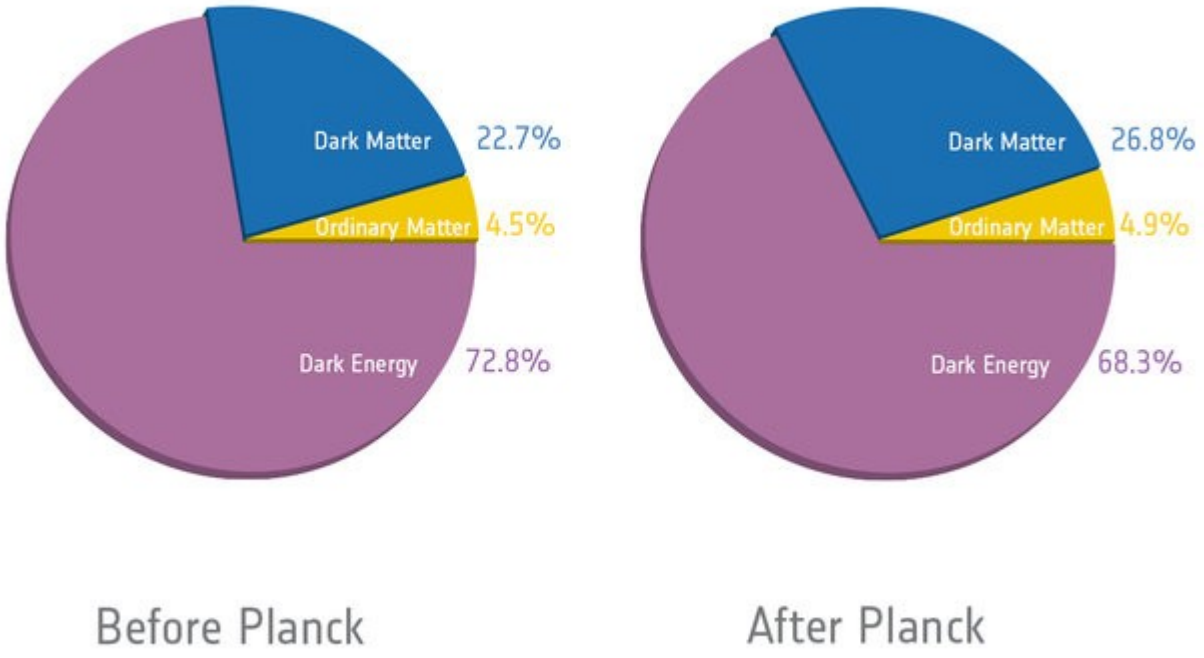

Dark matter evidence at ~44σ

Information compression

- Time domain (1 year): $5 \cdot 10^{11}$ data
- Maps: $4 \cdot 10^{9}$ data
- CMB map: $5 \cdot 10^{7}$ data
- Power spectrum: 2500 data
- Cosmological parameters: 6 numbers

  + calibration parameters (many)

  + foregrounds parameters (13)

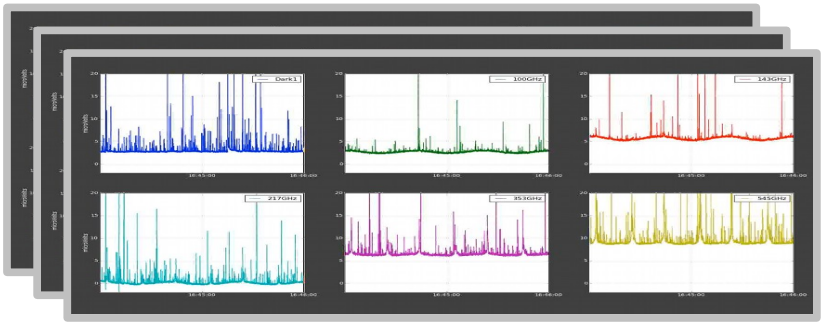

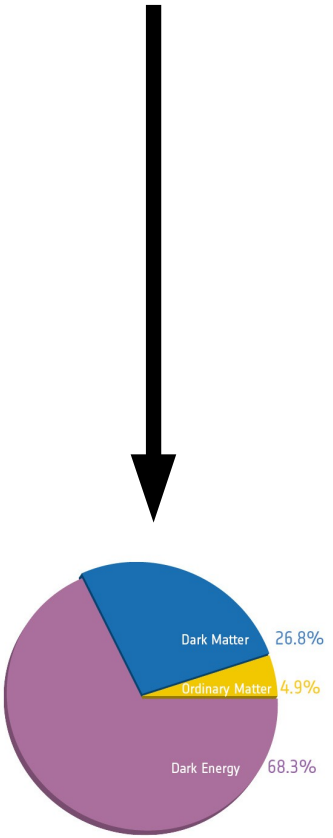

Gravitational lensing with Planck

Lensing of the CMB

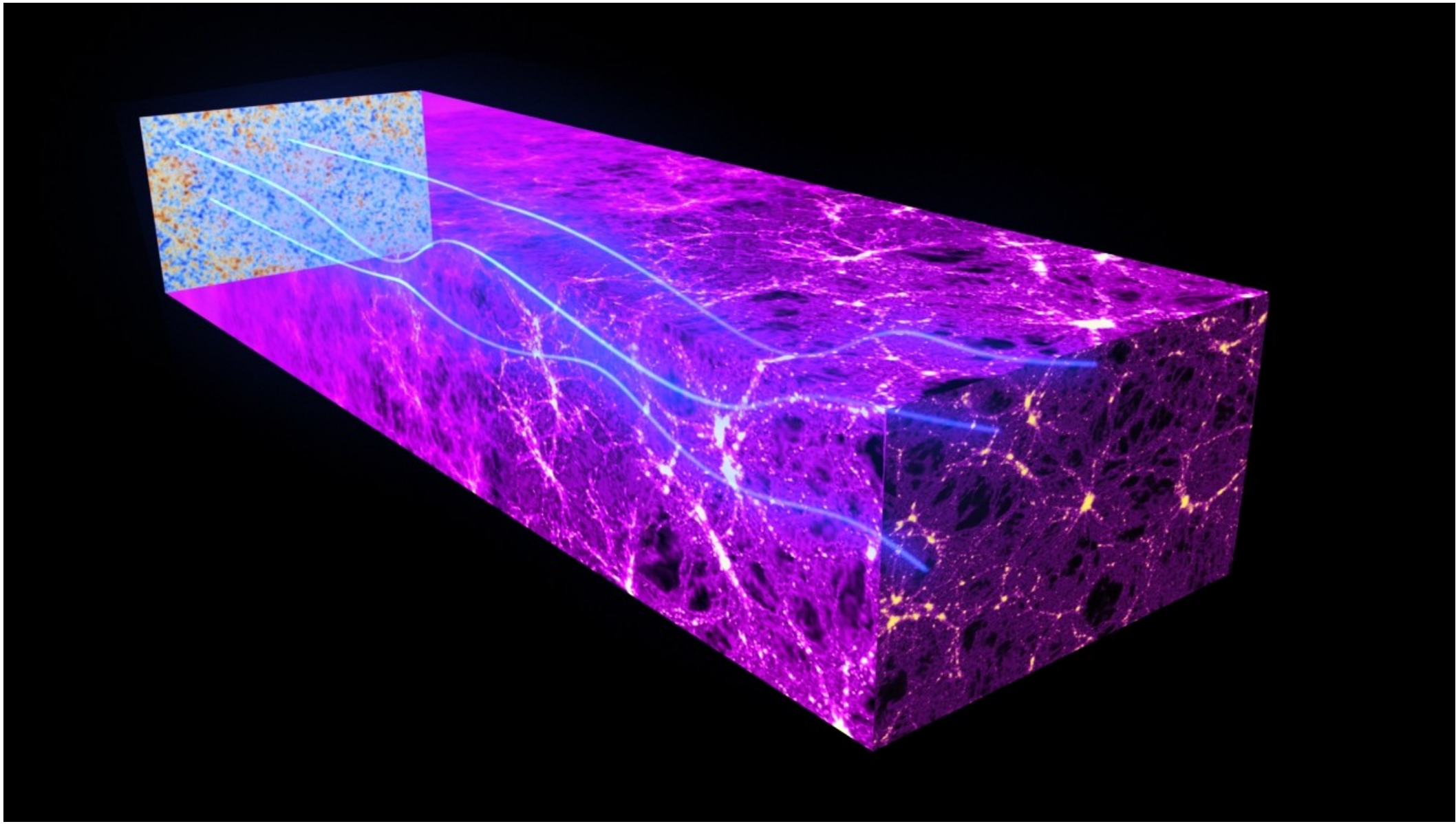

Lensing of the CMB

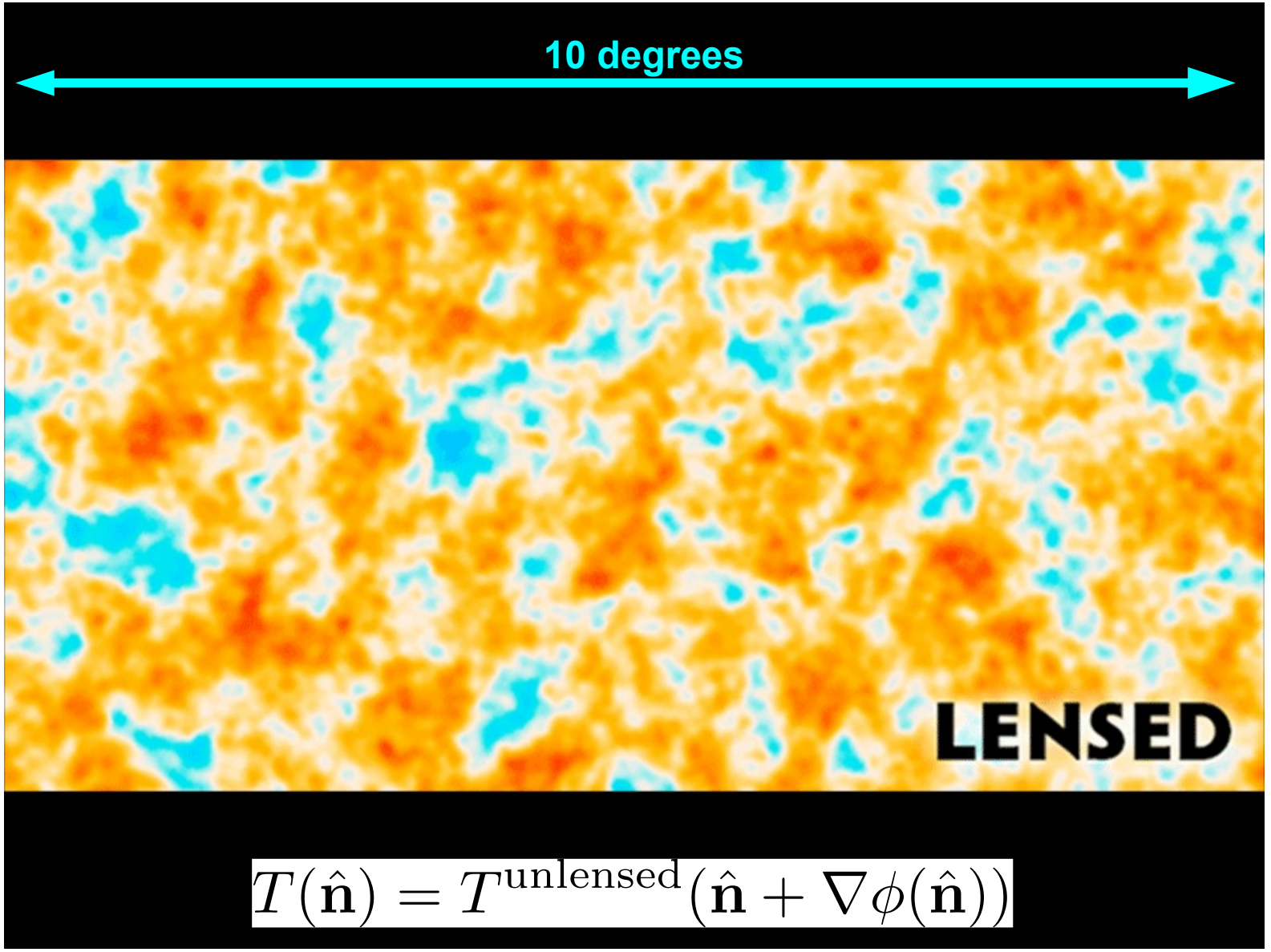

Deflection 2'.5

Coherence 2 deg

Lensing of the CMB

- Measuring the gravitational lensing of the CMB radiation, it is possible to map the distribution of matter in the universe
  - Related <T grad(T)> correlation
  - Obtained with a statistical method based on the 4-points correlation function (tri-spectrum)
  - It reveals the gradient of the projected gravitational potential along the line of sight
  - The underlying gravitational potential can be reconstructed
  - This can be used to
    - check model consistency (predicted/measured power spectrum)
    - Improve cosmological parameters estimation adding the lensing data

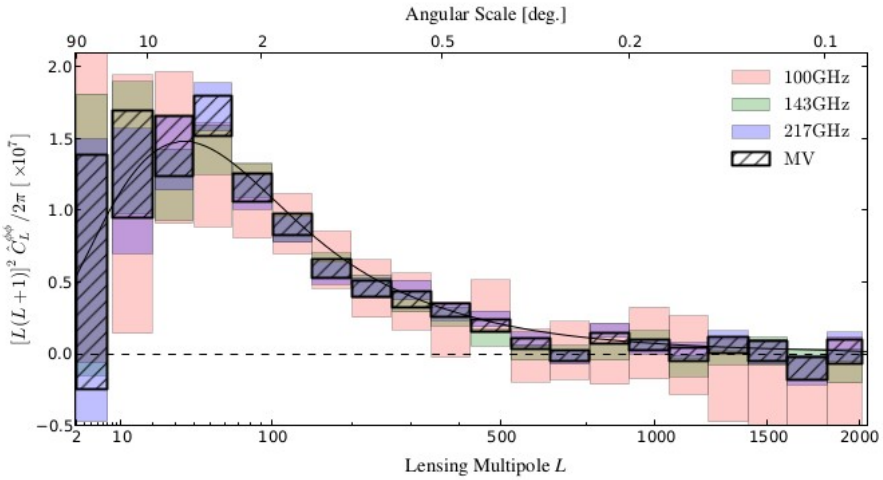

Fig. 10. Lensing potential power spectrum estimates based on the individual 100, 143, and 217 GHz sky maps, as well our fiducial minimum-variance (MV) reconstruction which forms the basis for the *Planck* lensing likelihood. The black line is for the best-fit ΛCDM model of Planck Collaboration XVI (2013).

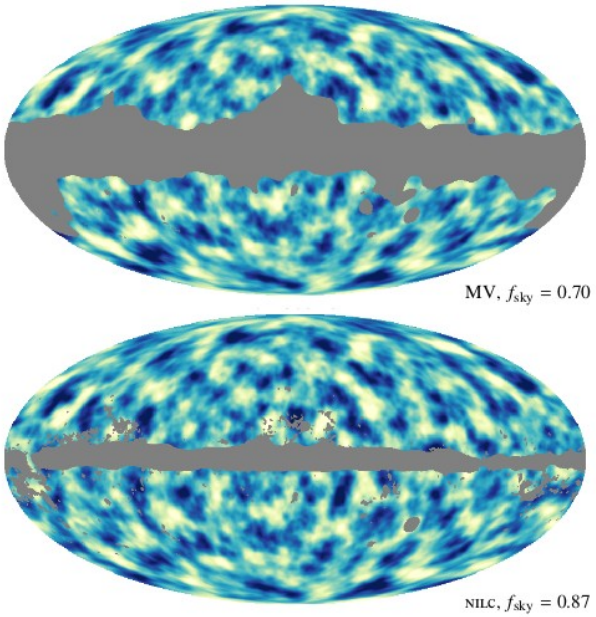

Fig. 19. Wiener-filtered potential maps in Galactic coordinates, as in Fig. 8, plotted here in Mollweide projection. Top is the MV reconstruction, bottom is an extended reconstruction on the NILC component-separated map.

Lensing of the CMB

Planck 2013 results. XVII. Gravitational lensing by large-scale structure

http://arxiv.org/abs/1303.5077

relatively low redshift catalogs. From the perspective of cross-correlation, the *Planck* lensing potential represents a mass survey with a well understood redshift kernel over the full-sky, and we anticipate that correlations with it will prove useful as a direct probe of the correlation between luminous and dark matter.

Dark matter annihilation with Planck

Dark matter annihilation

- Dark matter annihilation in **early universe (z>1000)** plasma can inject energy, and modify the recombination history
- Single parameter p_ann

The rate of energy release, dE/dt, per unit volume by a relic annihilating DM particle is given by

$$\frac{dE}{dt}(z) = 2\, g\, \rho_c^2 c^2 \Omega_c^2 (1+z)^6 p_{\rm ann}(z), \qquad (97)$$

where $p_{\rm ann}$ is, in principle, a function of redshift z, defined as

$$p_{\rm ann}(z) \equiv f(z) \frac{\langle \sigma v \rangle}{m_\chi}, \qquad (98)$$

where $\langle \sigma v \rangle$ is the thermally averaged annihilation cross-section, m_χ is the mass of the DM particle, ρ_c is the critical density of the Universe today, g is a degeneracy factor equal to 1/2 for Majorana particles and 1/4 for Dirac particles (in the following, constraints will refer to Majorana particles), and the parameter $f(z)$ indicates the fraction of energy which is absorbed *overall* by the gas at redshift z. We note that the presence of the brackets in $\langle \sigma v \rangle$ denote a thermal average over the velocity distribution of particles.

$$p_{\rm ann} < 3.1\times10^{-6}\ {\rm m^3\ s^{-1}\ kg^{-1}} \quad (95\%;\ \textit{Planck}{+}{\rm lensing}{+}{\rm WP})$$

Our results are consistent with previous work and show no evidence for DM annihilation. Future release of *Planck* polarization data will help to break the degeneracies which currently limit the accuracy of the constraints presented here.

Galactic Haze – Planck

- 30-44 GHz (previously detected in WMAP)
- Synchrotron radiation, with quite energetic electrons in the galactic center

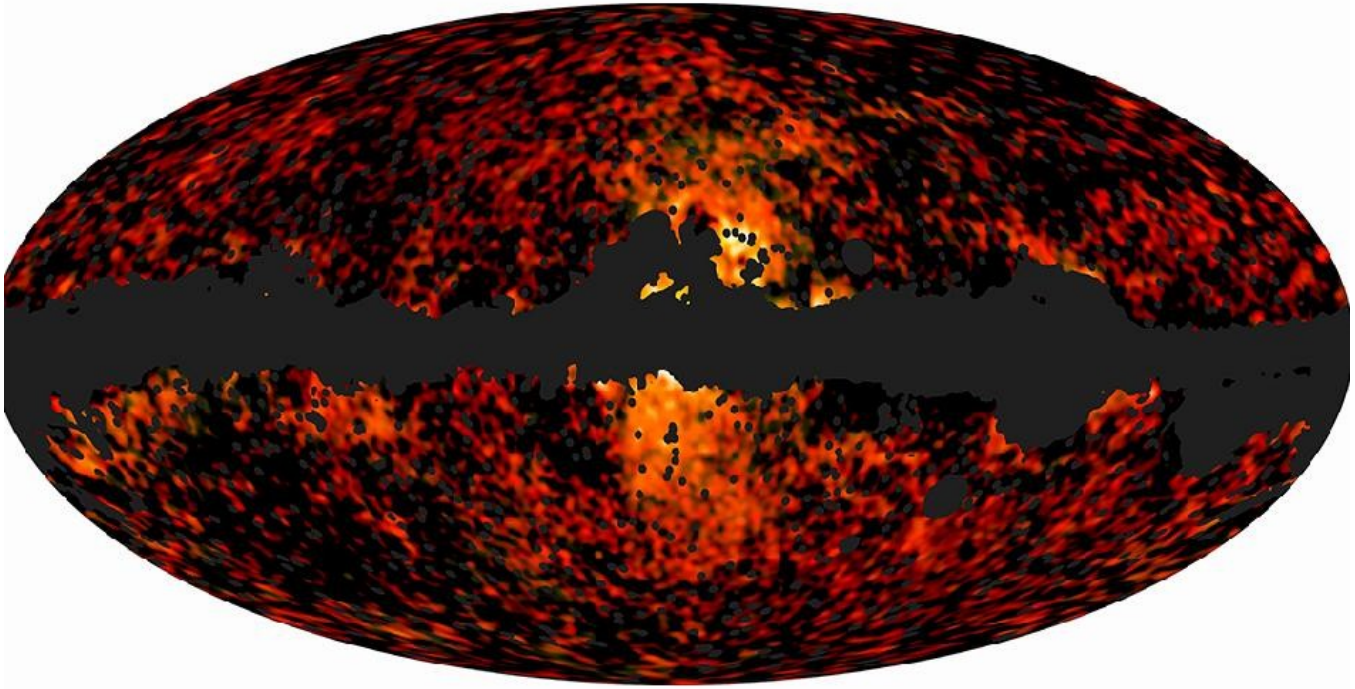

Galactic Haze – Planck + FERMI

- Fermi at 10-100 GeV, superimposed to Planck
- Several hypotheses, among which, energy injection by dark matter annihilation

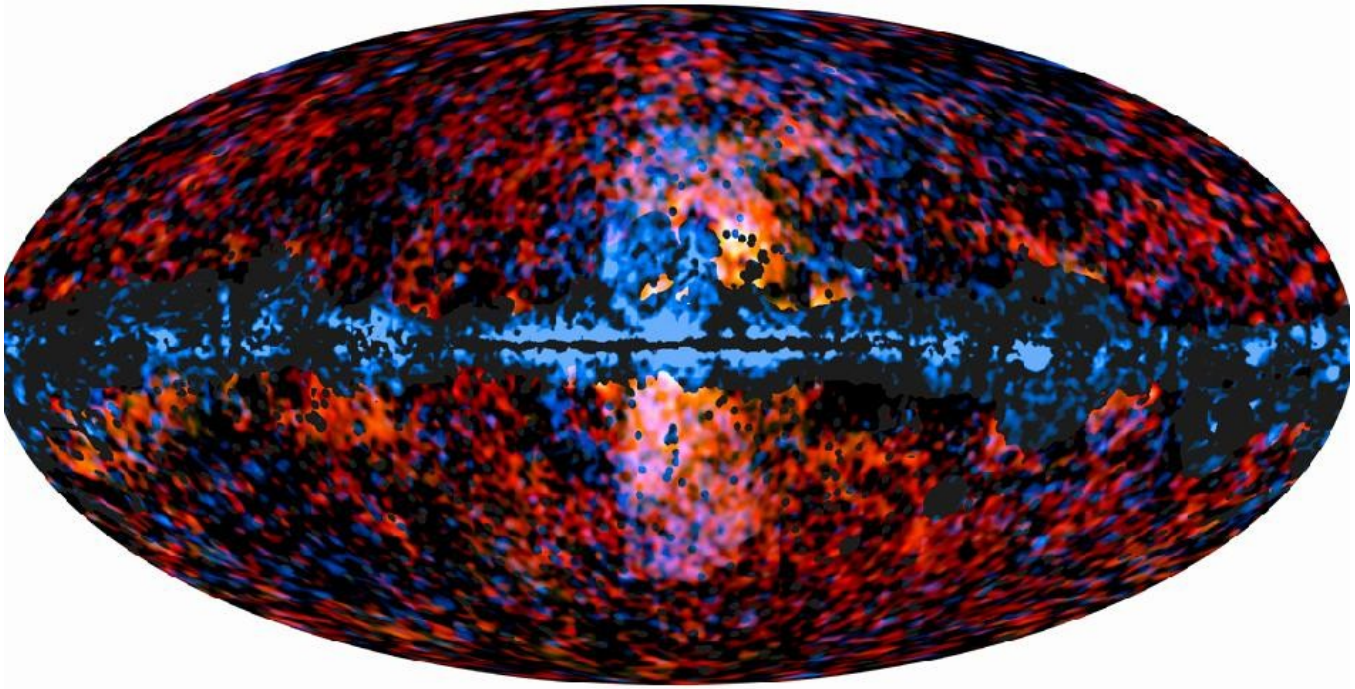

CSIRO telescope

- 2.3 GHz
- "Our data indicate that the process of gas accretion onto the Galactic nucleus inescapably involves **star formation** which, in turn, energizes an outflow."

compatible with no dark matter annihilation

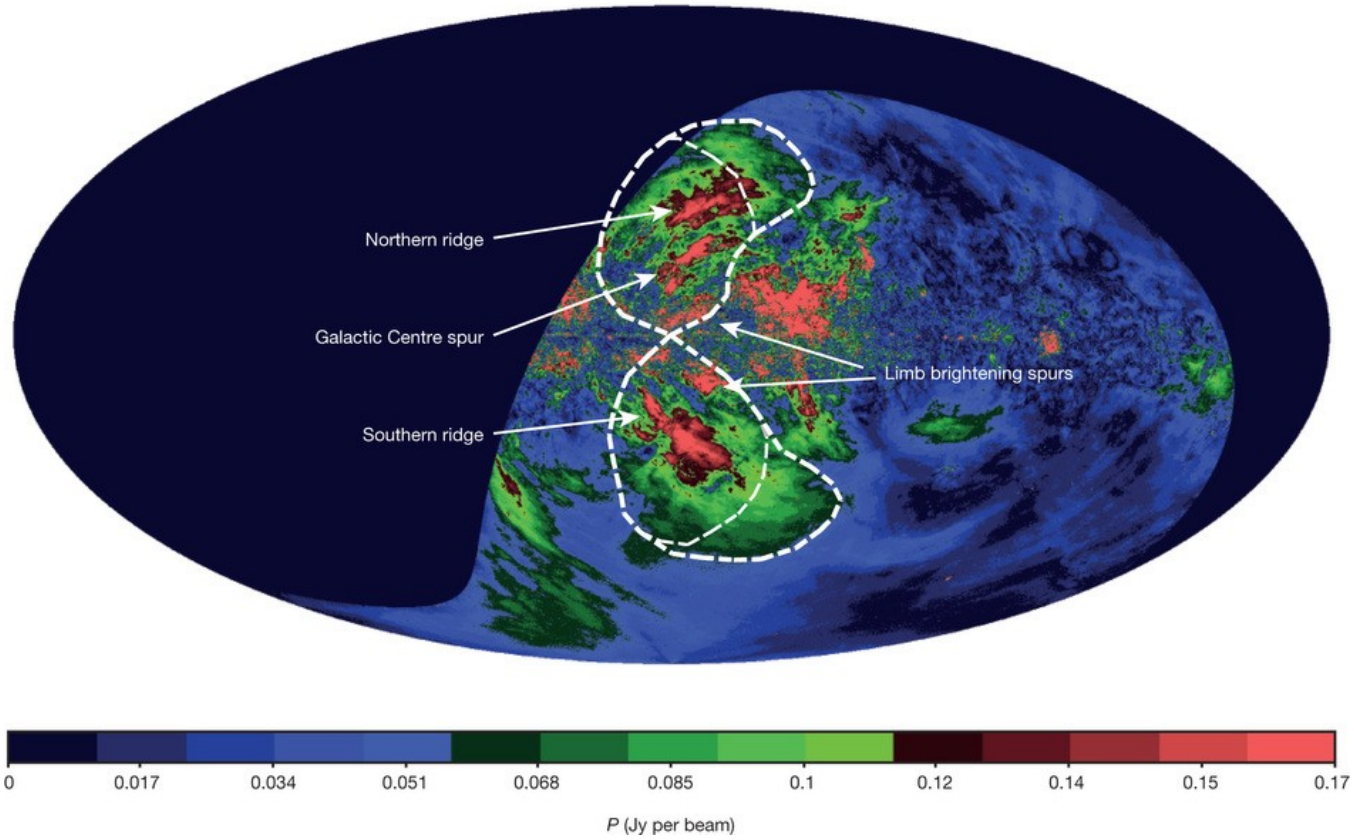

E. Carretti et al. Nature, Volume 493, Issue 7430, pp. 66-69 (2013)

CMB polarization

CMB polarization

- Thomson scattering can polarize incoming radiation

$$\frac{d\sigma}{d\Omega} = \frac{3\sigma_T}{8\pi}|\hat{\epsilon}\cdot\hat{\epsilon}'|^2$$

  - Incoming radiation must have quadrupolar asymmetry

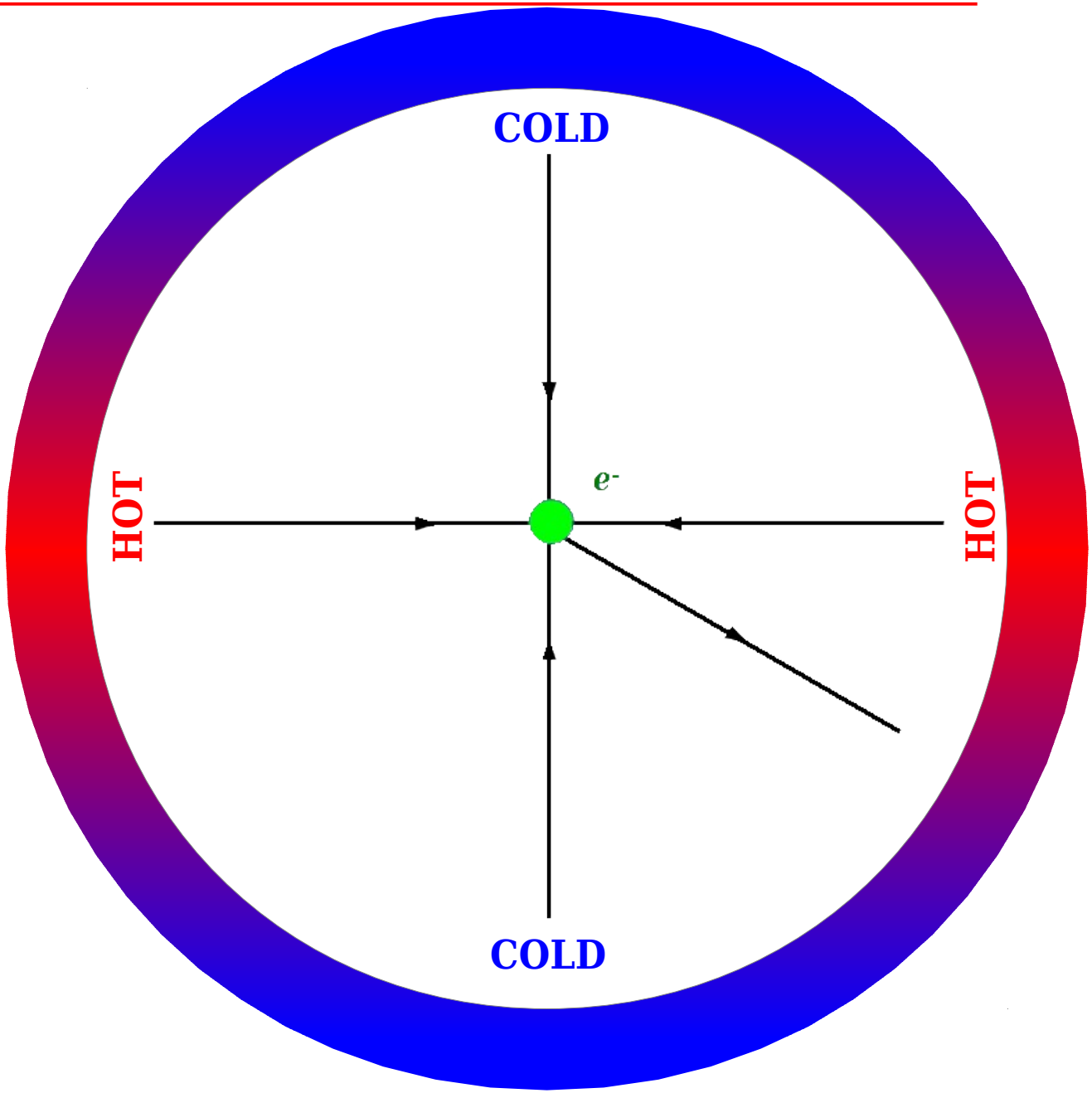

CMB polarization

- Plasma accelerated flows generate quadrupolar asymmetry

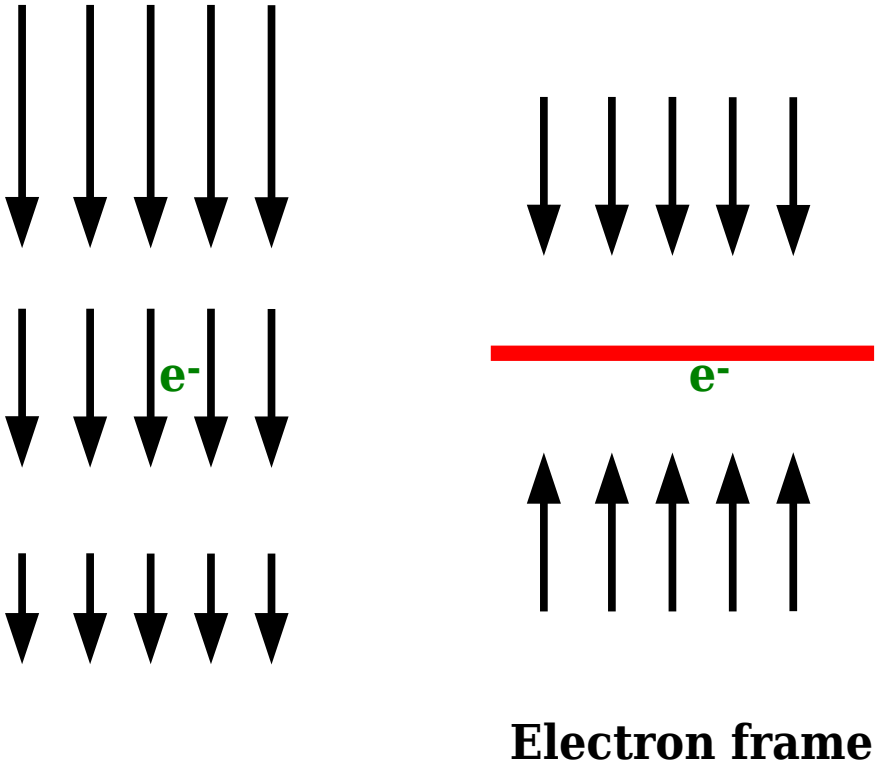

- Gravitational waves stretch space, causing red-shift and blue-shift

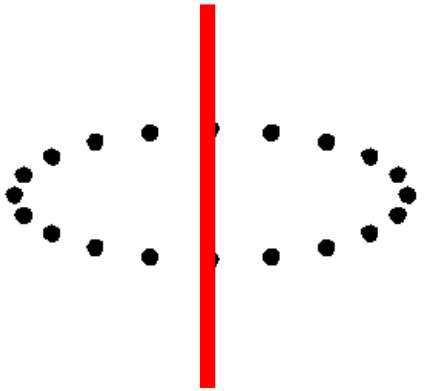

Polarization – E and B modes

- CMB polarization pattern can be decomposed in two “modes” with different symmetry properties
  - ***E*** is generated by a polarization with vector properties (as the Electric field)
  - ***B*** is generated by a polarization with pseudo-vector properties (as the Magnetic field)
    - Sign flip under a reflection

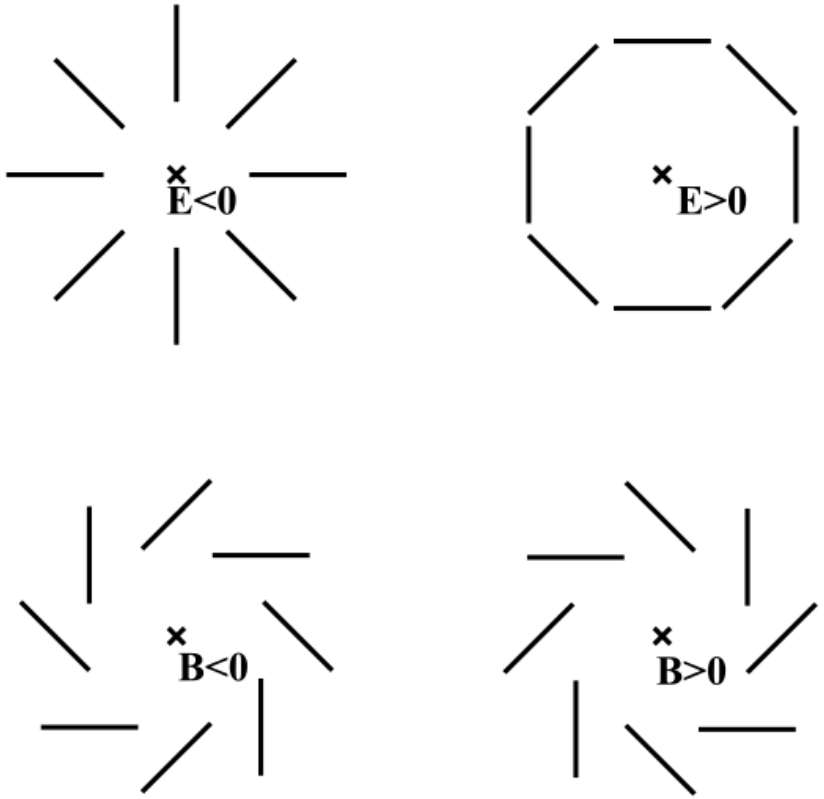

Polarization – B modes

- Only gravitational waves in early universe can generate mode *B* polarization
  - The **CMB polarization is an antenna for gravitational waves** in the early universe
  - Detection of B-mode polarization is the objective of next generation CMB experiments
  - It can shed light on the inflation mechanisms and energy

E-mode from a gravitational wave

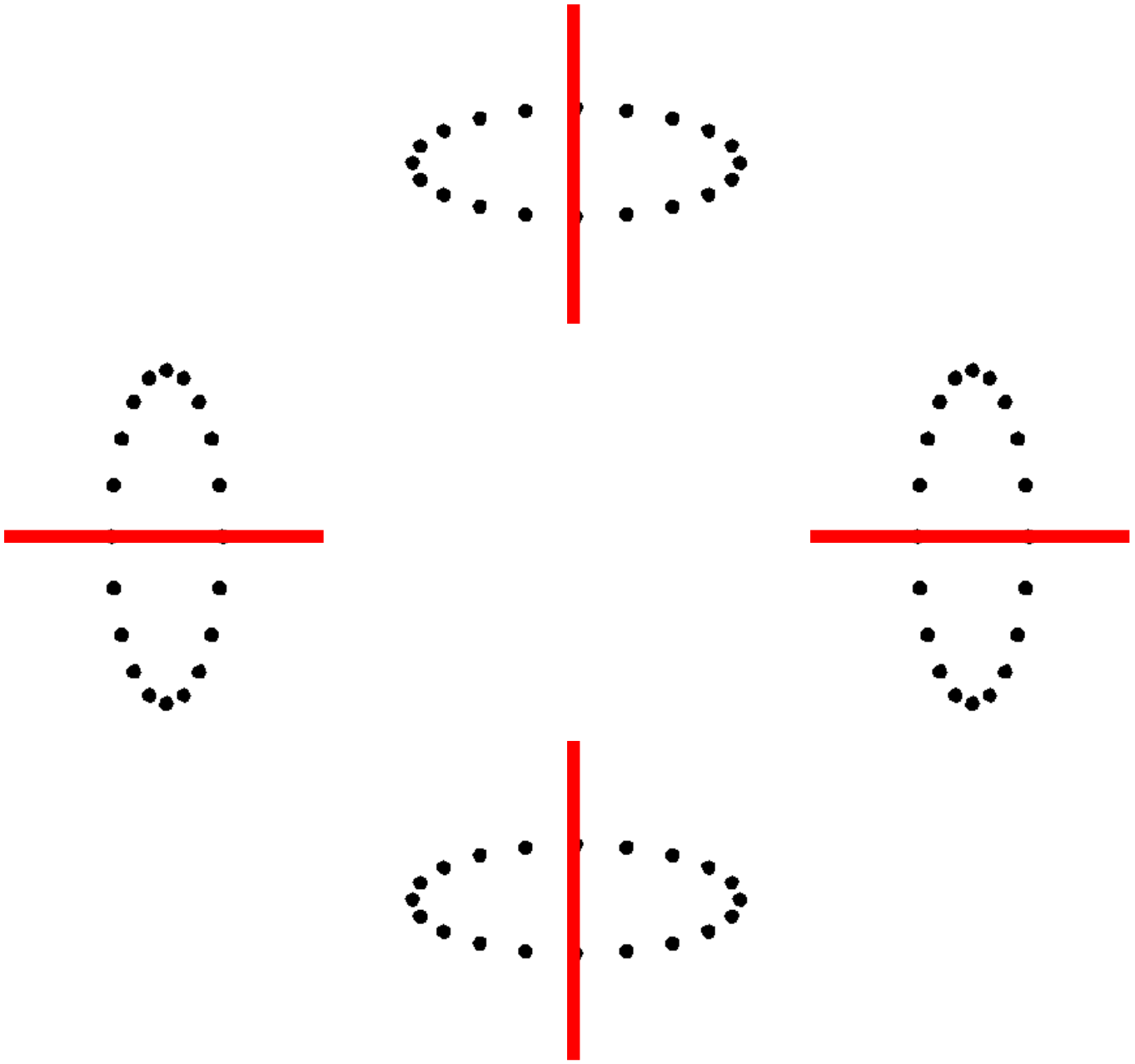

B-mode from a gravitational wave

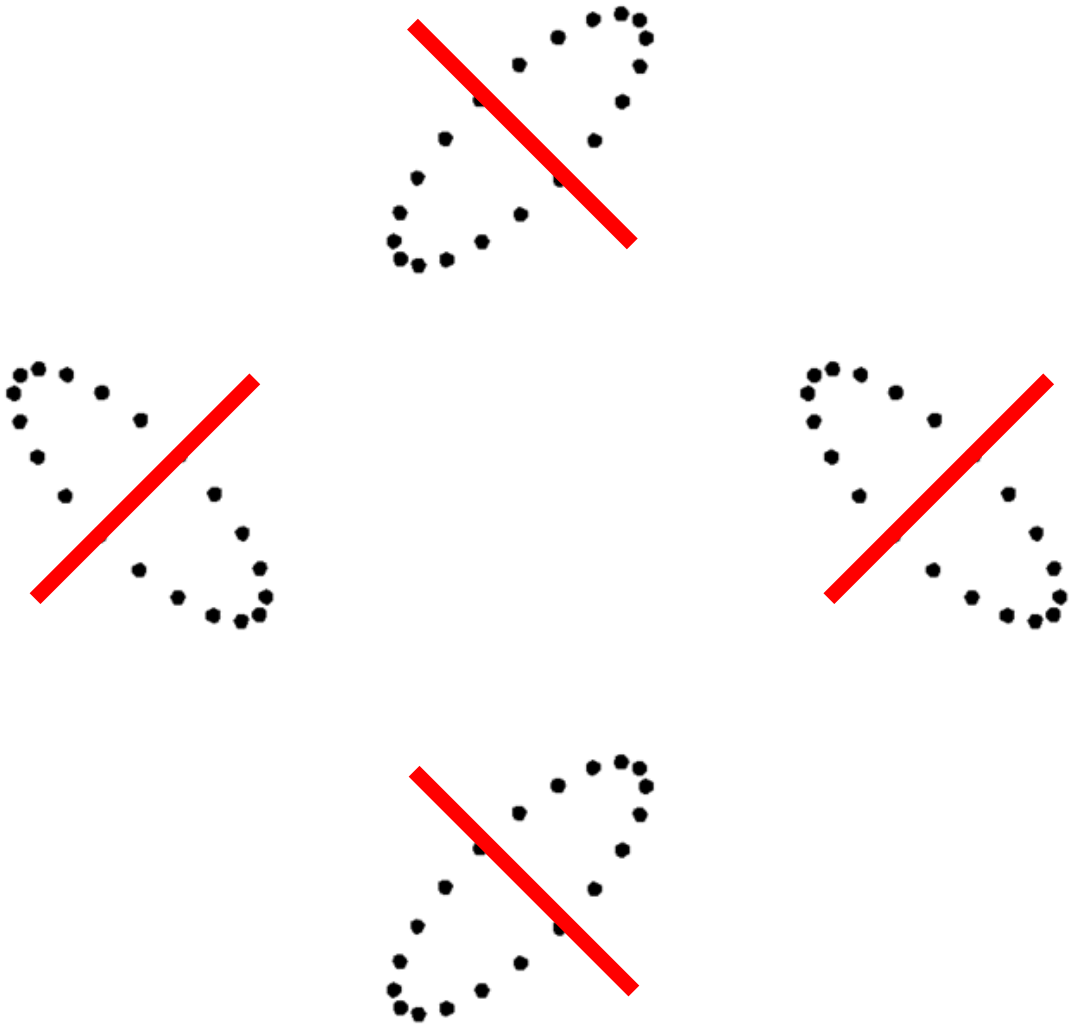

B-modes and inflation

- Scalar perturbations, in linear regime, can't produce vorticity
- Scalar perturbations only produce ***E***-mode polarization
- The presence of gravitational waves in the early universe is an effect of the inflation
  - Measuring ***B***-mode polarization will shed light on the inflation

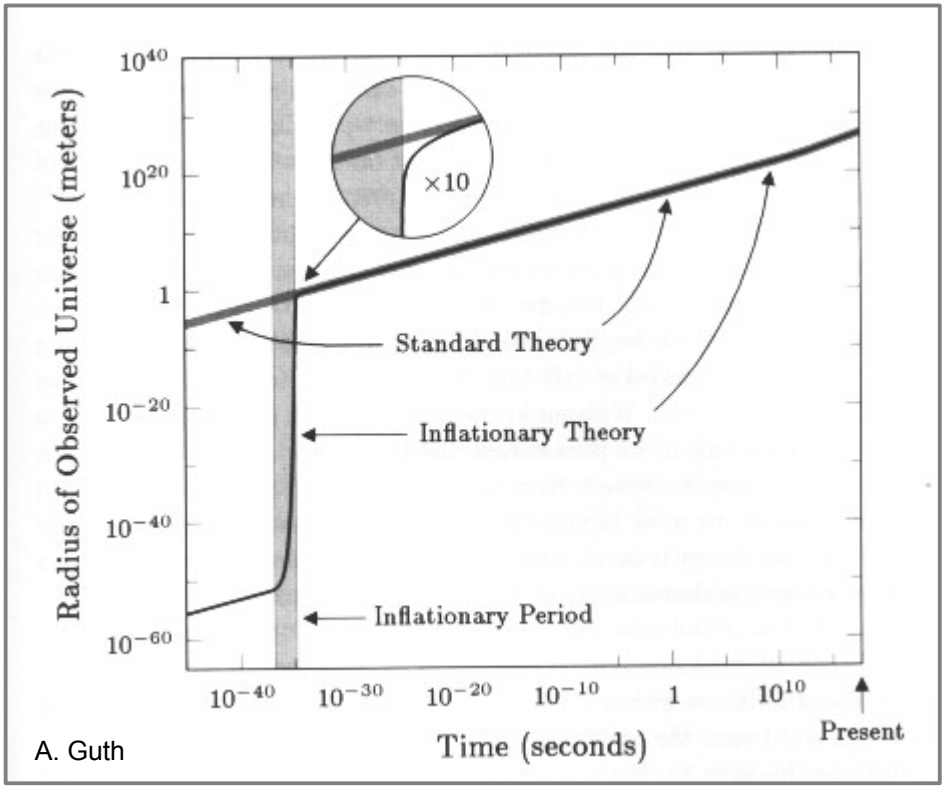

A. Guth

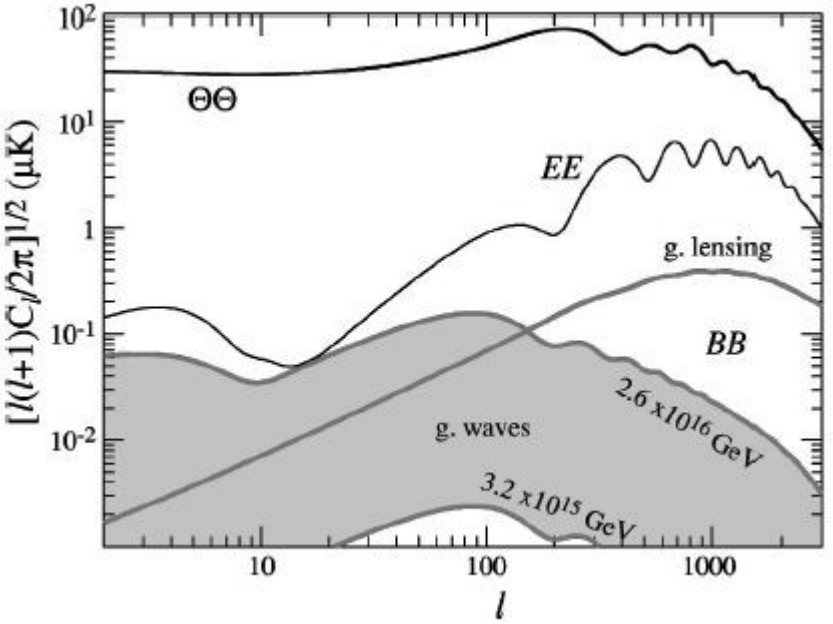

$$\left[\ell(\ell+1)C_\ell^{BB}\right]^{1/2} = 0.024(E_{\rm inf}/10^{16}{\rm GeV})^2\mu{\rm K}$$

W. Hu et al. 2003

Planck polarization

- Planck is designed to measure CMB polarization too
- For this release, polarization is used presented only as consistency tests
  - Results illustrate a remarkable concordance
  - Polarization data is still affected by systematic effects at small multipoles

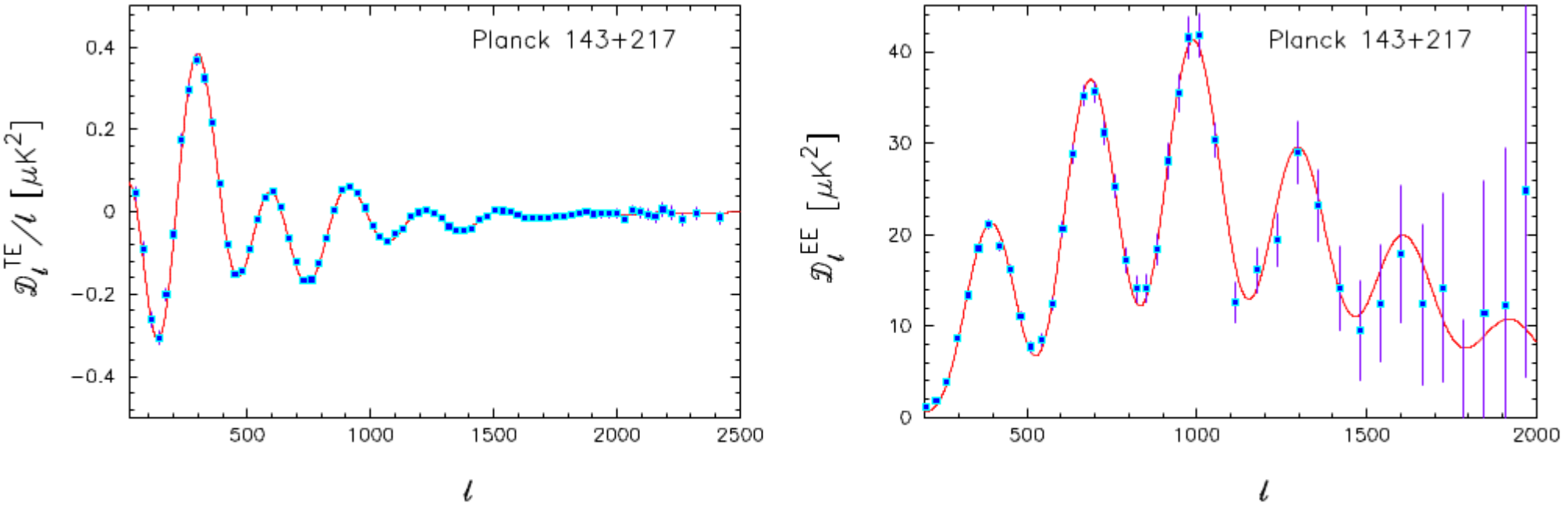

Fig. 11. *Planck TE* (left) and *EE* spectra (right) computed as described in the text. The red lines show the polarization spectra from the base ΛCDM *Planck*+WP+highL model, *which is fitted to the TT data only*.

Lensing induced B-modes

- Gravitational lensing can distort E-mode polarization into B-mode polarization
- We can estimate a template of B-mode lensing polarization map from:
  - E-mode map
  - Gravitational potential map
- We can then cross-correlate this template map with the measured polarization map
  - The correlation part is an estimation of the lensing B-modes
  - Done with South-Pole-Telescope data in combination with Herschel data
  - Can be done with Planck polarization data
- Not the “primordial B-mode” yet

Planck cosmology – Summary

From an analysis of an extensive grid of models, we find no strong evidence to favour any extension to the base ΛCDM cosmology, either from the CMB temperature power spectrum alone, or in combination with the Planck lensing power spectrum and other astrophysical data sets.

We find the following notable results using CMB data alone:

- The deviation of the scalar spectral index from unity is robust to the addition of tensor modes and to changes in the matter content of the Universe. For example, adding a tensor component we find $n_s = 0.9600 \pm 0.0072$, a $5.5\,\sigma$ departure from $n_s = 1$.
- A 95% upper limit on the tensor-to-scalar ratio of $r_{0.002} < 0.11$. The combined contraints on n_s and $r_{0.002}$ are on the borderline of compatibility with single-field inflation with a quadratic potential (Fig. 23).
- A 95% upper limit on the summed neutrino mass of $\sum m_\nu < 0.66\,\mathrm{eV}$.
- A determination of the effective number of neutrino-like relativistic degrees of freedom of $N_{\mathrm{eff}} = 3.36 \pm 0.34$, compatible with the standard value of 3.046.
- The results from *Planck* are consistent with the results of standard big bang nucleosynthesis. In fact, combining the CMB data with the most recent results on the deuterium abundance, leads to the constraint $N_{\mathrm{eff}} = 3.02 \pm 0.27$, again compatible with the standard value of 3.046.
- New limits on a possible variation of the fine-structure constant, dark matter annihilation and primordial magnetic fields.

Next generation CMB experiments

Quest for primordial B-mode

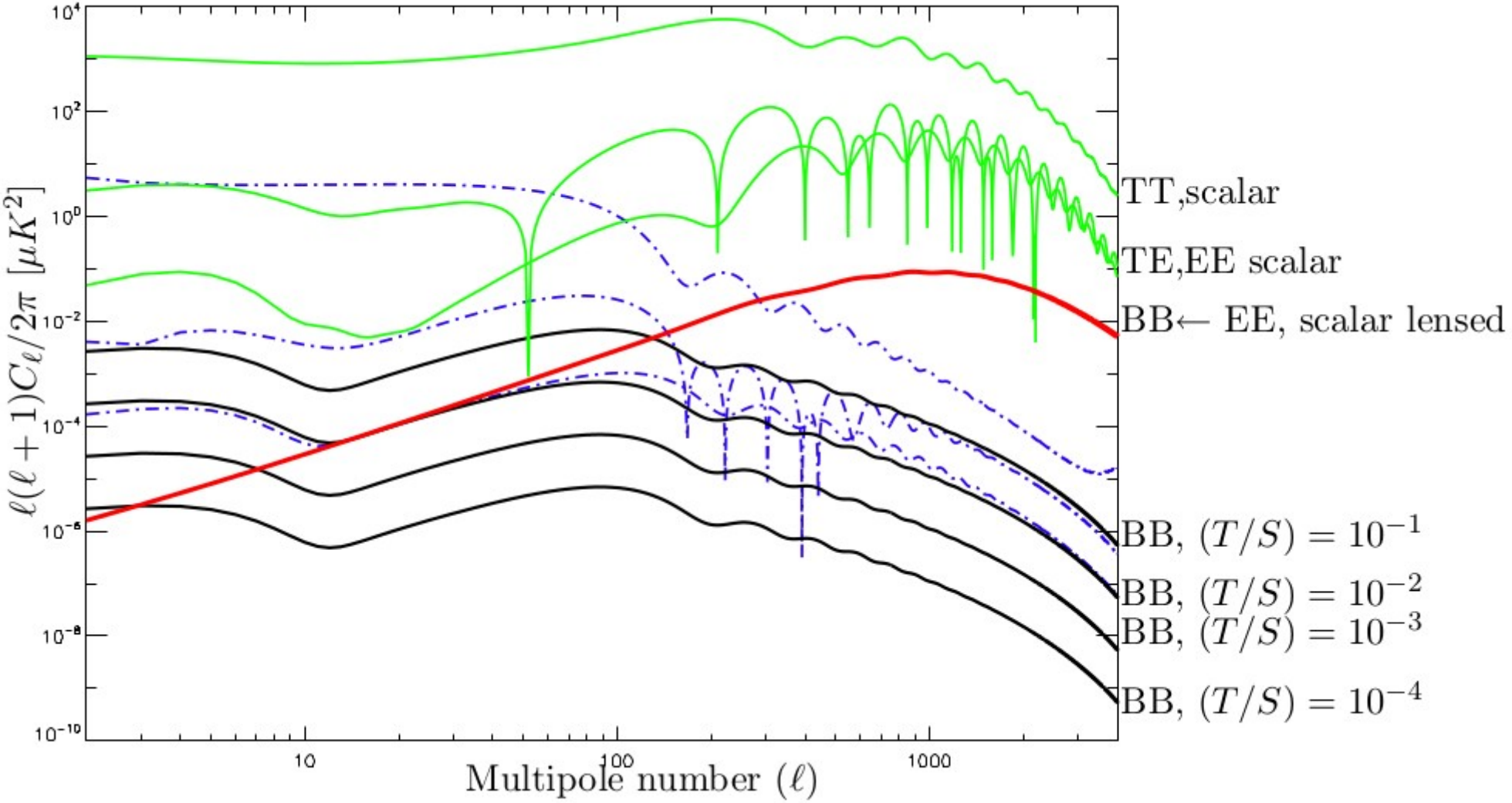

Next generation CMB mission?

- ESA calls for medium (M-class) missions
  - M1/M2 B-Pol proposed Solar orbiter/Euclid accepted
  - M3 COrE proposed EChO, LOFT, MarcoPolo-R, PLATO, STE-QUEST
  - M4 2014
- And Large (L-class) missions
  - L1 JUICE (Jupiter Icy Moon Explorer) selected
  - L2 PRISM mission was proposed (and refused)

Possible improvement – S/N

- The sensitivity of the detector is now limited by the photon noise of the CMB itself
- In order to increase S/N:
  - Longer mission, 4 times the mission, 2 times the S/N
  - More detectors, 4 times the number of detectors, 2 times the S/N
    - Planck had 74 detectors
    - Current ground based and balloon projects have thousands
  - New detector technology
    - Transition Edge Superconductors (TES)
    - Kinetic Inductance Detectors (KID)
    - Cold Electron Bolometers (CEB)

Transition Edge Superconductors

- SPT polarization
  - A total of 768 polarization-sensitive pixels (1536 detectors)
  - The focal plane is ~ 225 mm in diameter.

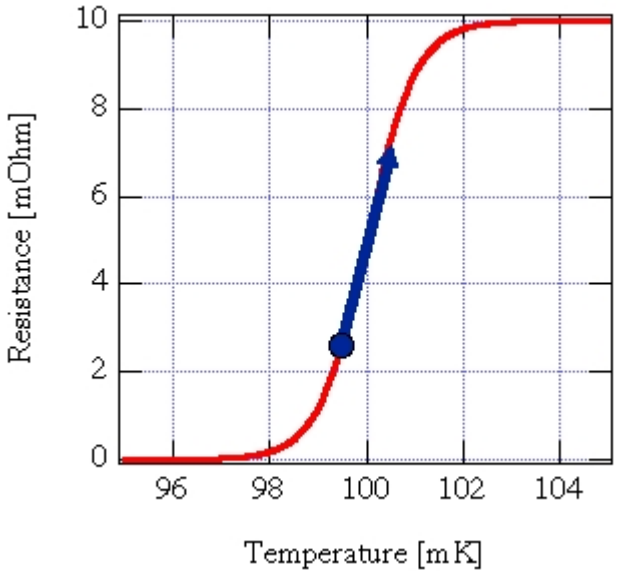

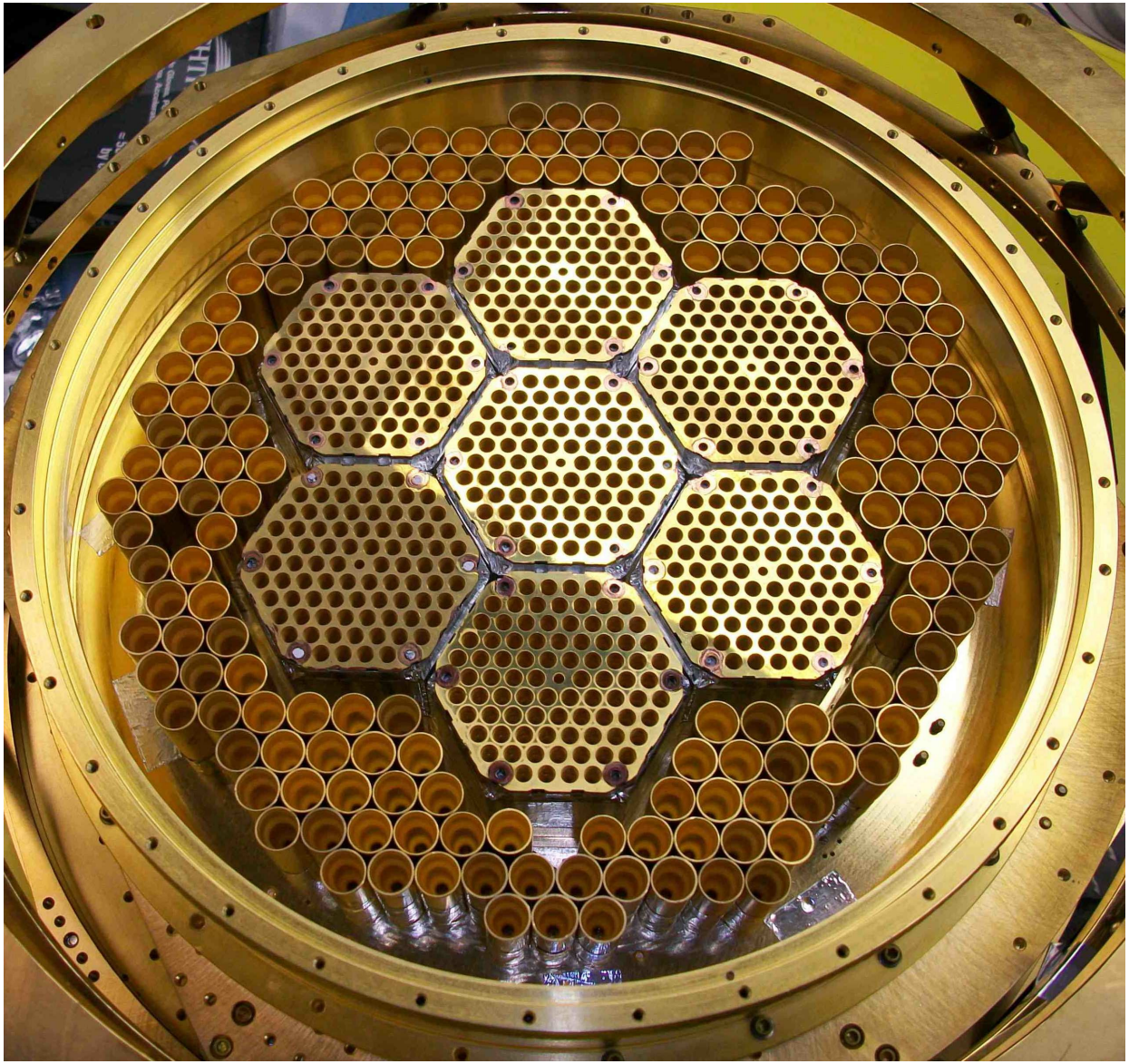

Kinetic Inductance Bolometers

NIKA instrument for IRAM 30 meters telescope in Sierra Nevada

A. Monfardini et al.

Photons are absorbed by a superconducting film, producing a quasi-particles

This changes the inductance of the element

The element is part of a resonant circuit

Amplitude and phase of an excitation RF signal are changed

Cold Electron Bolometers

- S-I-N tunnel junction plays the role of
  - Electron cooling
  - RF capacitive coupling of an absorber to the antenna through capacitance of the SIN tunnel junctions

5-7 19th ISSTT, Groningen, April 2008 1

Distributed Antenna-Coupled Cold-Electron Bolometers for Focal Plane Antenna

Leonid Kuzmin,
Chalmers University of Technology, S-41296 Gothenburg, Sweden,

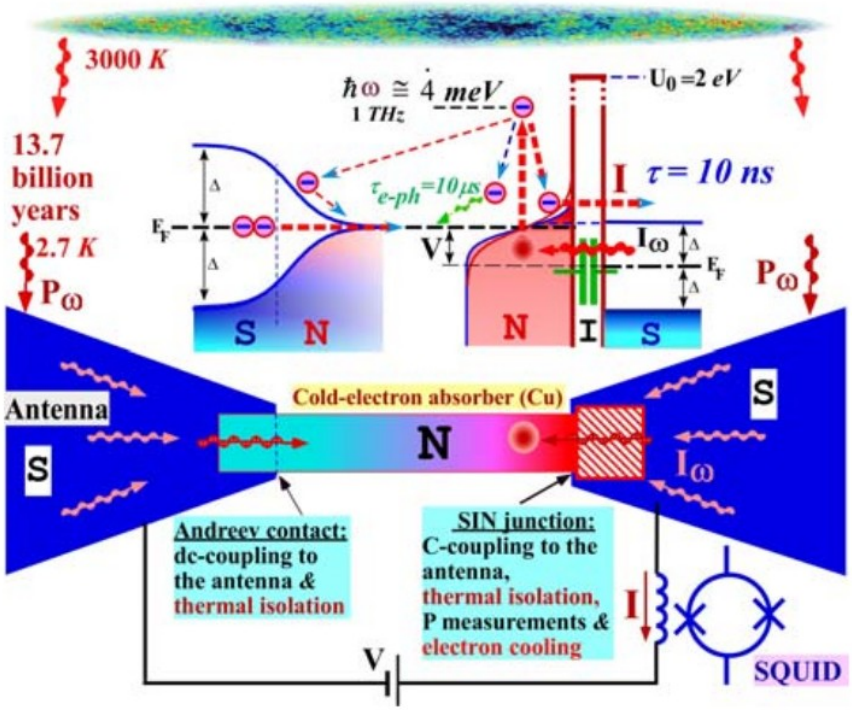

Fig 1. Schematic of the **optimal Cold-Electron Bolometer (CEB) with capacitive coupling to the antenna** and a SQUID readout. The CEB comprises a planar superconducting antenna and an absorber coupled through the capacitance of an SIN tunnel junction, and an SN Andreev contact. The SIN tunnel junction is used also for electron cooling, and for reading out the signal with a SQUID.

Control of systematic effects

- Wide bi-refringent Half Wave Plates
  - Each detectors can be used to resolve polarization, decoupled from beam asymmetry
  - Avoid introducing new half wave plate related systematic effects

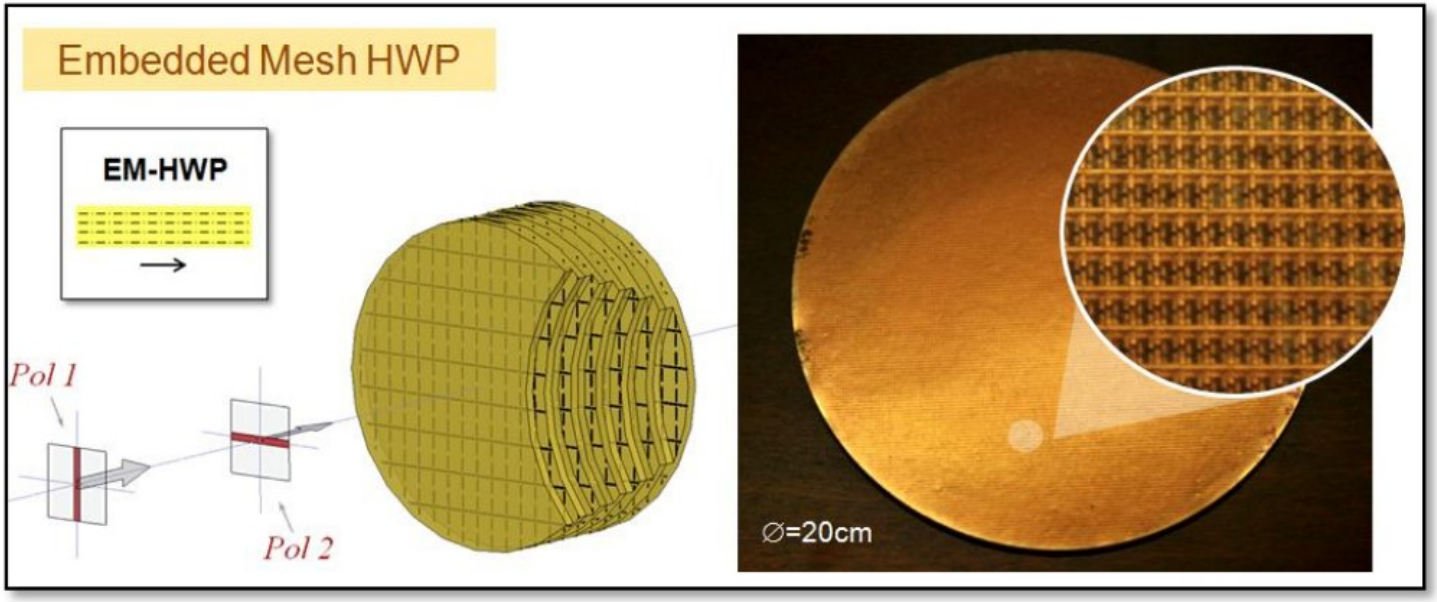

G. Pisano et al
M. Salatino et al.

COrE – Cosmic Origin Explorer

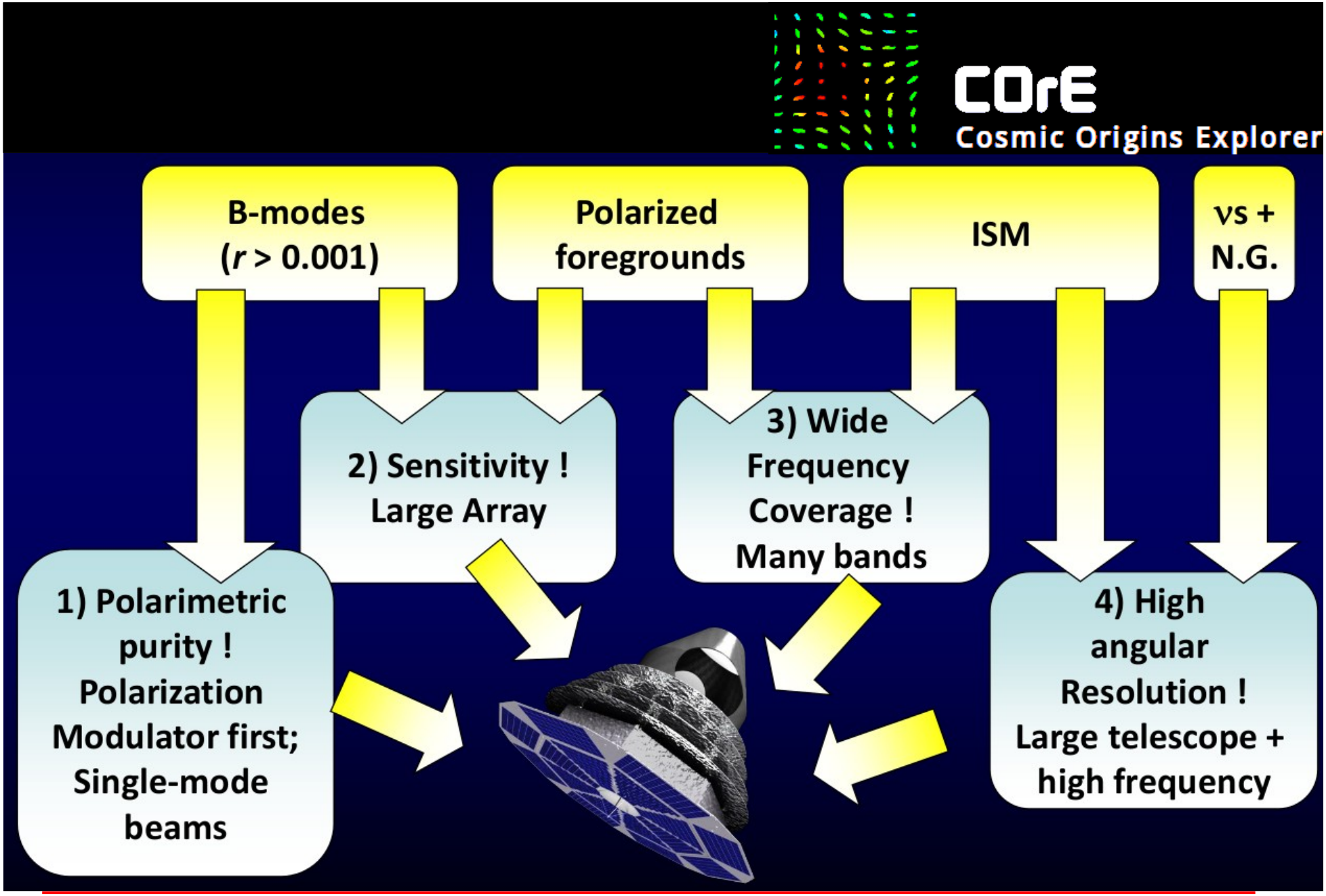

COrE

- Proposed in 2010 as M-class mission
  - Budget < 500 G€

- The **5 mK arcmin sensitivity** must be achieved with a wide sky and frequency coverage.
- This level of sensitivity allows a measurement of the sum of **neutrino masses** at the 0.05 eV level, thus allowing to investigate their hierarchy.
- **Frequency coverage is essential** because polarized foregrounds are overwhelming, and sufficient leverage is needed to separate them and extract a clean cosmological signal (w. redundancy)
- In addition, **polarimetry of ISM** (and the related study of the Galactic magnetic field) at high frequencies is one of the main targets of COrE

Technological development

- After CORE was rejected
  - ESA has granted a number of technological development, related to a CORE-like mission:
    - Development of Cryogenic technology
    - Development of large radii Half Wave Plates
    - Development of compact focal planes and detectors
    - Development of optical system

Large mission – PRISM

- Very ambitious
  - Combine CMB polarization with spectroscopy
  - Cost order of 1000 Geuro
  - Proposed in 2013
- Goals
  - Ultimate galaxy clusters survey
  - Cosmic Infrared Background
  - Inflationary gravitational waves
  - CMB spectral distortion
  - Galactic astrophysics

http://www.prism-mission.org/

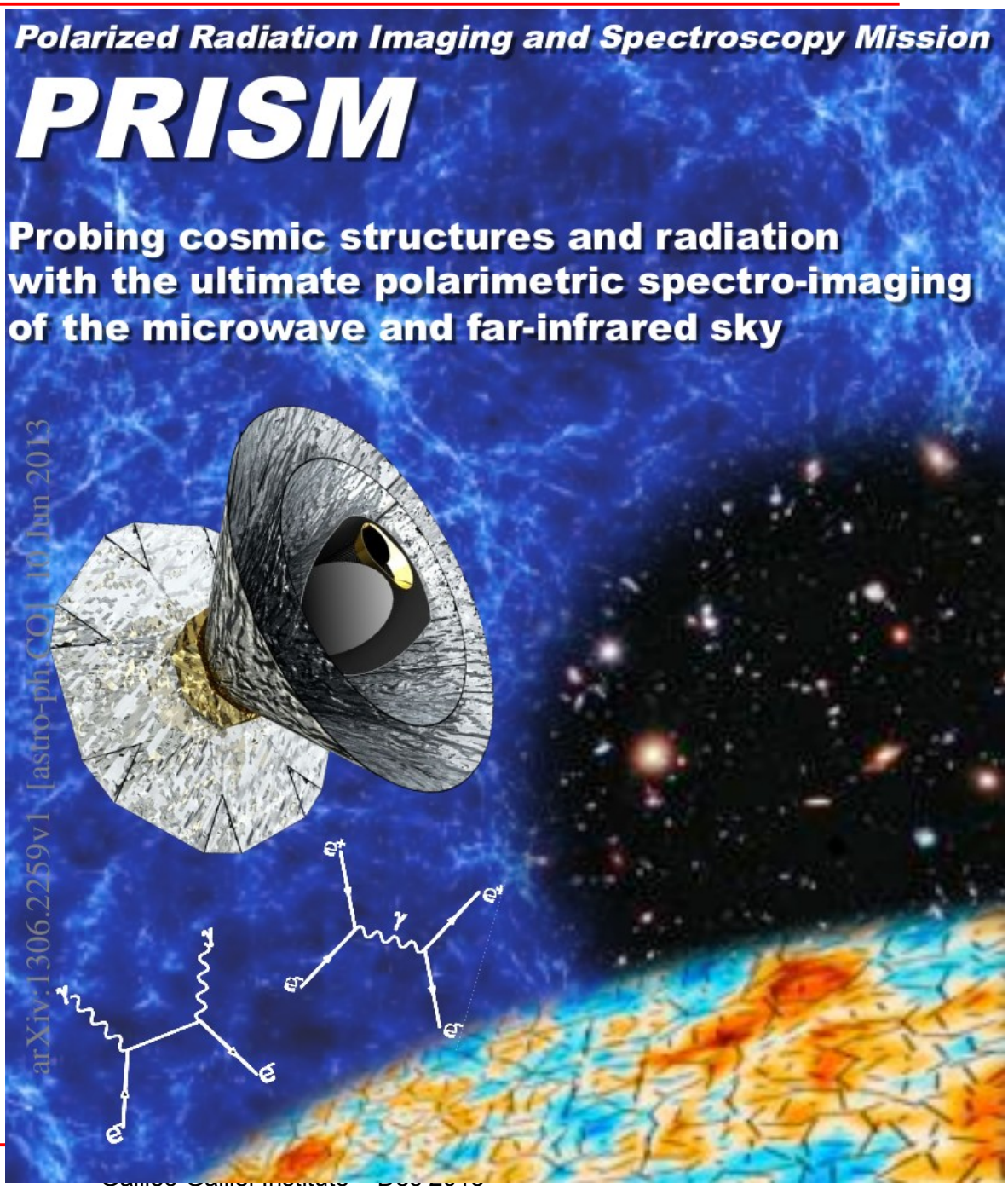

PRISM instruments

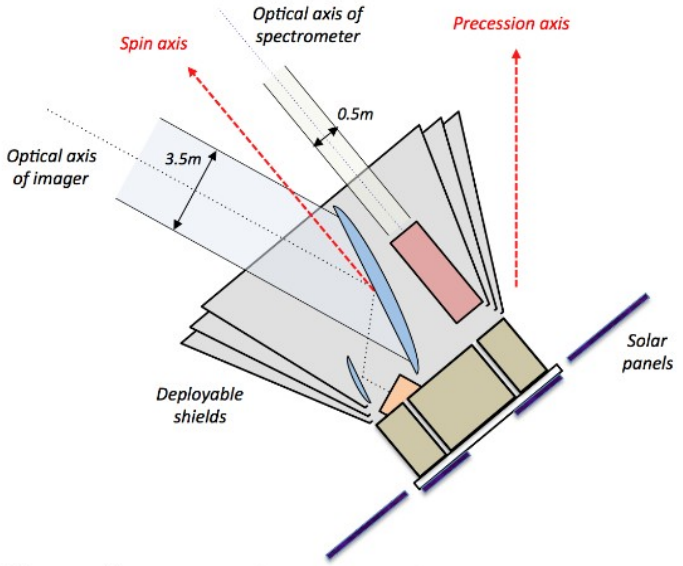

Figure 7: The PRISM spacecraft with its two instruments: PIM, with a 3.5-diameter telescope with a FOV at ∼30° from the spacecraft spin axis, and ASP, aligned with the spin axis.

ν_0	Range	$\Delta\nu/\nu$	n_{det}	$\theta_{\rm fwhm}$	σ_I per det 1 arcmin		$\sigma_{(Q,U)}$ per det 1 arcmin		Main molec. & atomic lines
GHz	GHz				μK$_{\rm RJ}$	μK$_{\rm CMB}$	μK$_{\rm RJ}$	μK$_{\rm CMB}$	
30	26-34	.25	50	17'	61.9	63.4	87.6	89.7	
36	31-41	.25	100	14'	57.8	59.7	81.7	84.5	
43	38-48	.25	100	12'	53.9	56.5	76.2	79.9	
51	45-59	.25	150	10'	50.2	53.7	71.0	75.9	
62	54-70	.25	150	8.2'	46.1	50.8	65.2	71.9	
75	65-85	.25	150	6.8'	42.0	48.5	59.4	68.6	
90	78-100	.25	200	5.7'	38.0	46.7	53.8	66.0	HCN & HCO^+ at 89 GHz
105	95-120	.25	250	4.8'	34.5	45.6	48.8	64.4	CO at 110-115 GHz
135	120-150	.25	300	3.8'	28.6	44.9	40.4	63.4	
160	135-175	.25	350	3.2'	24.4	45.5	34.5	64.3	
185	165-210	.25	350	2.8'	20.8	47.1	29.4	66.6	HCN & HCO^+ at 177 GHz
200	180-220	.20	350	2.5'	18.9	48.5	26.7	68.6	
220	195-250	.25	350	2.3'	16.5	50.9	23.4	71.9	CO at 220-230 GHz
265	235-300	.25	350	1.9'	12.2	58.5	17.3	82.8	HCN & HCO^+ at 266 GHz
300	270-330	.20	350	1.7'	9.6	67.1	13.6	94.9	
320	280-360	.25	350	1.6'	8.4	73.2	11.8	103	CO, HCN & HCO^+
395	360-435	.20	350	1.3'	4.9	107	7.0	151	
460	405-520	.25	350	1.1'	3.1	156	4.4	221	CO, HCN & HCO^+
555	485-625	.25	300	55"	1.6	297	2.3	420	C-I, HCN, HCO^+, H_2O, CO
660	580-750	.25	300	46"	0.85	700	1.2	990	CO, HCN & HCO^+
					nK$_{\rm RJ}$	kJy/sr	nK$_{RJ}$	kJy/sr	
800	700-900	.25	200	38"	483	9.5	683	13.4	
960	840-1080	.25	200	32"	390	11.0	552	15.6	
1150	1000-1300	.25	200	27"	361	14.6	510	20.7	
1380	1200-1550	.25	200	22"	331	19.4	468	27.4	N-II at 1461 GHz
1660	1470-1860	.25	200	18"	290	24.5	410	34.7	
1990	1740-2240	.25	200	15"	241	29.3	341	41.5	C-II at 1900 GHz
2400	2100-2700	.25	200	13"	188	33.3	266	47.1	N-II at 2460 GHz
2850	2500-3200	.25	200	11"	146	36.4	206	51.4	
3450	3000-3900	.25	200	8.8"	113	41.4	160	58.5	O-III at 3393 GHz
4100	3600-4600	.25	200	7.4"	98	50.8	139	71.8	
5000	4350-5550	.25	200	6.1"	91	70.1	129	99.1	O-I at 4765 GHz
6000	5200-6800	.25	200	5.1"	87	96.7	124	136	O-III at 5786 GHz

Table 1: The 32 broad-band channels of the polarized imager with a total of 7600 detectors. Sensitivities are averages for sky regions at galactic latitude and ecliptic latitude both higher than 30°. A detector noise level equal to the sky photon noise is assumed. The mission sensitivity per frequency channel is the sensitivity per detector divided by $\sqrt{n_{det}}$.

Reply to PRISM proposal

→ REPORT OF THE SENIOR SURVEY COMMITTEE ON THE SELECTION OF THE SCIENCE THEMES FOR THE L2 AND L3 LAUNCH OPPORTUNITIES IN THE COSMIC VISION PROGRAMME

October 2013

Prepared by the Senior Survey Committee:
Dr. Catherine Cesarsky (CEA, Chair)
Prof. Willy Benz (Bern University)
Dr. Sergio Bertolucci (CERN)
Prof. Giovanni Bignami (INAF)
Dr. Thérèse Encrenaz (Meudon Observatory)
Prof. Reinhard Genzel (MPE)
Dr. Jason Spyromilio (ESO)
Prof. John Zarnecki (Open University)

Reply to PRISM proposal

other means. Yet, it is the non-CMB science that is the technology and cost driver for the proposed mission, especially in terms of the size and temperature of the telescope. The core CMB science can in principle be carried out with a smaller space mission (which could thus be implemented on a different, faster implementation path). Given the very active ongoing activities in CMB studies by the worldwide scientific community, it's not impossible for the CMB science goals of a PRISM-like mission implemented in either L2 or L3 (thus 15 or more years in the future) to be undercut by a smaller (M mission scale) mission focused on CMB science only.

In summary, the SSC was fully convinced of the great importance of the core CMB science and encourages the CMB community to consider proposing this science for a future M-class mission. The SSC did not see that an L mission is needed for the CMB science, nor justified in itself by the other science goals presented.

In the meanwhile

- Ground based and balloon based experiments:
  - Much cheaper and simple
  - Test technology
  - Improve measurements
  - Miss full sky and purity of a satellite based mission

- Balloon
  - SPIDER
  - EBex
  - LSPE (Italy)
  - PIPER

- Ground based
  - SPT
  - ACT
  - QUBIC (Italy)
  - BICEP
  - Keck array
  - Quijote
  - Polar bear
  - Simons array
  - Ground bird
  - CLASS

Conclusion

- Planck worked incredibly well
  - Considering that the Planck satellite and its complex cryogenic payload have operated without interruption over a lifetime that is longer than initially planned by a factor of ~2, and that the performance of its payload is the same or better than expected from pre-launch ground testing, we can conclude that it has been a tremendous technical success.
  - 2nd year and Polarization results are coming along
  - Knowledge of the calibration parameter is as important as knowledge of the cosmological model
- Combination of CMB and other astrophysical datasets is providing more and more information on the Dark Matter distribution and evolution
- Next generation CMB experiment has the potential to constrain inflationary parameters
  - An evolution of COrE will be presented as M4 mission in 2014
  - Squeezed between “single number mission (maybe)” and “over-killer”
  - Technological development, ground-based and balloon based experiment are progressing fast
- Planck (Max) started a revolution, completed in less than 30 years
- We are not there yet!

Planck acknowledgements

The scientific results presented today are the product of the Planck Collaboration, including individuals from more than 50 scientific institutes in Europe, the USA and Canada

Back-up slides

Planck 2013 results. XVI. Cosmological parameters

Abstract: This paper presents the first cosmological results based on *Planck* measurements of the cosmic microwave background (CMB) temperature and lensing-potential power spectra. We find that the *Planck* spectra at high multipoles ($\ell \gtrsim 40$) are extremely well described by the standard spatially-flat six-parameter ΛCDM cosmology with a power-law spectrum of adiabatic scalar perturbations. Within the context of this cosmology, the *Planck* data determine the cosmological parameters to high precision: the angular size of the sound horizon at recombination, the physical densities of baryons and cold dark matter, and the scalar spectral index are estimated to be $\theta_* = (1.04147 \pm 0.00062) \times 10^{-2}$, $\Omega_b h^2 = 0.02203 \pm 0.00028$, $\Omega_c h^2 = 0.1199 \pm 0.0027$, and $n_s = 0.9603 \pm 0.0073$, respectively (68% errors). For this cosmology, we find a low value of the Hubble constant, $H_0 = 67.3 \pm 1.2\,\mathrm{km\,s^{-1}\,Mpc^{-1}}$, and a high value of the matter density parameter, $\Omega_m = 0.315 \pm 0.017$. These values are in tension with recent direct measurements of H_0 and the magnitude-redshift relation for Type Ia supernovae, but are in excellent agreement with geometrical constraints from baryon acoustic oscillation (BAO) surveys. Including curvature, we find that the Universe is consistent with spatial flatness to percent level precision using *Planck* CMB data alone. We use high-resolution CMB data together with *Planck* to provide greater control on extragalactic foreground components in an investigation of extensions to the six-parameter ΛCDM model. We present selected results from a large grid of cosmological models, using a range of additional astrophysical data sets in addition to *Planck* and high-resolution CMB data. None of these models are favoured over the standard six-parameter ΛCDM cosmology. The deviation of the scalar spectral index from unity is insensitive to the addition of tensor modes and to changes in the matter content of the Universe. We find a 95% upper limit of $r_{0.002} < 0.11$ on the tensor-to-scalar ratio. There is no evidence for additional neutrino-like relativistic particles beyond the three families of neutrinos in the standard model. Using BAO and CMB data, we find $N_{\mathrm{eff}} = 3.30 \pm 0.27$ for the effective number of relativistic degrees of freedom, and an upper limit of 0.23 eV for the sum of neutrino masses. Our results are in excellent agreement with big bang nucleosynthesis and the standard value of $N_{\mathrm{eff}} = 3.046$. We find no evidence for dynamical dark energy; using BAO and CMB data, the dark energy equation of state parameter is constrained to be $w = -1.08^{+0.11}_{-0.09}$. We also use the *Planck* data to set limits on a possible variation of the fine-structure constant, dark matter annihilation and primordial magnetic fields. Despite the success of the six-parameter ΛCDM model in describing the *Planck* data at high multipoles, we note that this cosmology does not provide a good fit to the temperature power spectrum at low multipoles. The unusual shape of the spectrum in the multipole range $20 \lesssim \ell \lesssim 40$ was seen previously in the *WMAP* data and is a real feature of the primordial CMB anisotropies. The poor fit to the spectrum at low multipoles is not of decisive significance, but is an "anomaly" in an otherwise self-consistent analysis of the *Planck* temperature data.

http://arxiv.org/abs/1303.5076

Low multipoles anomaly

Planck Collaboration: The *Planck* mission

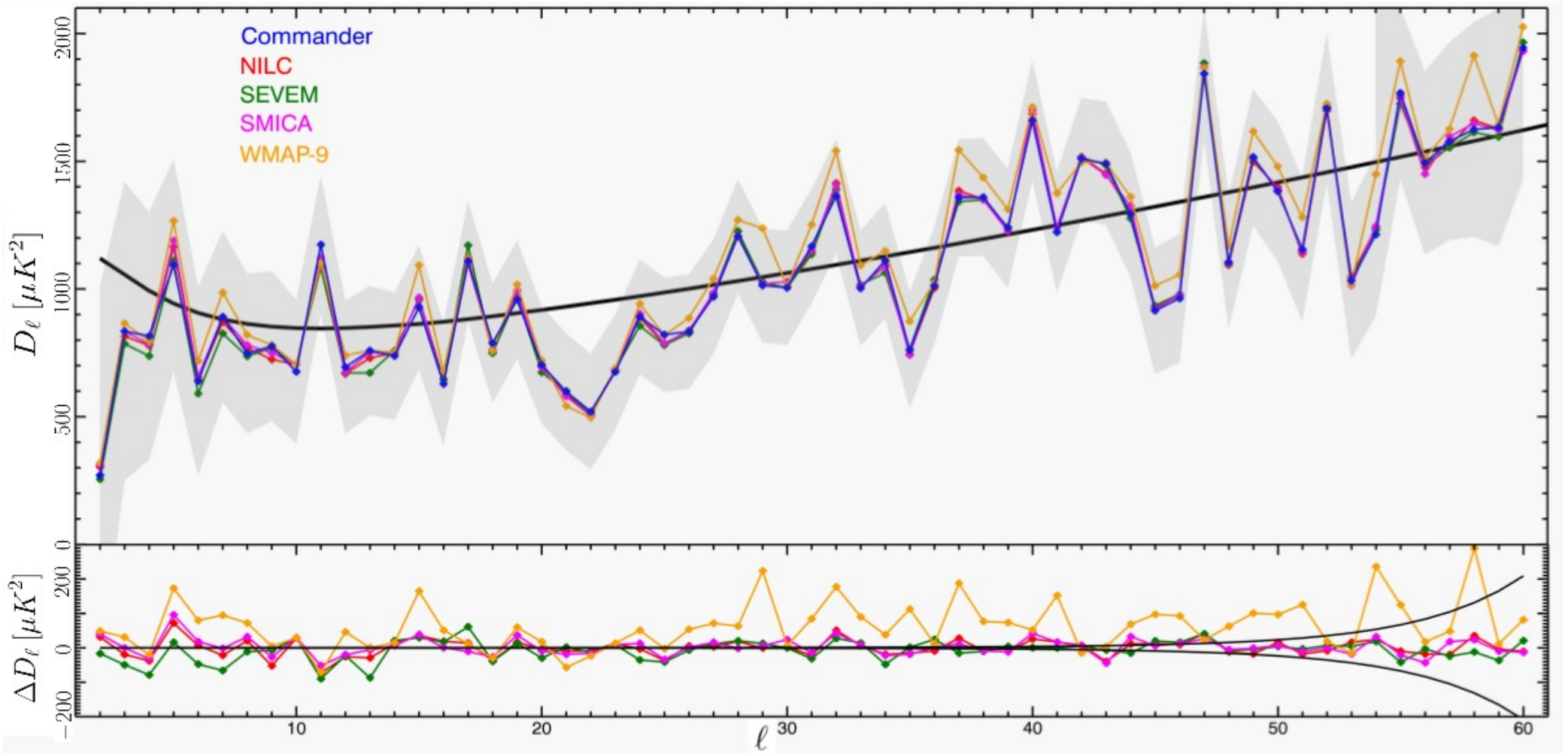

Fig. 12. Top panel: temperature power spectra evaluated from downgraded *Planck* maps, estimated with `Commander`, `NILC`, `SEVEM`, or `SMICA`, and the 9-year *WMAP* ILC map, using the `Bolpol` quadratic estimator. The grey shaded area indicates the $1\,\sigma$ Fisher errors while the solid line shows the *Planck* ΛCDM best fit model. Bottom panel: Power spectrum differences for each algorithm/data set relative to the `Commander` spectrum, estimated from the spectra shown in the panel above. The black lines show the expected $1\,\sigma$ uncertainty due to (regularization) noise. This is Fig. 34 of Planck Collaboration XV (2013)

Hubble constant

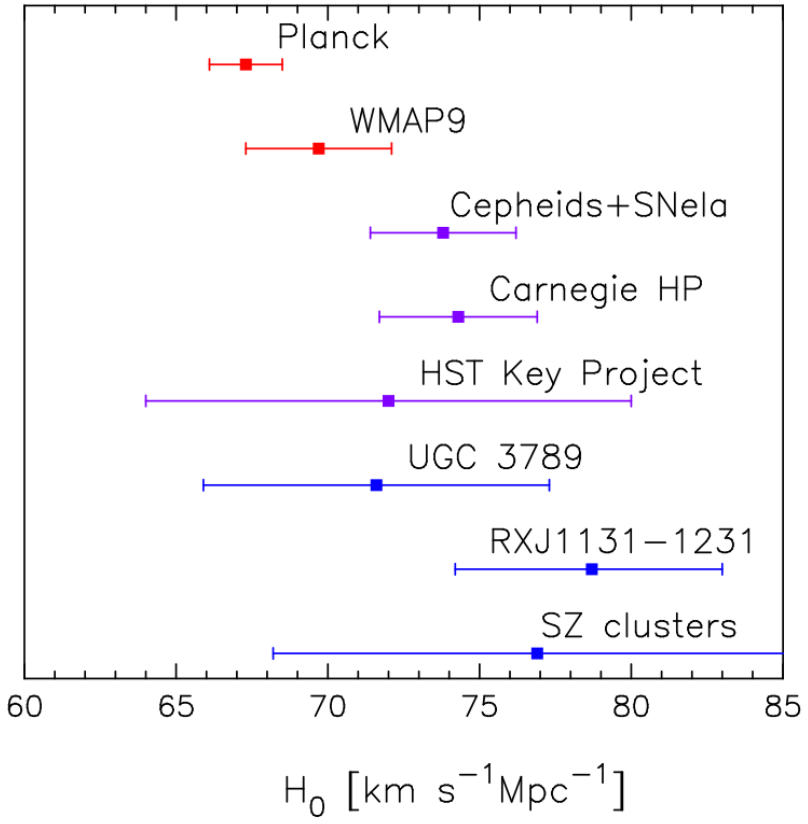

Sample	Ω_m	H_0
6dF	$0.305^{+0.032}_{-0.026}$	$68.3^{+3.2}_{-3.2}$
SDSS	$0.295^{+0.019}_{-0.017}$	$69.5^{+2.2}_{-2.1}$
SDSS(R)	$0.293^{+0.015}_{-0.013}$	$69.6^{+1.7}_{-1.5}$
WiggleZ	$0.309^{+0.041}_{-0.035}$	$67.8^{+4.1}_{-2.8}$
BOSS	$0.315^{+0.015}_{-0.015}$	$67.2^{+1.6}_{-1.5}$
6dF+SDSS+BOSS+WiggleZ	$0.307^{+0.010}_{-0.011}$	$68.1^{+1.1}_{-1.1}$
6dF+SDSS(R)+BOSS	$0.305^{+0.009}_{-0.010}$	$68.4^{+1.0}_{-1.0}$
6dF+SDSS(R)+BOSS+WiggleZ	$0.305^{+0.009}_{-0.008}$	$68.4^{+1.0}_{-1.0}$

Supernovae calibrated on HST Cepheids
Riess et al. 2011 $H_0 = 73.8 \pm 2.4$ km/s/Mpc

$H_0 = 67.3 \pm 1.2\,\mathrm{km\,s^{-1}\,Mpc^{-1}}$ (68%; *Planck*+WP+highL)

$H_0 = 69.7 \pm 2.4\,\mathrm{km\,s^{-1}\,Mpc^{-1}}$ (68%; *WMAP*-9)

Curvature

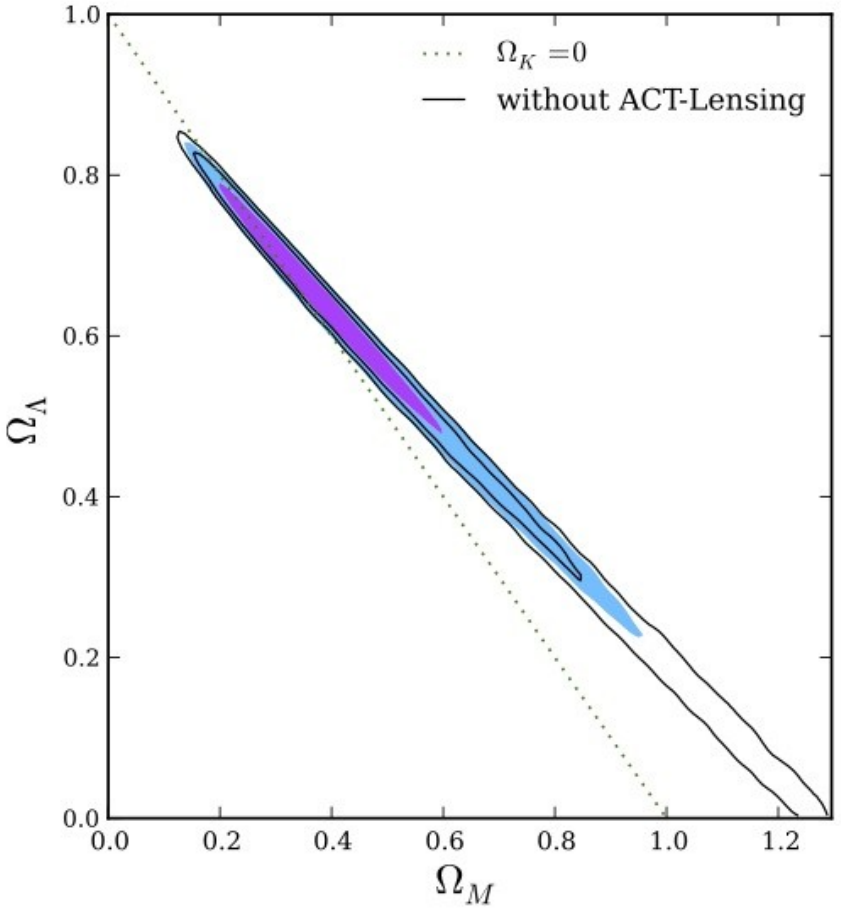

$100\Omega_K = -4.2^{+4.3}_{-4.8}$, (95%, *Planck*+WP+highL,

$100\Omega_K = -1.0^{+1.8}_{-1.9}$, (95%, *Planck*+lensing+WP+highL).

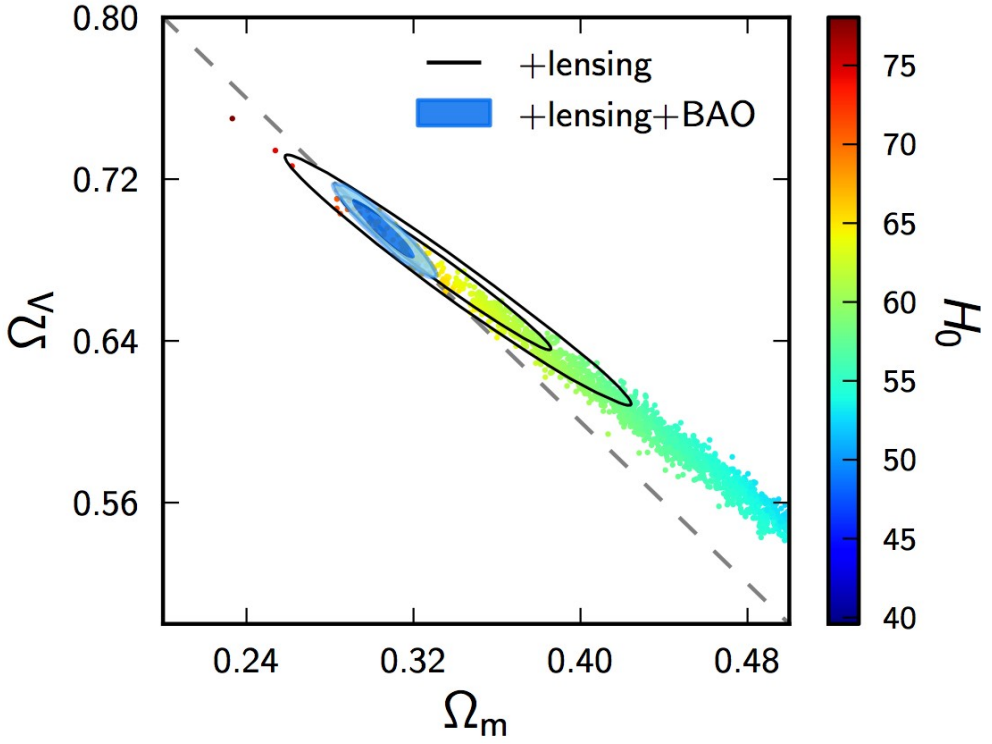

Dark energy

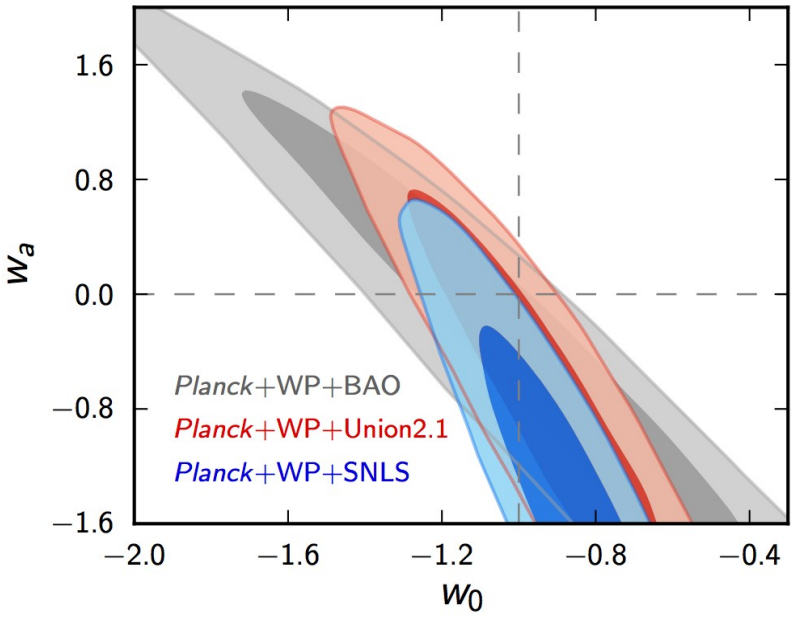

$w = -1.13 \pm 0.24$ (95%, *Planck* + WP + BAO)

$w = -1.09 \pm 0.17$ (95%, *Planck* + WP + Union2.1)

$w = -1.13^{+0.13}_{-0.14}$ (95%, *Planck* + WP + SNLS)

$w = -1.24^{+0.18}_{-0.19}$ (95%, *Planck* + WP + H_0)

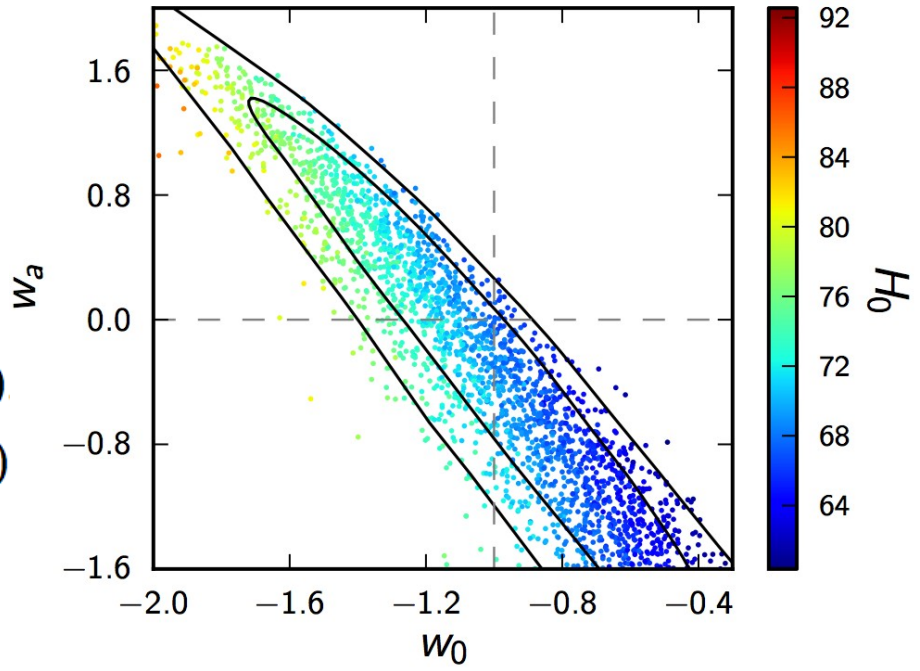

$w_0 = -1.04^{+0.72}_{-0.69}$ (95%, *Planck* + WP + BAO)

$w_a < 1.32$ (95%, *Planck* + WP + BAO)

Neutrino physics

T_ν. We account for the additional energy density in neutrinos by assuming that they have a thermal distribution with an effective energy density

$$\rho_\nu = N_{\rm eff}\,\frac{7}{8}\left(\frac{4}{11}\right)^{4/3}\rho_\gamma, \qquad (1)$$

with $N_{\rm eff} = 3.046$ in the baseline model (Mangano et al. 2002, 2005). This density is divided equally between three neutrino species while they remain relativistic.

The physics of how $N_{\rm eff}$ is constrained by CMB anisotropies is explained in Bashinsky & Seljak (2004), Hou et al. (2011) and Lesgourgues et al. (2013). The main effect is that increasing the radiation density at fixed θ_* (to preserve the angular scales of the acoustic peaks) and fixed $z_{\rm eq}$ (to preserve the early-ISW effect and so first-peak height) increases the expansion rate before recombination and reduces the age of the Universe at recombination. Since the diffusion length scales approximately as the square root of the age, while the sound horizon varies proportionately with the age, the angular scale of the photon diffusion length, $\theta_{\rm D}$, increases, thereby reducing power in the damping tail at a given multipole. Combining *Planck*, *WMAP* polarization and the high-ℓ experiments gives

$$N_{\rm eff} = 3.36^{+0.68}_{-0.64} \quad (95\%;\ \textit{Planck}{+}{\rm WP}{+}{\rm highL}). \qquad (74)$$

Cosmological models, with and without neutrino mass, have different primary CMB power spectra. For observationally-relevant masses, neutrinos are still relativistic at recombination and the unique effects of masses in the primary power spectra are small. The main effect is around the first acoustic peak and is due to the early integrated Sachs-Wolfe (ISW) effect; neutrino masses have an impact here even for a fixed redshift of matter–radiation equality (Lesgourgues & Pastor 2012; Hall & Challinor 2012; Hou et al. 2012; Lesgourgues et al. 2013). To date, this effect has been the dominant one in constraining the neutrino mass from CMB data, as demonstrated in Hou et al. (2012). As we shall see here, the *Planck* data move us into a new regime where the dominant effect is from gravitational lensing. Increasing neutrino mass, while adjusting other parameters to remain in a high-probability region of parameter space, increases the expansion rate at $z \gtrsim 1$ and so suppresses clustering on scales smaller than the horizon size at the non-relativistic transition (Kaplinghat et al. 2003; Lesgourgues et al. 2006). The net effect for lensing is a suppression of the CMB lensing potential and, for orientation, by $\ell = 1000$ the suppression is around 10% in power for $\sum m_\nu = 0.66\,{\rm eV}$.

Neutrino physics

- *N_eff* specifies the energy density when the species are relativistic in terms of the neutrino temperature assuming exactly three flavors and instantaneous decoupling
- In the Standard Model, *N eff* = 3.046, due to non-instantaneous decoupling corrections

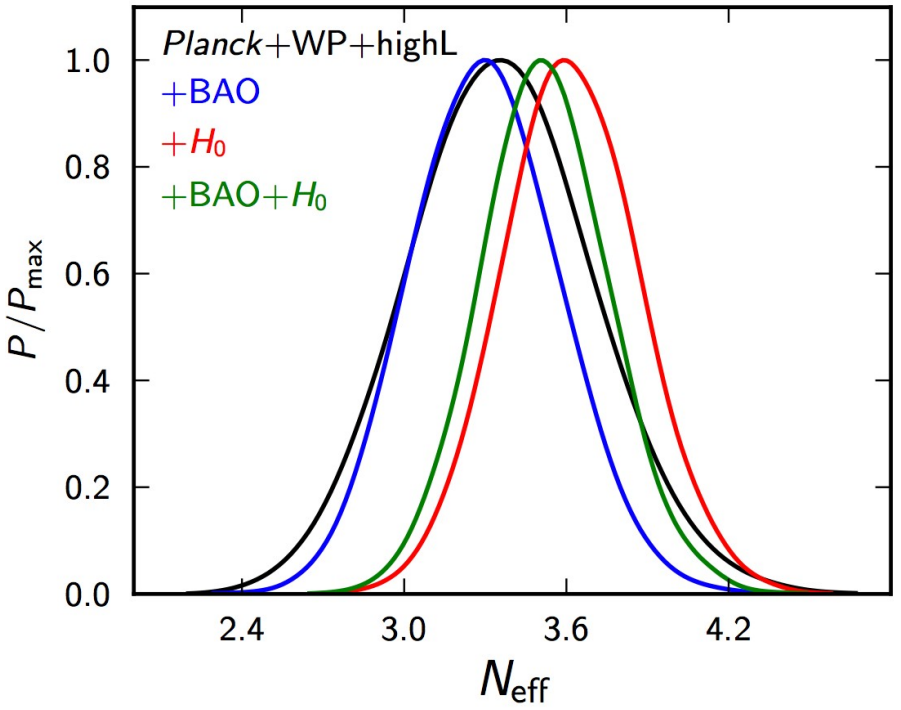

$N_{\rm eff} = 3.36^{+0.68}_{-0.64}$ (95%; *Planck*+WP+highL)

$N_{\rm eff} = 3.62^{+0.50}_{-0.48}$ (95%; *Planck*+WP+highL+H_0)

$N_{\rm eff} = 3.52^{+0.48}_{-0.45}$ (95%; *Planck*+WP+highL+H_0+BAO).

Neutrino physics

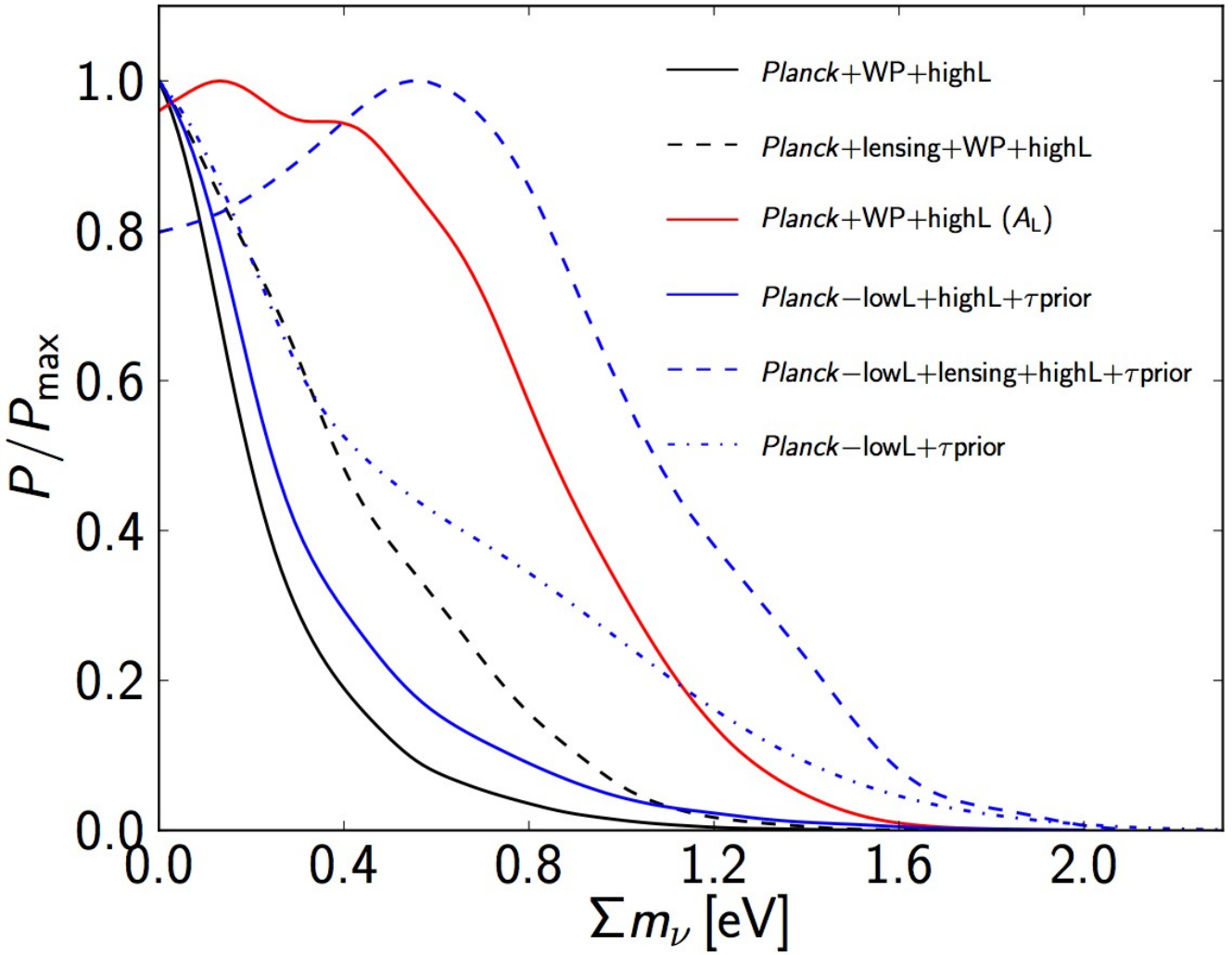

AL means marginalization over lensing, without using the lensing likelihood. Lensing plays a major role in setting the neutrino mass

Including lensing likelihood pushes for higher masses

$$\sum m_\nu < 0.85\,\text{eV} \quad (95\%;\ \textit{Planck}+\text{lensing}+\text{WP}+\text{highL}),$$

$$\sum m_\nu < 0.23\,\text{eV} \quad (95\%;\ \textit{Planck}+\text{WP}+\text{highL}+\text{BAO}).$$

$$\left.\begin{aligned} N_{\rm eff} &= 3.32^{+0.54}_{-0.52} \\ \textstyle\sum m_\nu &< 0.28\,\text{eV} \end{aligned}\right\} \quad (95\%;\ \textit{Planck}+\text{WP}+\text{highL}+\text{BAO})$$

Comparison with WMAP

Parameter	*Planck* ("CMB+Lens")	*WMAP* (9-year)	Difference value	Difference *WMAP* σ
$\Omega_b h^2$	0.02217 ± 0.00033	0.02264 ± 0.00050	-0.00047	0.9
$\Omega_c h^2$	0.1186 ± 0.0031	0.1138 ± 0.0045	0.0048	1.1
Ω_Λ	0.693 ± 0.019	0.721 ± 0.025	-0.028	1.1
τ	0.089 ± 0.032	0.089 ± 0.014	0	0
t_0 (Gyr)	13.796 ± 0.058	13.74 ± 0.11	56 Myr	0.5
H_0 (km s^{-1}Mpc^{-1})	67.9 ± 1.5	70.0 ± 2.2	-2.1	1.0
σ_8	0.823 ± 0.018	0.821 ± 0.023	0.002	0.1
Ω_b	0.0481^{b}	0.0463 ± 0.0024	0.0018	0.7
Ω_c	0.257^{b}	0.233 ± 0.023	0.024	1.0

H0 slightly lower (and thus modified densities)

WMAP Team Comparison Source http://lambda.gsfc.nasa.gov

Maps HFI

Table 4. HFI Nominal Maps — Main Characteristics.

Quantity	Units							Notes
Reference frequency ν	[GHz]	100	143	217	353	545	857	*a*1
Number of bolometers		8	11	12	12	3	4	*a*2
Effective beam solid angle Ω	[arcmin^2]	105.78	59.95	28.45	26.71	26.53	24.24	*b*1
Error in solid angle σ_Ω	[arcmin^2]	0.55	0.08	0.03	0.02	0.03	0.03	*b*2
Spatial variation (*rms*) $\Delta\Omega$	[arcmin^2]	0.31	0.25	0.27	0.25	0.34	0.19	*b*3
Effective beam FWHM$_1$	[arcmin]	9.66	7.27	5.01	4.86	4.84	4.63	*b*4
Effective beam FWHM$_2$	[arcmin]	9.65	7.25	4.99	4.82	4.68	4.33	*b*5
Effective beam ellipticity ϵ		1.186	1.036	1.177	1.147	1.161	1.393	*b*6
Variation (*rms*) of the ellipticity $\Delta\epsilon$		0.023	0.009	0.030	0.028	0.036	0.076	*b*7
Sensitivity per beam solid angle	[μK]	10	6	12	39			*c*1
	[kJy sr^{-1}]					13	14	*c*1
Sensitivity	[μK deg]	1.8	0.8	1.0	3.5			*c*2
	[kJy sr^{-1} deg]					1.1	1.1	*c*2
Relative calibration accuracy	[%]	$\lesssim$ 0.2	-	$\lesssim$ 0.2	$\lesssim$ 1	$\lesssim$ 5	$\lesssim$ 5	*d*1
Absolute calibration accuracy	[%]	$\lesssim$ 0.5	$\lesssim$ 0.5	$\lesssim$ 0.5	$\lesssim$ 1.2	$\lesssim$ 10	$\lesssim$ 10	*d*2
Galactic zero-level offset	[MJy sr^{-1}]	0.0047	0.0136	0.0384	0.0885	0.1065	0.1470	*e*1
Galactic zero-level uncertainty	[MJy sr^{-1}]	0.0008	0.0010	0.0024	0.0067	0.0165	0.0147	*e*2
CIB monopole prediction	[MJy sr^{-1}]	0.0030	0.0079	0.033	0.13	0.35	0.64	*e*3

Side-lobes / residual tails

- Planck calibrates on the dipole
  - Dipole calibration is “transferred” to all scales by beams shape and time response transfer function

Frequency (GHz)	SR Spillover[f] (%)			PR Spillover[g] (%)		
	Mean	Min	Max	Mean	Min	Max
30	0.24	0.23	0.24	0.59	0.59	0.59
44	0.07	0.03	0.09	0.18	0.14	0.19
70	0.17	0.12	0.19	0.65	0.54	0.76
100	0.19	0.17	0.21	0.14	0.12	0.16
143	0.19	0.19	0.19	0.11	0.10	0.11
143 (unpol)	0.19	0.19	0.19	0.13	0.13	0.13
217	0.10	0.10	0.11	0.07	0.02	0.09
217 (unpol)	0.12	0.12	0.12	0.12	0.12	0.12
353	0.02	0.02	0.02	0.02	0.02	0.02
353 (unpol)	0.02	0.02	0.02	0.02	0.02	0.02
545 (unpol)	0.02			0.3		
857 (unpol)	0.0001			0.03		

- The integrated power in the **side-lobes** is estimated by models, validated with survey difference maps
  - In survey 1 and 2 the side-lobes see different parts of the Galactic emission
- HFI residual **long time constant effects** are estimated by looking at long tails after Jupiter scans

		tails	NSL	color correction	pointing error and noise
Band [GHz]	Ω_{SB} [arcmin^2]	$\Delta\Omega_\tau$	$\Delta\Omega_{NSL}$	$\Delta\Omega_{CC}$	$\Delta\Omega_{MC}$
100	104.2	−0.03 ± 0.04 %	0.11 (0.21) %	< 0.3 %	0.53 %
143	58.4	−0.03 ± 0.01 %	0.13 (0.17) %	< 0.3 %	0.14 %
217	26.9	−0.03 ± 0.01 %	0.11 (0.13) %	< 0.3 %	0.11 %
353	25.1	−0.002± 0.01 %	0.18 (0.22) %	< 0.5 %	0.10 %
545	25.4	0.04 ± 0.01 %	0.16 %	< 2.0 %	0.13 %
857	23.0	0.09 ± 0.01 %	0.21 %	< 1.0 %	0.15 %

5+ surveys

Table 1. *Planck* "surveys" (see Sect. 4.1 for the definition of a survey).

Survey	Instrument	Beginning	End	Coverage[a]
1	LFI & HFI	12 August 2009 (14:16:51 UT)	2 February 2010 (20:51:04 UT)	93.1 %
2	LFI & HFI	2 February 2010 (20:54:43)	12 August 2010 (19:27:20 UT)	93.1 %
3[b]	LFI & HFI	12 August 2010 (19:30:44)	8 February 2011 (20:55:55 UT)	93.1 %
4	LFI & HFI	8 February 2011 (20:59:10)	29 July 2011 (17:13:32)	86.6 %
5[c]	LFI & HFI	29 July 2011 (18:04:49)	1 February 2012 (05:26:29 UT)	80.1 %
6	LFI	14 January 2012	July 2012	
7	LFI	July 2012	Jan 2013	
8	LFI	Jan 2013	August 2013	

[a] Fraction of the sky covered by all frequencies
[b] End of Nominal period = 28 November 2010 (12:00:53 UT)
[c] End of data acquisition with HFI = 13 January 2012 (14:54:07 UT)
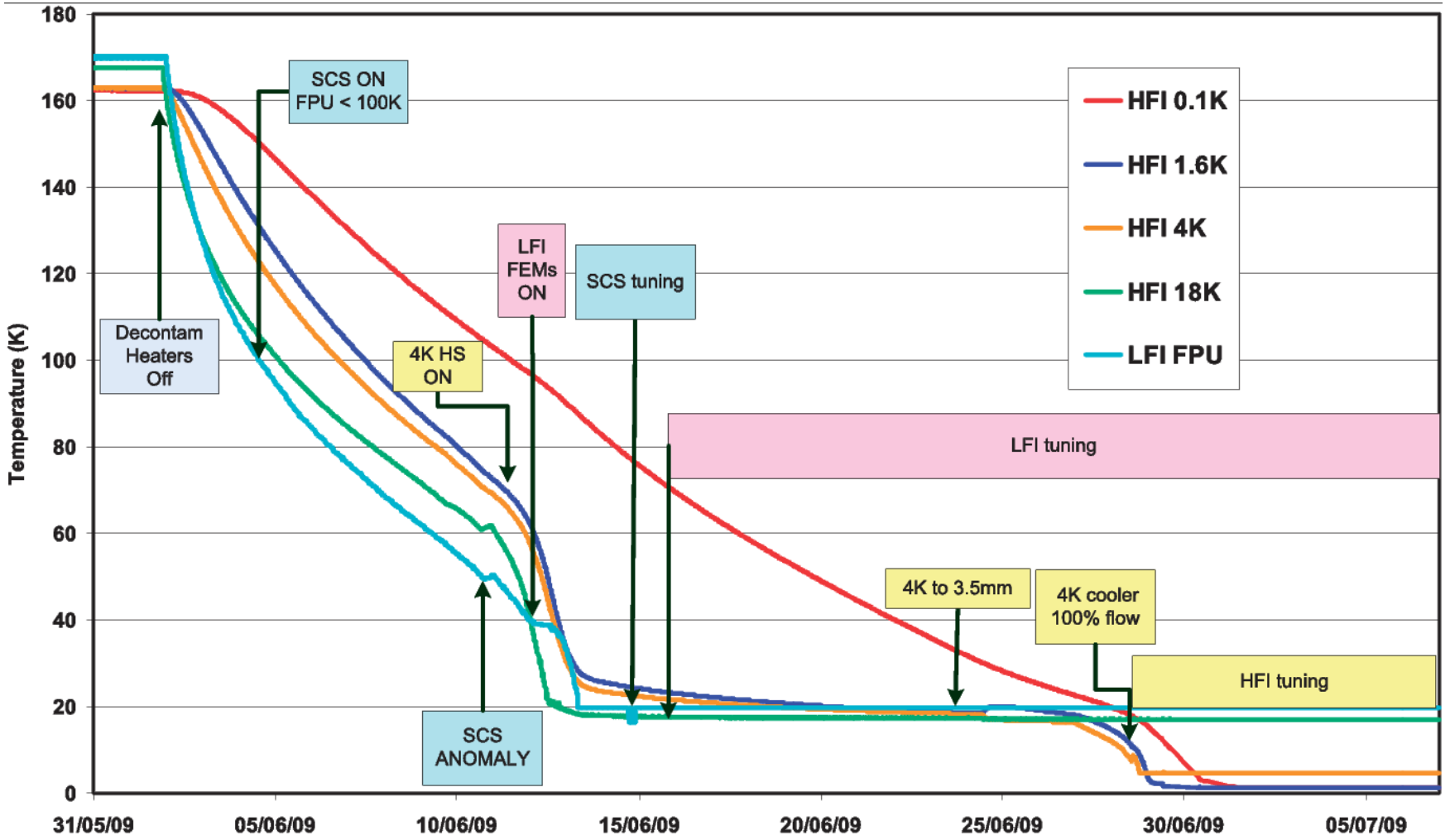
In-flight cooldown